

Baichoo, Nameeta (2007) The effect of rapid cooling on the fat phase of chocolate. PhD thesis, University of Nottingham.

**Access from the University of Nottingham repository:**

[http://eprints.nottingham.ac.uk/11397/1/nameeta\\_baichoo\\_thesis.pdf](http://eprints.nottingham.ac.uk/11397/1/nameeta_baichoo_thesis.pdf)

**Copyright and reuse:**

The Nottingham ePrints service makes this work by researchers of the University of Nottingham available open access under the following conditions.

- Copyright and all moral rights to the version of the paper presented here belong to the individual author(s) and/or other copyright owners.
- To the extent reasonable and practicable the material made available in Nottingham ePrints has been checked for eligibility before being made available.
- Copies of full items can be used for personal research or study, educational, or not-for-profit purposes without prior permission or charge provided that the authors, title and full bibliographic details are credited, a hyperlink and/or URL is given for the original metadata page and the content is not changed in any way.
- Quotations or similar reproductions must be sufficiently acknowledged.

Please see our full end user licence at:

[http://eprints.nottingham.ac.uk/end\\_user\\_agreement.pdf](http://eprints.nottingham.ac.uk/end_user_agreement.pdf)

**A note on versions:**

The version presented here may differ from the published version or from the version of record. If you wish to cite this item you are advised to consult the publisher's version. Please see the repository url above for details on accessing the published version and note that access may require a subscription.

For more information, please contact [eprints@nottingham.ac.uk](mailto:eprints@nottingham.ac.uk)

# **THE EFFECT OF RAPID COOLING ON THE FAT PHASE OF CHOCOLATE**

**Nameeta Baichoo,**

BSc. (Hons) University of Nottingham

Thesis submitted to the University of Nottingham for the  
degree of Doctor of Philosophy

**February 2007**

“It was the best of times, it was the worst of times, it was the age of wisdom, it was the age of foolishness, it was the epoch of belief, it was the epoch of incredulity, it was the season of Light, it was the season of Darkness, it was the spring of hope, it was the winter of despair, we had everything before us, we had nothing before us, we were all going direct to Heaven, we were all going direct the other way . . .”

**-A Tale of Two Cities**

## Table of Contents

<b>TABLE OF CONTENTS.....</b>	<b>I</b>
<b>ABSTRACT .....</b>	<b>III</b>
<b>ACKNOWLEDGEMENTS.....</b>	<b>V</b>
<b>CHAPTER 1: INTRODUCTION .....</b>	<b>1</b>
1.1    THESIS OUTLINE .....	4
<b>CHAPTER 2: LITERATURE REVIEW .....</b>	<b>6</b>
2.1    HISTORY OF CHOCOLATE .....	7
2.2    MODERN DAY CHOCOLATE .....	9
2.3    POLYMORPHISM .....	10
2.4    MODERN DAY CHOCOLATE PRODUCTION .....	21
2.5    TECHNIQUES USED TO STUDY POLYMORPHISM .....	32
<b>CHAPTER 3: MATERIALS AND METHODS.....</b>	<b>46</b>
3.1    MATERIALS .....	47
3.2    TEMPERING .....	48
3.3    DIFFERENTIAL SCANNING CALORIMETRY (DSC) .....	52
3.4    X-RAY DIFFRACTION .....	59
<b>CHAPTER 4: LAB-SCALE TEMPERING AND CHARACTERISATION OF CHOCOLATE AND CHOCOLATE FATS.....</b>	<b>66</b>
4.1    INTRODUCTION.....	67
4.2    DETERMINATION OF TEMPERING PROFILE FOR CHOCOLATE.....	68
4.3    TEMPERING OF CHOCOLATE FATS .....	79
4.4    TEMPERING OF COCOA BUTTER.....	84
4.5    CONCLUSIONS .....	86
<b>CHAPTER 5: EFFECT OF THE RATE OF COOLING AND HEATING ON THE PHASE BEHAVIOUR OF CHOCOLATE USING DIFFERENTIAL SCANNING CALORIMETRY.....</b>	<b>87</b>
5.1    INTRODUCTION.....	88
5.2    EFFECT OF SLOW COOLING ON TEMPERED CHOCOLATE.....	89
5.3    EFFECT OF RAPID COOLING ON TEMPERED CHOCOLATE .....	91
5.4    EFFECT OF COOLING RATE ON UNTEMPERED CHOCOLATE.....	99
5.5    HYPOTHESIS DEVELOPED FROM DSC RESULTS.....	103
5.6    CONFIRMATION OF RESULTS: EXPERIMENTS USING COCOA BUTTER AND	

CHOCOLATE FATS .....	107
5.7 CONCLUSION .....	110
<b>CHAPTER 6: TEMPERATURE CONTROLLED X-RAY STUDY OF POLYMORPHIC TRANSITIONS IN COCOA BUTTER AND CHOCOLATE FATS DURING COOLING AND HEATING.....</b>	<b>112</b>
6.1 EFFECT OF SLOW COOLING .....	113
6.2 EFFECT OF RAPID COOLING .....	119
6.3 CONCLUSIONS FROM SLOW AND RAPID COOLING OF COCOA BUTTER AND CHOCOLATE FATS.....	127
6.4 DIRECT CONTACT COOLING .....	129
6.5 CONCLUSIONS .....	139
<b>CHAPTER 7: USE OF STEPSCAN DSC TO STUDY THE EFFECT OF COOLING RATE ON CHOCOLATE.....</b>	<b>141</b>
7.1 INTRODUCTION .....	142
7.2 OPTIMISATION OF STEPSCAN PARAMETERS .....	143
7.3 RESULTS AND DISCUSSION .....	145
7.4 CONCLUSION .....	166
<b>CHAPTER 8: GENERAL DISCUSSION AND FUTURE WORK.....</b>	<b>168</b>
8.1 RAPID COOLING TO PRODUCE FORM V .....	169
8.2 GOOD DEMOULDING PROPERTIES FOLLOWING RAPID COOLING.....	173
8.3 FUTURE IMPLICATIONS .....	177
<b>CHAPTER 9: REFERENCES .....</b>	<b>178</b>

## **Abstract**

The aim of the project was to understand the science behind rapid cooling of chocolate used in the Frozen Cone® process.

Differential scanning calorimetry was used to study the effect of slow and rapid cooling on tempered chocolate. On rapid cooling, lower melting polymorphs of cocoa butter were generated. Upon heating these recrystallised into the more stable Form V. Results were confirmed by similar observations with tempered chocolate fats. A hypothesis was formed whereby upon rapid cooling, lower melting polymorphs nucleate and grow at the expense of Form V nuclei produced during tempering. Upon subsequent warming, these polymorphs melt and recrystallise into Form V. Rapid cooling on untempered chocolate did not show any recrystallisation during warming; proving that tempering is required for the formation of Form V crystals in the final matrix.

These results were confirmed by temperature-controlled X-ray diffraction on cocoa butter and chocolate fats. The polymorph generated upon rapid cooling was identified as Form I. This co-existed and eventually transformed to Form II and Form V upon warming. X-ray results showed that following rapid cooling, Form V crystals created during tempering did not grow until above 5 °C. Direct contact cooling at different temperatures was carried out to mimic the Frozen Cone® process. It was found that above -15 °C, the adhesion of the sample to the holder increases and seems to be correlated to the presence of Form II. These results suggest that the molecular structure and adhesive property of the polymorphs formed at specific temperatures are important for

the release of chocolate.

Stepscan differential scanning calorimetry was used to separate the simultaneous melting and recrystallisation events occurring in chocolate following slow and rapid cooling, by deconvoluting the total heat flow into reversing and non-reversing components. The general applicability and limitations of Stepscan DSC are also discussed.

## Acknowledgements

I gratefully acknowledge the University of Nottingham and Cadbury Schweppes for sponsoring my PhD. I would like to thank my supervisors at Nottingham University, Prof. John Mitchell and Dr Imad Farhat for their invaluable support and encouragement throughout my research period and my industrial supervisors, Dr Ian Smith and Mr Mike Polgreen for their contribution to the project. I have been very lucky to have worked with people of such talent and wisdom.

Most of this work would not have been possible without Dr William MacNaughtan, (Uncle Bill-one of the most brilliant persons I have ever met), whose constant encouragement, help and discussions about life and science kept me going through the bad times. Mike Chapman (who can fix anything) deserves a big thank you as had he not fixed the countless problems with my equipment, I wouldn't have anything to work with! Phil Glover, Val Street, Liz Rogers, Lynne Moseley and Carolyn Newton: thank you for your patience and kindness; you are truly the people who make everything work smoothly in the background. The librarians at James Cameron Gifford library also deserve special thanks

To all the friends that I've made throughout my research period: your support in the lab and the good times we shared made it all worthwhile. Special mention goes to Jane Newton, for being my best friend and the best housemate ever.



And last but not least, my thanks go to my family for always supporting me despite being so far away and to whom I dedicate this thesis.

# **Chapter 1: Introduction**

*This chapter gives an introduction to the project background and then lays out the details and overall scope of this thesis.*

# 1 Introduction

Cooling is an essential process in the manufacture of most chocolate confectionery. Conventionally, products are formed from liquid tempered chocolate and must be cooled so that they can be handled and wrapped. It is commercially desirable for cooling to be fast so that unstable material is minimised and output (desired polymorphic form) maximised. But there is a limit to the rate of chocolate cooling (approx.  $2\text{ }^{\circ}\text{C}\cdot\text{min}^{-1}$ ) beyond which product quality is impaired. 'White work' or bloom is produced in which the polymorphic cocoa butter has crystallised in lower melting point crystals despite the melt having been pre-seeded with higher melting point Form V crystals. Bloomed chocolate has a white matt appearance and is difficult to demould.

There are, however, processes used in confectionery manufacture in which chocolate is momentarily cooled at rates in the order of tens of degrees Kelvin per minute to temperatures around  $-15\text{ }^{\circ}\text{C}$  without producing white work. These include the Erikson Roller and Aasted Frozen Cone® processes. There is also a patent by Willcocks et al., (2002) and Nice, (2005) which claims the intellectual ownership of very rapid cooling of enrobed products and also mentions that it is possible with very rapid cooling to set a thin layer of chocolate that has not been tempered, such that it has the final appearance of having been tempered.

These methods of rapid cooling are at variance with conventional wisdom and

although there is literature explaining how to do it, there appears to be little satisfactory explanation of how it actually works. As the use of the Frozen Cone process in particular has increased, so has the importance of understanding the science of it. A thorough scientific understanding of why these processes work and what their limitations are is an essential foundation for the use of these technologies and is the objective of the project.

The project aims to address two issues of technological significance:

1. Issue 1: The use of rapid cooling to produce acceptable chocolate. The overall questions to be addressed in this area are
  - a. What are the structural changes resulting from the rapid cooling of chocolate to  $-30\text{ }^{\circ}\text{C}$  or lower at very fast cooling rates?
  - b. What are the processing windows for the production of acceptable chocolate products by rapid cooling as defined above? Within this context it is important to understand changes occurring upon subsequent reheating.
2. Issue 2: The Frozen Cone process. The questions to be addressed in this area are
  - a. What are the mechanisms governing shape retention and subsequent frozen surface release?
  - b. What are the processing windows for shape retention and release?

To understand these technological issues at the heart of the thesis is an

investigation of the polymorphic forms in chocolate and chocolate fats that result during cooling and heating. The main novelty in this work is that the cooling rates are particularly much more rapid than those previously investigated. Furthermore, Stepscan DSC has been applied for the first time to study chocolate and indeed confectionery fats in general.

## **1.1 Thesis outline**

The thesis is laid out as follows. Following this introduction, the thesis comprises six further chapters.

Chapter 2 covers the background processing theory relevant to this work. It deals with polymorphism and industrial processes vital to the production of chocolate. Then techniques used to study polymorphism such as X-ray diffraction and calorimetry are discussed.

Chapter 3 looks at the materials used in this study. It also details the experimental conditions used for each analytical technique.

Chapter 4 details the determination and optimisation of the tempering profiles of chocolate, cocoa butter and chocolate fats and tests carried out to check for correct temper.

Chapter 5 shows the effect of cooling and heating rate on the phase behaviour of chocolate, using data acquired by differential scanning calorimetry. This is

further strengthened by looking at polymorphic transitions in the fat phase of chocolate occurring on rapid cooling using temperature controlled X-ray diffraction.

Chapter 6 describes the use of Stepscan differential scanning calorimetry to study the effect of rapid cooling in chocolate

Chapter 7 discusses the results as a whole, conclusions from the work completed as well as implications of the findings for chocolate manufacture and suggestions for future work.

## **Chapter 2: Literature review**

*This chapter gives insight into the background of chocolate manufacture, the key ingredients and processes as well as background information on techniques to be used in the following chapters*

## 2 Introduction

Chocolate has been described as a mysteriously appealing food (Ollivon, 2004). It is unique in the sense that it is solid at room temperature yet melts easily within the mouth. This cooling sensation and flavour release added to the sweetness of modern chocolate contributes to chocolate's popularity.

Chocolate production involves the creation of a formulation containing cocoa butter, cocoa solids, vegetable fats (optional), sugar, lecithin, and in the case of milk chocolate, milk fat and milk solids. Figure 2.1 shows the composition of a typical milk chocolate that can be purchased in the UK. These substances are mixed together and undergo heating and cooling regimes to produce a product that is enjoyed worldwide by millions.

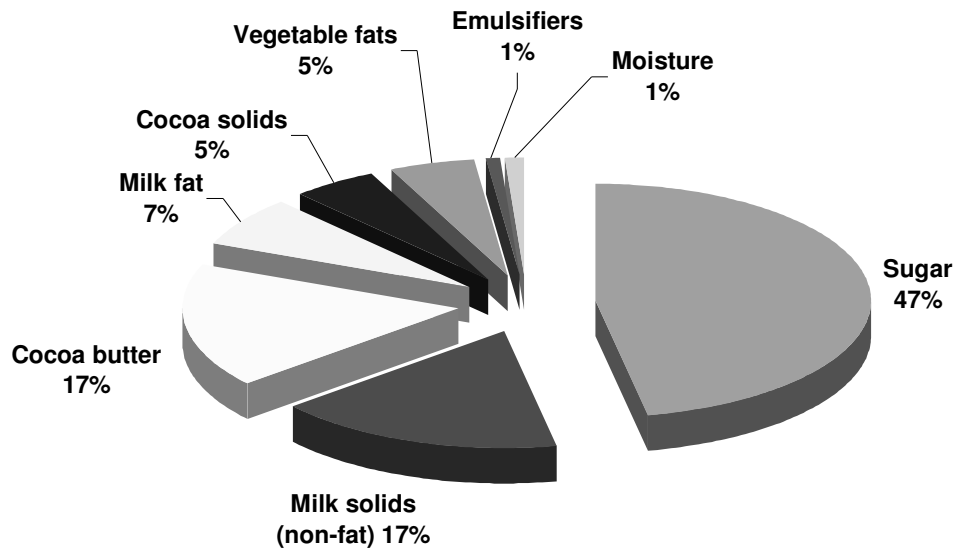


**Figure 2.1 Typical composition of a British milk chocolate**

### 2.1 History of chocolate

The earliest known cocoa plantations are believed to have been established by



the Maya in 600 A.D and the Aztecs of Mexico and the Inca of Peru are also known to have had cocoa plantations at the time when the Europeans discovered America (Beckett, 2000). The beans were highly prized and used a currency as well as to produce a rather astringent, thick, fatty and spicy unpleasant drink called 'chocolatl'. It was believed that this drink conferred mysterious powers to the drinker (Whymper, 1912). The Aztec Emperor Montezuma was said to consume 50 jars of this drink daily.

Cocoa was brought to Spain in the 16<sup>th</sup> century after Don Cortez conquered Mexico. Sugar was added to the 'chocolatl' drink to atone the bitterness of the drink. A century later, the chocolate drink now also mixed with milk was introduced to the rest of Europe and was regarded as an expensive luxury.

In the 1800s, solid chocolate became popular, with the invention of moulding processes. Mechanical grinders crushed cocoa beans to a fine powder that could be heated and poured into moulds, forming shapes as it cooled. The Dutchman Van Houten perfected the extraction of cocoa butter from cocoa beans in 1825. This technique enabled the ground cocoa beans and sugar to be added together with the extra fat, producing a palatable chocolate bar without the unpleasant coarse mouthfeel. The technique of eating chocolate however was not perfected until the Victorian times.

In the 1880s, Rudolphe Lindt of Switzerland invented the conching machine, enabling addition of extra cocoa butter during chocolate manufacture, to make it smoother, glossier and better tasting. The manufacture of milk chocolate was

perfected in 1875, by the Swiss Daniel Peter using Henri Nestlé's recently-invented condensed milk was easy to mix with cocoa paste, unlike liquid milk. In the UK, the Cadbury family were mainly responsible for perfecting drinking chocolate and eventually milk chocolate bars. Cadbury's 'Dairy Milk', first developed in 1905, is the UK's most popular chocolate bar.

## **2.2 Modern day chocolate**

From Figure 2.1, it can be seen that the major component of milk chocolate is sugar followed by cocoa butter and milk fats. For the purpose of this review, the only ingredient to be elaborated on will be cocoa butter as most of the chemical and physical properties of chocolate are related directly to the nature of cocoa butter. The properties of cocoa butter have drawn the attention of numerous investigators, owing to the significance they assume in confectionery production and storage.

### **2.2.1 Cocoa Butter: Structure and composition**

The physical properties of chocolate are influenced by the polymorphism of cocoa butter, which is the major component of solid fat present in chocolate. Hence, the control of the molecular structure and polymorphic forms of this fat is particularly important in the manufacture of chocolate.

Cocoa butter, which amounts to 25-36 % in finished dark chocolate, is responsible for the smooth texture, contraction, flavour release, and gloss of

chocolate. It is a yellow fat that shows brittleness below 20 °C, begins softening at 30 to 32 °C, and exhibits a sharp complete melting below body temperature (Schlichter-Aronhime and Garti, 1988). This quick meltdown in a narrow range of temperature results in a cool sensation, which is a very appreciated organoleptic feature. Although cocoa butter is a tasteless fat, its melting behaviour is not only responsible for mouth feel but also for flavour release from cocoa powder, which is dispersed within the fat. Since fat constitutes the main phase in chocolate and binds together other ingredients, its physical properties will determine the acceptability and quality of confectionery products.

Cocoa butter is a mixture of triacylglycerols and trace compounds. It is a simple fat in terms of the number of constituent triacylglycerols in its make up. Three main triacylglycerols POP, StOSt and POSt (where O = oleic acid, P = palmitic acid and St = stearic acid) make up approximately 83% of the cocoa butter fat components. Both climate and agriculture impact on the relative distribution of the triglycerides, which make up cocoa butter fat (Berbert and Alvim, 1972, Berbert, 1976, Lehrian, Keeney and Butler, 1980, Chaiseri and Dimick, 1989) .

### **2.3 Polymorphism**

Polymorphism in triglycerides has been known to exist for over 150 years with the first work being carried out by Duffy, (1853). Polymorphism is defined as the ability of a substance to exist in more than one crystalline form under

thermodynamically different conditions (Chapman, 1956, Chapman, 1962, Hernqvist, 1984, Sato et al., 1989). Due to their structural make up, triacylglycerols (TAGs) can exist in more than one crystalline form and therefore exhibit polymorphism. Wille and Lutton, (1966) demonstrated this phenomenon in cocoa butter by X-ray diffraction techniques.

### **2.3.1 Packing behaviour and identification of polymorphs**

X-ray diffraction is commonly used to ascertain the identity of polymorphs. For each polymorph to produce a different X-ray pattern there must be an underlying difference in their structure. The crystallisation characteristic must be due to the packing of the hydrocarbon chains. Polymorphism of most fats is based around three main forms:  $\alpha$ ,  $\beta'$  and  $\beta$ . This nomenclature is based on work carried out using X-ray diffraction (Carter and Malkin, 1939, Malkin and Meara, 1939)

TAG molecules can be considered as three-legged molecules that can pack with the acyl chains (legs) in one of two configurations, neither of which involves all the chains packing alongside each other. They can pack into a 'chair' configuration (Chapman, 1962, Garti and Sato, 1988) where the acyl chain in the 2 position is alongside the chain on either the 1 or 3 positions. Alternatively, a 'tuning fork' configuration can be adopted where the acyl chain in the 2 position is alone and the chains in the 1 and 3 positions pack along side each other. This configuration is shown in Figure 2.2.

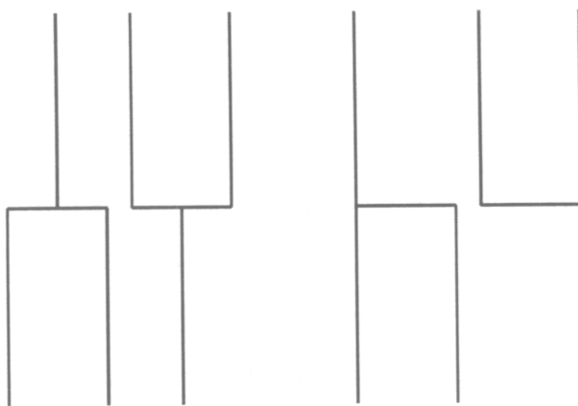


**Figure 2.2: Triacylglycerol molecule in the tuning fork configuration**

Either configuration naturally packs in a chair-like manner. The stacking of these chairs can be either in a double (Figure 2.3) or triple (Figure 2.4) chain structure and these stack side by side in crystal planes, sometimes at an angle.

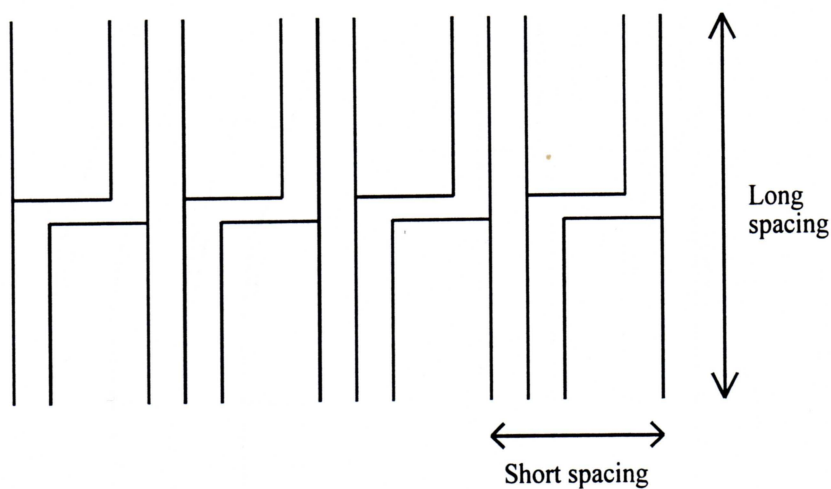


**Figure 2.3: Schematic representation of double chain structure**

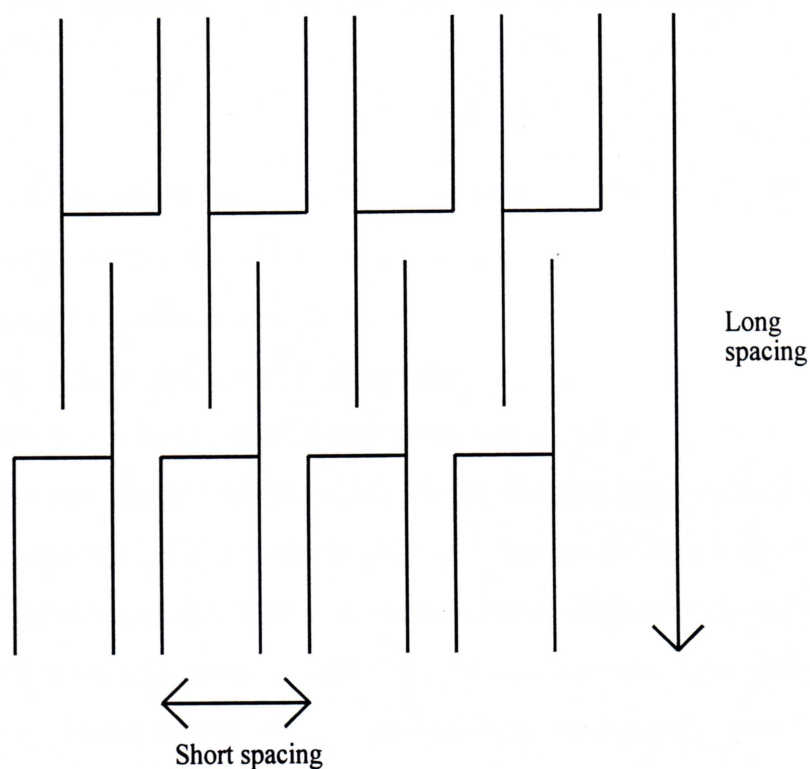


**Figure 2.4: Schematic representation of triple chain structure**

The differences in the polymorphs are most apparent from a top view of these planes which show the sub-cell structure as shown in Figure 2.5. These structures can be identified by X-ray diffraction patterns where the long spacings give information on the repeat distance between crystal planes (chain length packing) and the short spacings give information on subcell structure (interchain distances) ((Hernqvist, 1988) . These interchain distances depend on how the chains pack together and are complicated by the ‘zigzag’ arrangement of successive carbon atoms in the aliphatic chains. Closer packing is achieved when the zigzag of adjacent chains are in step with each other (parallel) as opposed to out of step (perpendicular) (Hernqvist, 1988, Larsson, 1994).

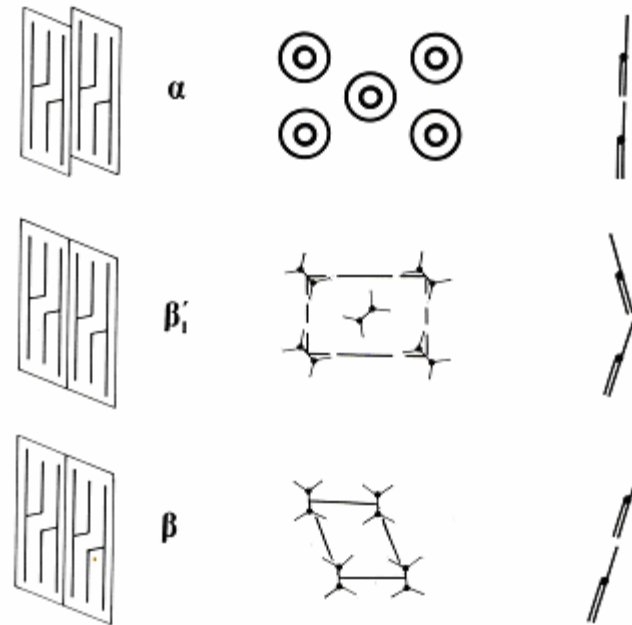


**Figure 2.5: Subcell structures of the three most common polymorphs in triacylglycerols (from Hernqvist, 1988)**

The main features of the three main polymorphic forms are as follows (from (Larsson, 1994, Timms, 2003) :

- The  $\alpha$ -form is characterised by one strong spacing line in the X-ray diffraction near 0.42nm. The chains are arranged in a hexagonal structure (H) with no angle of tilt and are far apart enough for the zigzag nature of the chains not to influence packing.
- The  $\beta'$  form is characterised by two strong spacings at about 0.38 and 0.42 nm. The chain packing is orthorhombic and perpendicular ( $O\perp$ ) which means that the adjacent chains cannot pack closely. The chains have a tilt angle between  $50^\circ$  and  $70^\circ$ .
- The  $\beta$  form is characterised by a strong spacing at about 0.46nm and a number of other strong lines between 0.36 and 0.39nm. This is the densest form and has a triclinic chain packing ( $T_{//}$ ), in which the chains

pack snugly together. The chains normally have a tilt angle between  $50^\circ$  and  $70^\circ$ .

In addition, the  $\beta$ -form can exist in double or triple chain structures and are termed  $\beta_2$  and  $\beta_3$ , respectively. An example of these chains is shown in Figure 2.6 (from Timms, 1984)

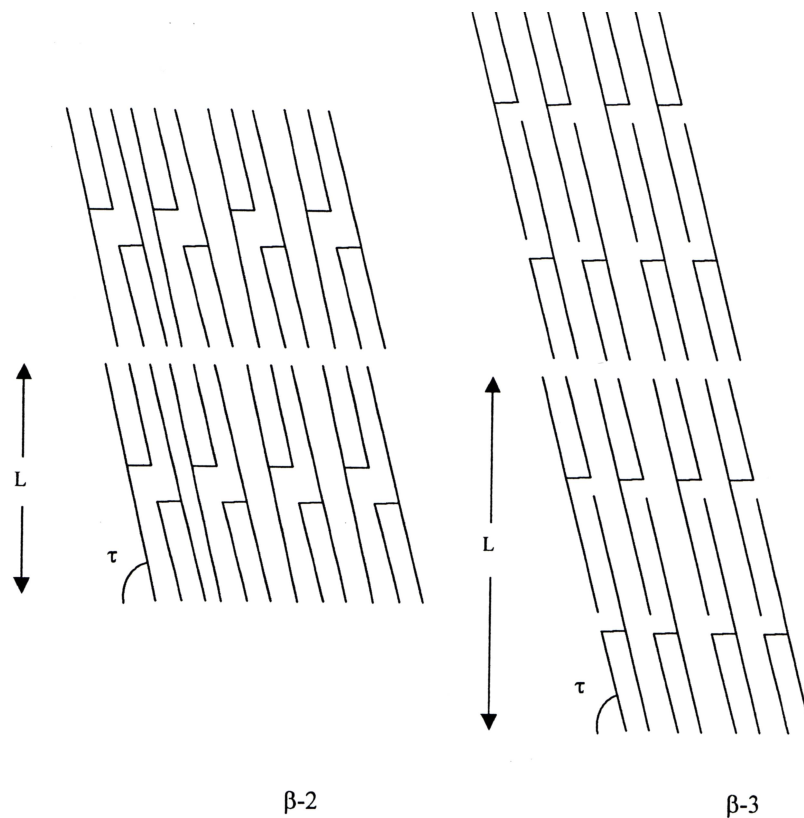


**Figure 2.6: Schematic example of the  $\beta$  form in the double and triple chain arrangement ( $\tau$  is the tilt angle)**

### 2.3.2 Crystallisation behaviour of polymorphs

There are 2 types of polymorphism: enantiotropy and monotropy ((Jovanovic, Karlovic and Jakovljevic, 1995) ). Enantiotropic polymorphism is characterised by a greater number of stable crystal forms in the given temperature range, i.e., the transformations of the crystal forms are reversible. In monotropic



polymorphism only one stable crystal form exists while the transformation of the other crystal forms to the only stable form is irreversible. According to Jovanovic, Karlovic and Jakovljevic, (1995), in vegetable oils and fats, three polymorphic forms predominate ( $\alpha$ ,  $\beta'$ ,  $\beta$ ), the formation of which depend on crystallisation conditions, i.e., degree of cooling below the saturation temperature as shown in Figure 2.7

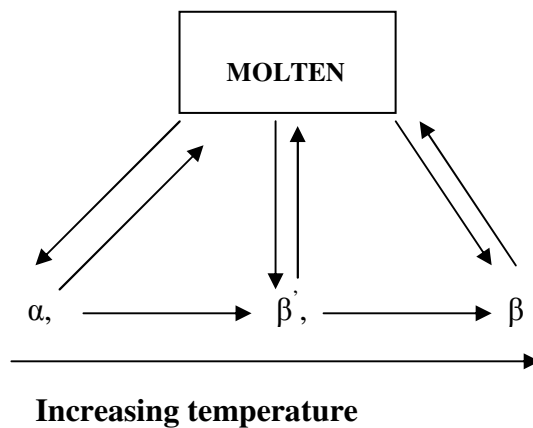


**Figure 2.7: Pathway for polymorphic transformations in fats**

Melted liquid fat can directly transform into any polymorphic form but the transformation rate is different. Every polymorphic form can transform into a liquid state. The formed polymorph may transform into another form only following the pathway  $\alpha \rightarrow \beta' \rightarrow \beta$ , which means that the process is irreversible and therefore polymorphism in fats is monotropic. As the  $\beta$  form is the most stable form with the highest melting point, cocoa butter stored for a long period of time consists of only this crystalline form.

The relative stability of two polymorphs and the driving force for transformations between them at constant temperature and pressure are determined by their respective Gibbs free energies ( $G$ ). The polymorph which

has the lowest Gibbs free energy is the most stable. Figure 2.8 shows the Gibbs energy relationship between the polymorphs. As can be seen, the transition of the molecules from the liquid state to the solid state (which is more energetically stable), has to go through unstable transitory states that require overcoming energy barriers. The phase with the lowest melting free energy ( $\Delta G_f$ ) i.e. the least stable phase, also has the lowest energy barrier,  $\Delta G^*$ , to form from the liquid.

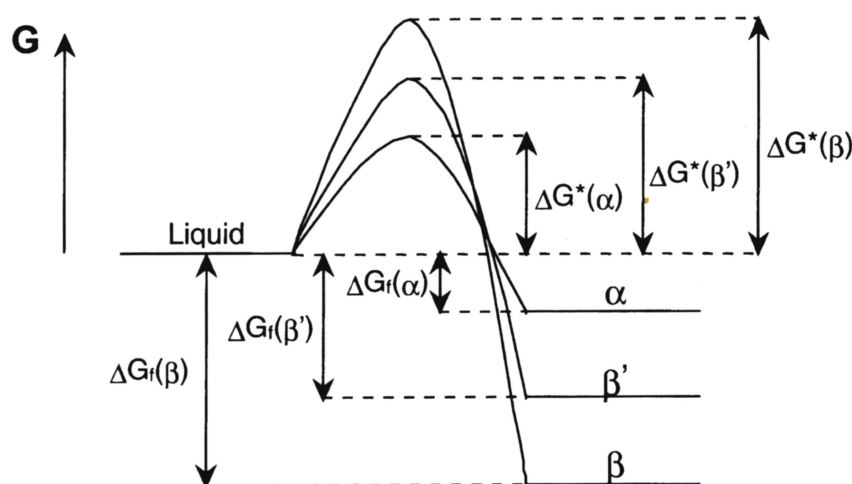


**Figure 2.8: Schematics of the free energy of fusion ( $\Delta G_f$ ) and of activation ( $\Delta G^*$ ) for the three polymorphic phases of a TAG, at given conditions (P, T) below their temperature of fusion (from Rousset, 2002 )**

Due to its monotropic nature, the Gibbs free energy values are the largest for the  $\alpha$ -form (the least dense crystal packing), intermediate for the  $\beta'$ -form and the smallest for the  $\beta$ -form (the most dense packing). The transformation pathways among the three main polymorphs (shown in Figure 2.7) can be summarised as follows (from Sato, 1989)

- The three polymorphs can all be directly crystallised from melt
- Although any polymorph can be returned to the liquid phase by raising

the temperature above its melting point, interpolymorphic transformations are irreversible (i.e.  $\beta$  cannot transform back to  $\beta'$  and  $\beta'$  cannot revert back to  $\alpha$ ).

- Two different modes of transformations are possible
  - i. Transformations within the solid state and,
  - ii. Recrystallisation of the more stable forms after the less stable forms have melted. This is termed melt-mediated transformation (Sato, 1989)
- It has been found by Gibon, Durant and Deroanne, (1986), Lavigne, Bourgaux and Ollivon, (1993) and Ueno et al., (1997) that a liquid crystalline phase exists as an intermediate phase and occurs before the crystallisation of the polymorphic crystals or during melt-mediated transformations.

### **2.3.3 Polymorphism of cocoa butter**

Cocoa butter polymorphism has been extensively studied but contradictions over the number of forms and their characteristics still exist. As early as 1900, it was reported that cocoa butter had various melting points. Subsequent research carried out then showed that cocoa butter could crystallize in a stable and at least one unstable form (quoting from Vaeck, 1951). In the late 1920's, work carried out by Abers, (1928) showed that three polymorphic forms of cocoa butter were known to exist with melting temperatures of 24 °C, 29°C and 34°C. More than twenty years later a study was conducted that described cocoa butter as having four polymorphic forms known as  $\gamma$ ,  $\alpha$ ,  $\beta'$ , and  $\beta$  with

melting points at 17°C, 23°C, 28°C and 35°C. Duck, (1958) later identified a fifth form with a melting temperature of 33°C.

The development of X-ray techniques allowed for a more detailed analysis and the

identification of six polymorphic forms of cocoa butter. (Wille and Lutton, 1966) carried out a comprehensive study on cocoa butter using different cooling temperatures and X-ray diffraction and determined the existence of the following polymorphic forms in order of increasing stability: I (sub- $\alpha$  or  $\gamma$ ), II ( $\alpha$ ), III, IV ( $\beta$ ), V ( $\beta$ ) and VI .

X-ray diffraction data collected for the polymorphic forms observed by Wille and Lutton, (1966) have been confirmed by other research groups (Chapman, Akehurst and Wright, 1971; Lovegren, Gray and Feuge, 1976a, Lovegren, Gray and Feuge, 1976b). These six forms have also been confirmed using DSC (Chapman, Akehurst and Wright, 1971; Huyghebaert and Hendrickx, 1971, Lovegren, Gray and Feuge, 1976a, Lovegren, Gray and Feuge, 1976b) . Chapman, Akehurst and Wright, (1971) however, found the melting temperatures of each form to be several degrees lower than previously reported.

Even though six distinctive polymorphic forms of cocoa butter have been observed by several research groups, others have recognized only four forms (Vaeck, 1960, Merken and Vaeck, 1980). It has been proposed that Form III is merely a mixture of variable proportions of Forms II and IV. Form III has never been isolated in its pure state and its formation conditions are quite

similar to that of Form IV (Merken and Vaeck, 1980). Schlichter-Aronhime, Sarig and Garti, (1988) reported that cocoa butter does not behave differently than a pure triacylglycerol and consists mainly of three possible polymorphic forms. The fact that six polymorphs have been detected is related to the fact that complex mixtures of saturated and unsaturated triacylglycerols are present. Therefore, form III can be interpreted as being a mixture of two solid phases of polymorph II and IV (Schlichter-Aronhime, Sarig and Garti, 1988). However, some researchers may not have observed Form III because the samples were not tempered in order to develop a particular form and only one sample of cocoa butter was used (Timms, 1984). It has been suggested that Form VI is not a distinctive polymorph but is identical to Form V only lacking the liquid triacylglycerol fraction. Form VI was determined to be simply a separation of the solid solution Form V into two distinct phases (Merken and Vaeck, 1980). It is possible that Merken and Vaeck, (1980) were unable to detect form VI because they failed to provide the long tempering time required for its formation as shown in previous studies.

The determination of the various polymorphic forms of cocoa butter is one of the most controversial areas in confectionery science. There is not only a discrepancy in the number of polymorphic forms but also in the nomenclature used to classify these various forms. Table 2.1 shows the classification of cocoa butter polymorphs by eminent workers and the controversy in nomenclature. Techniques such as microscopy, X-ray diffraction and differential scanning calorimetry have been used to characterise the polymorphs. The Wille & Lutton nomenclature using roman numerals is best known in the confectionery industry and will be used in this report.

**Table 2.1: Classification and melting temperature (°C) of cocoa butter polymorphs**

(Vaeck, 1951)	(Vaeck, 1960)	(Duck, 1964)	(Wille and Lutton, 1966)	(Chapman, Akehurst and Wright, 1971)	(Lovegren, Gray and Feuge, 1976a)
$\gamma$ 18.0	$\gamma$ 17.0	$\gamma$ 18.0	I 17.3	I	VI 13.0
$\alpha$ 23.5	$\alpha$ 21-24	$\alpha$ 23.5	II 23.3	II	V 20.0
			III 25.5	III	IV 23.0
$\beta'$ 28.0	$\beta'$ 28	$\beta'$ 28.0	IV 27.5	IV 25.6	III 25.0
$\beta$ 34.5	$\beta$ 34-35	$\beta'$ 33.0	V 33.8	V 30.8	II 30.0
		$\beta$ 34.4	VI 36.3	VI 32.2	I 33.5

For chocolate, Form V is the most desirable as it gives rise to better demoulding, desirable gloss and snap at room temperature. Also Form V melts just below body temperature, which is highly desirable. Undesirable polymorphic forms, which are generally unstable such as Forms III and IV, would give rise to poor quality chocolate. It is therefore vital that good polymorphic control of cocoa butter is maintained in chocolate production.

## 2.4 Modern day chocolate production

The formation of crystalline particles from a liquid phase is an industrial process that involves detailed and elaborate production processes to control the mechanisms of the crystallisation process. Chocolate manufacture is a

relatively complex process as illustrated in Figure 2.9. Each stage must be carefully monitored, in particular the conching stage and tempering. Conching is the last process in the manufacture of bulk chocolate. This process involves reducing particle size, viscosity and removing unwanted volatile flavours. It is a crucial step for the development of the full desirable chocolate flavour and the conversion of the powdery, crumbly refined product into a flowable, smooth mixture.

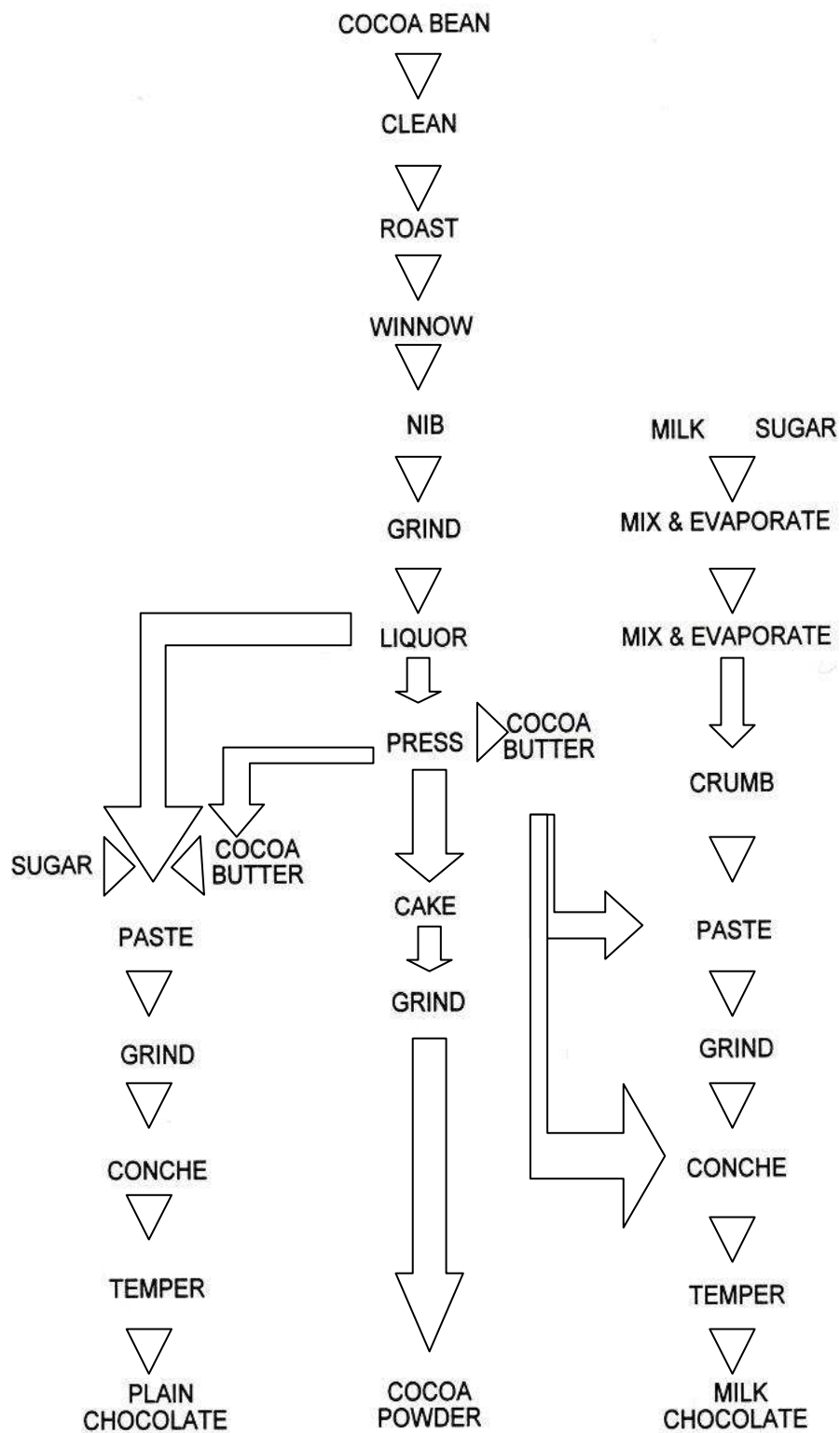


**Figure 2.9: Industrial chocolate manufacture**



### **2.4.1 Industrial tempering**

In order to produce high quality chocolate with its desirable gloss and snap, it is essential to subject the chocolate mass to the process of tempering. Tempering is a complex process which in simple terms involves mixing and cooling the liquid chocolate under carefully controlled conditions to ensure that the fat phase in the chocolate composed principally of cocoa butter, crystallises in its most desirable form, i.e. the Form V or  $\beta_2$ -modification (Sato and Koyano, 2001). The importance of tempering has been reviewed by many workers most recently by Cebula, Dilley and Smith, (1991), Jovanovic, Karlovic and Jakovljevic, (1995), Loisel et al., (1997), Nelson, (1999a) and Stapley, Tewkesbury and Fryer, (1999) .

The process of tempering consists of cooling the chocolate down under continuous shear to produce a sufficient number of stable fat seed crystals and distribute these throughout the liquid chocolate mass (Hachiya, Koyano and Sato, 1989). Tempered chocolate typically contains about 3- 8% of cocoa butter crystals in the whole chocolate mass (Minifie, 1989) and the tempering quality is related to the quantity of stable crystalline seed present in the fat phase (Adenier, Chaveron and Ollivon, 1984). A good temper has been described by Seguine, (1991) 'as consisting of the largest number of the smallest possible crystals in the right crystalline form'. Under these conditions, viscosity of the chocolate is the lowest and the large number of nuclei assists in further crystal growth in the correct form. This results in a chocolate which can flow easily, release entrapped air bubbles and produce uniform coating. It will

also set readily in air or cooling tunnels. It will also have a good gloss, good mould release and maximum contraction during cooling and solidification. Well-tempered chocolate shows better resistance to fat migration, softening and bloom appearance.

The most commonly used method of tempering involves the following steps (Talbot, 1999):

- Complete melting
- Cooling to the point of crystallisation
- Crystallisation
- Melting of unstable crystals

Figure 2.10 shows a typical tempering profile of milk chocolate.

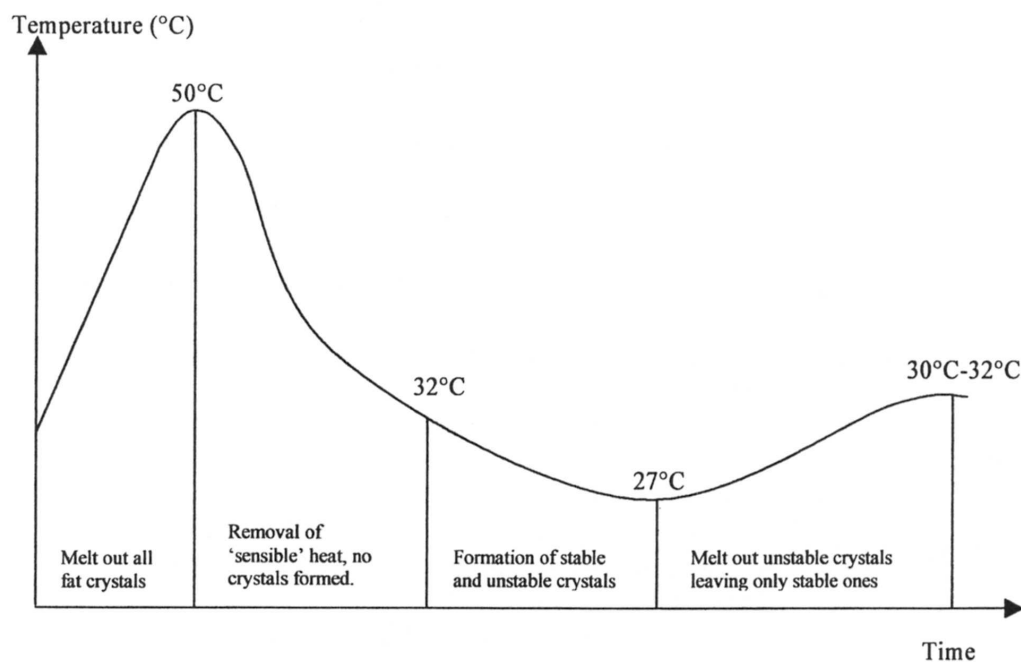


**Figure 2.10: A typical tempering sequence (Talbot, 1999)**

Chocolate has to be heated to at least 50 °C to ensure complete melting of the fat thus avoiding any 'memory effect' of the cocoa butter (van Langevelde et

al., 2001a). The molten chocolate is rapidly cooled to a minimum temperature depending on its composition (normally between 26 and 29 °C) and mixed to induce pre-crystallisation. This is very important as it is necessary to produce a large number of small seed crystals in the highest possible melting point in the fat phase of the melted mass. The rapid crystallisation also causes the formation of metastable forms. This is due to the extensive supercooling, which is the driving force for nucleation and crystal growth in fat. Metastable forms such as Forms III and IV have lower free energies of crystallisation than Form V and hence crystallise more rapidly. However these must be eliminated as they cause poor demoulding and induce fat bloom.

The chocolate is then heated to around 30 °C (higher for plain chocolate) to melt the unstable crystals and create a uniform sized crystal population of Form V nuclei. At the end of the tempering process, small stable crystals uniformly distributed in the chocolate mass act as seed to promote growth and stabilisation of the Form V crystals during cooling. The effect of shear on the generation of Form V crystals has been studied by MacMillan et al., (2002) and they concluded that the absence of shear generates the formation of Form IV nuclei at the expense of Form V, resulting in the formation of chocolate which will easily bloom and is of unsuitable quality.

Highly sophisticated machinery has been developed for this process and the control of it is one of the skills of the chocolatier. In chocolate manufacturing, careful control of the tempering process is very important. First of all, it significantly influences the rheological properties of chocolate, which

determines the workability of chocolate (Nelson, 1999b). Secondly, the physical properties of the end product such as snap, gloss, texture, heat resistance and fat bloom stability are also influenced by the tempering processes (Reade, 1985). Snap is associated with the chocolate's ability to break apart easily and fat bloom stability enables chocolate to be stored without the appearance of 'whitish mould' forming on the surface of the chocolate. Bloom is mainly due to poor storage conditions or poor manufacture of the chocolate enabling formation of undesirable crystals. It is normally associated with the formation of Form VI crystals.

The degree of temper of chocolate can be assessed by obtaining a temperature-time curve for the chocolate while it is cooling. An instrument called a tempermeter can be used to obtain such curves. The concept of the tempermeter and the results obtained from it is further elaborated in Chapter 3. After being tempered, the chocolate is further cooled in either moulds or on top of fillings.

#### **2.4.2 Cooling processes**

Tempered commercial chocolate is then moulded and cooled so that subsequent crystal growth occurs upon the existing seed crystals. Moulding involves depositing a small amount of liquid chocolate into a mould. The mould should be at a similar temperature to the chocolate. If the mould temperature is too high the chocolate may de-temper, if too cold it may set insufficiently. Once in the mould, it is shaken to remove any bubbles and then

cooled. The process of pouring the tempered chocolate over the solid centre of the product is known as Enrobing.

Cooling is a combination of conduction, convection and radiation. Every chocolate has a natural rate of solidification and the best results are obtained when cooling is directed in such a way that the chocolate solidifies at this rate, neither too fast nor too slow (Reade, 1985). The natural rate is dependent partly on the fat blend in the chocolate and also on the style and the degree of temper of that sample. According to Nelson, (1999a), to cool and solidify chocolate, it must first be allowed to cool gently, in either radiant or gently moving air conditions. Chocolate leaving the enrober must also not be subjected to fierce cooling because this has the effect of drawing the cocoa butter up the surface of the product, quickly resulting in fat bloom. The second stage of cooling may be forced by cooling at mild temperatures ( $\sim 13^{\circ}\text{C}$ ), or by convection/ radiation. Finally a slight warming of the air is used to reduce the possibility of condensation forming on the chocolate once it reaches the warmer packing area.

To increase the cooling rate of chocolate, cooling tunnels are employed, cooling the chocolate in 10 to 30 minutes depending on the type of cooling tunnel used and the rate of heat removal. Convection is the main cooling effect used in the cooling tunnels in which air is blown over the chocolate at varying speeds. The speed is slow initially, as high velocities will cause uneven solidification and eventually leading to fat bloom. The air velocity is then increased and the temperature lowered considerably to encourage convective heat removal in the warmer packing area. According to Willcocks et al.,

(2002), conventional cooling can be considered to operate through a crystal growth mechanism where crystallisation is taking place at a number of nuclei sites which have been generated through tempering and grown in size. The cooling tunnel operating conditions (10-20°C) provides a driving force for crystallisation through undercooling. However, since the actual cooling rate of chocolate is low given the relatively low heat transfer rates used, the conditions favour crystal growth.

The moulding of chocolate is technically challenging as it is difficult to achieve the required Form V crystals by simple cooling of chocolate. If the cooling rate is excessive other polymorphs can nucleate and grow during moulding. (Tewkesbury, Stapley and Fryer, 2000) developed a computational model to predict the temperature in the mould as a function of space and time. Temperature control is crucial to the moulding process and their work was intended to study the spatial and temporal variation of temperature in chocolate moulds. It was discovered that crystallisation caused a significant reduction in the cooling rate resulting in the evolution of latent heat. However, the major problem in modelling the cooling in crystallising systems occurs in predicting this latent heat production. The study confirmed previous work that the effective specific heat of chocolate is a strong function of cooling rate and process history. This was achieved using both tempered and untempered chocolate, where different cooling behaviour was observed. Cooling rates were found to be in the range of 0.5-2 °C.min<sup>-1</sup>. It was concluded that overall this study showed that it is possible to develop a mathematical model that can accurately represent the behaviour of chocolate and fillings in commercial manufacture.

### **2.4.3 Rapid cooling techniques**

Given the huge demand of chocolate, the chocolate manufacturing industry is continuously trying to improve existing production processes or invent new methods for manufacturing. The requirements for cooling tunnels consuming lots of time and space are disadvantageous in the conventional process. Hence, quicker and simpler processes for the setting of high quality chocolate has been the driving force for the invention of new processes involving rapid cooling rates. Several patents have been published recently making use of rapid to aggressive cooling regimes to set chocolate (Aasted, 1993, Demmer et al., 2002, Willcocks et al., 2002). The patent to Demmer et al (2002) describes a process by which liquid chocolate mass is subjected to tempering, super-cooling and press-forming through an extrusion die and cooled stamps. Willcocks et al., (2002) make use of rapid cooling using increased convective heat transfer coefficients and/or low operating temperatures. The Frozen Cone® process, patented by Aasted, is described below.

#### *2.4.3.1 The Frozen Cone technique*

The Frozen Cone® method is designed to reduce the complexity of shell moulding and is becoming increasingly popular with confectionery manufacturers. The principle is illustrated in Figure 2.11.

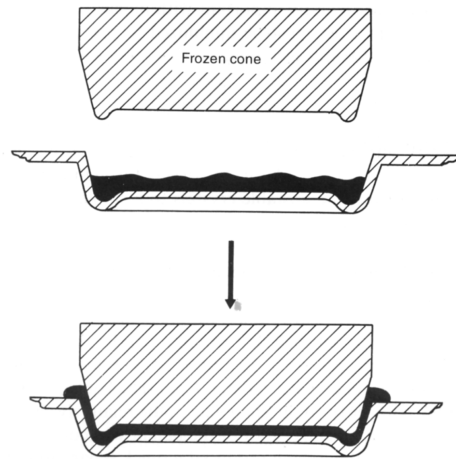


**Figure 2.11: The Frozen cone technique**

The process starts by pouring sufficient tempered chocolate into the mould to make the shell and to allow for small excess (Beckett, 1999). The excess is required to ensure that the chocolate reaches the top of the mould all the way round. A frozen plunger, in the shape of the sweet is then inserted into the chocolate. The liquid chocolate is thus squeezed up around the plunger and forms the shell. The Aasted system operates at temperatures between  $-15^{\circ}\text{C}$  to  $-21^{\circ}\text{C}$  and it takes only about 2seconds for the chocolate shell to be hard enough for the plunger to be removed.

According to conventional literature on the tempering and cooling of chocolate, it is expected that the very cold temperature of the plunger would cause the fat to set in its unstable crystalline form and so rapidly bloom. However, this does not seem to be the case, with even the inside of the products remaining glossy after long periods (Beckett, 1999). There is no suitable explanation to date to explain this observation. Part of the explanation according to Beckett, (1999) may lie in the fact that only the surface reaches the very low temperature due to the short contact time. The bulk fat remains



liquid and has to lose its latent and some specific heat in order to set. This heat must pass through the surface made by the plunger because the mould if made of plastic will be an insulator. In passing through this surface the temperature will rise and convert the unstable crystals to a stable form.

## **2.5 Techniques used to study polymorphism**

### **2.5.1 X-ray diffraction: Technique and Principles**

X-ray diffraction (XRD) is a very important tool for crystal phase identification and molecular structure determination. X-ray powder diffraction is ideally suited for the characterization and identification of the extent of polycrystalline phases in mixed amorphous - crystalline systems. The powder XRD technique, which is important for application to most foods, allows the presence of even small crystalline regions to be identified in complex matrices since results are independent of the presence of amorphous or liquid regions. X-ray diffraction has been extensively used in the study of confectionery fats and triacylglycerols. This technique was first used to determine the structure of triacylglycerols by Carter and Malkin, (1939) and Malkin and Meara, (1939) began work by looking at the structures of triacylglycerols using X-ray diffraction. The work of Wille and Lutton, (1966) is used as reference when discussing the structure of cocoa butter. Temperature controlled X-ray was used by Riiner, (1970) and Chapman, Akehurst and Wright, (1971) to investigate the changes in the polymorphism of fats with temperature. Since then major progress has been achieved using X-ray diffraction. Synchrotron X-ray diffraction uses a very powerful beam to take a complete and detailed

snapshot of a sample within a few seconds. Several authors have used this powerful technique to study polymorphism and crystallisation kinetics in various fat systems (Kellens et al., 1991, Keller et al., 1996, Loisel et al., 1998, Roberts et al., 1999, Sato, 1999, Sato, Ueno and Yano, 1999, Sato, 2001, Takeuchi et al., 2002, Higami et al., 2003, Mazzanti et al., 2003, Takeuchi, Ueno and Sato, 2003, Ueno et al., 2003, Mykhaylyk et al., 2004, Kalnin et al., 2005) . Coupling of synchrotron X-ray and DSC has been used by Loisel et al., (1998) and Ollivon et al., (2001) to allow simultaneous examination of the thermal behaviours of a fat.

### **2.5.2 Principles of X-ray diffraction**

X-ray diffraction is a very important tool for the crystal phase identification and molecular structural determination. The technique involves impinging X-rays onto a single crystal or polycrystalline material and analysing the diffraction patterns emitted. The emitted diffraction pattern then acts like a fingerprint and enables the characterisation of specific crystalline forms. XRD can be used to elucidate phase transformations and the specific arrangements of atoms in crystal structures. For a more detailed information on the principles of XRD the works of (Klug and Alexander, 1974) can be used as reference.

#### *2.5.2.1 X-ray scattering*

X-rays are short-wavelength, high-energy beams of electromagnetic radiation of wavelength of about 1 Angstrom ( $\text{\AA}$ ). The X-rays used in diffraction are generated when high-energy electrons bombard a metal target. The metal most commonly used is copper; whose characteristic wavelength for the K radiation

is  $1.5418 \text{ \AA}$ . If X-rays strike a regularly spaced row of atoms, the waves of the X-rays interact with the atoms. This causes each atom to produce a series of spherical waves to emanate out, each with the same frequency and wavelength (Klug and Alexander, 1974). These waves interfere with each other and cause regions of constructive and destructive interference. According to the same authors, all the points of intersection of the two sets of concentric arcs are points of constructive interference and are diffraction maxima. The waves are out of phase at points in between the intersections and this leads to various degrees of destructive interference. Figure 2.12 below is a schematic example of such an interference, where the wave crests and troughs from 2 atoms are shown (from Klug and Alexander, 1974).

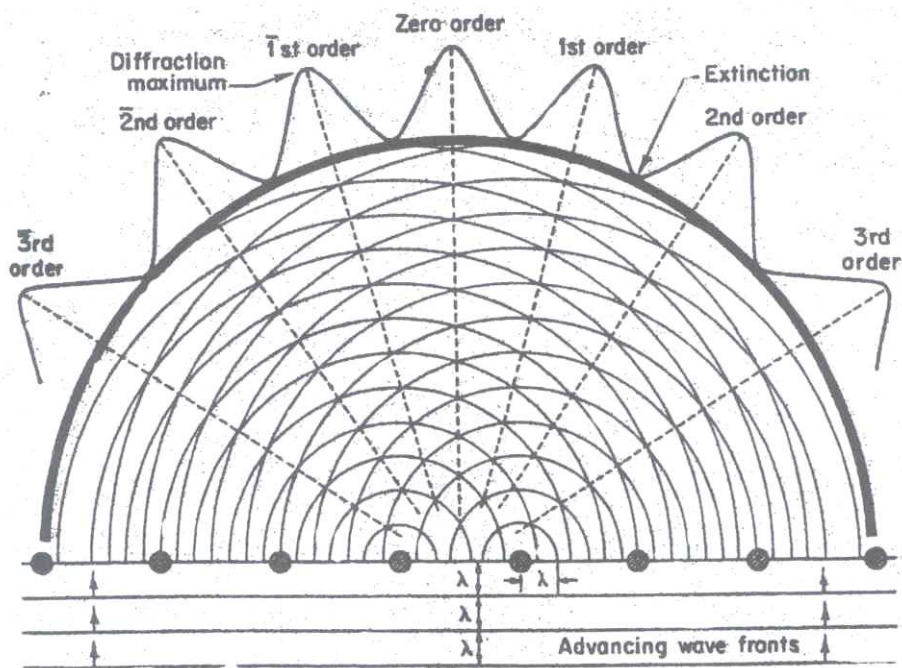


**Figure 2.12: Schematic diagram of scattering by a regularly spaced row of atoms (from Klug and Alexander, 1974)**

The diffraction order can also be calculated from the wave crest difference. When scattering from the two atoms is perpendicular to the original wave, it is

said to be ‘in-phase’ and gives rise to a zero order diffracted beam (Klug and Alexander, 1974). The first order diffracted beam is a constructive wave in which the crest intersections have a phase difference of one unit of the scattering wavelength. If the crest intersections have a difference of 2 units, then this results in a second order diffracted beam. This goes on and on to the  $n$ th-order. This is also shown in Figure 2.12

#### 2.5.2.2 Bragg's Law

Bragg's Law, which is shown in Equation 1, describes how the diffraction occurs.

$$n\lambda = 2d \sin \theta \quad \text{Equation 1}$$

Where  $n$  is an integer,  $\lambda$  is the wavelength of the X-rays,  $d$  is the interplanar spacing generating the diffraction and  $\theta$  is the diffraction angle.

Figure 2.13 demonstrates the geometry of Bragg's Law.

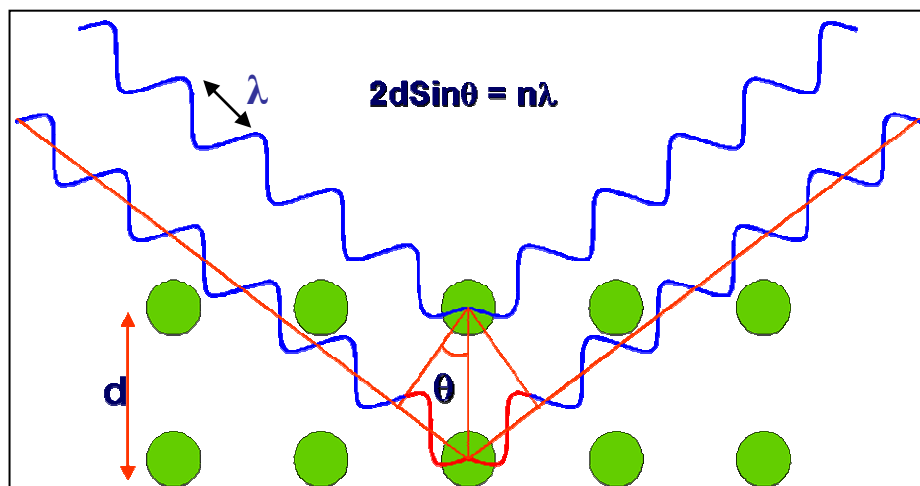


**Figure 2.13: The geometry of the Bragg reflection analogy (Alexander, 1969).**

The figure shows X-rays of wavelength  $\lambda$  striking at angle  $\theta$  on planes, separated by distance  $d$ . X-rays are reflected (diffracted) at this same angle  $\theta$  with these planes. The figure illustrates the case where  $n = 1$ , which is referred to as the reflection of first order from the given planes. The value of the  $d$ -spacing depends only on the shape of the unit cell. Bragg's Law indicates that each unique  $d$ -spacing diffracts different wavelengths at their own unique diffraction angles (Alexander, 1969) .

The range of angles covered determines the technique of X-ray diffraction. Small angle X-ray scattering (SAXS) involves scattering angles of  $2\theta$  smaller than  $3^\circ$  whereas wide angle scattering (WAXS) deals with  $2\theta$  up to  $180^\circ$ . Only WAXS measurements were performed in this study.

### **2.5.3 Wide angle X-ray diffraction patterns of the polymorphs of cocoa butter**

Figure 2.14, which is taken from data obtained by Wille and Lutton, (1966) shows the wide angle X-ray pattern of the six polymorphs of cocoa butter. The main features of the pattern given by Form I are two strong diffractions peaks at  $2\theta$  angle of  $21.18^\circ$  ( $d = 4.19\text{\AA}$ ) and  $24.02^\circ$  ( $d = 3.70\text{\AA}$ ). For Form II, a single strong diffraction peak is given at  $20.93^\circ$  ( $4.24\text{\AA}$ ) while Form III shows diffraction peaks at  $20.9^\circ$  ( $4.24\text{\AA}$ ),  $20.88^\circ$  ( $4.25\text{\AA}$ ) and  $23.01^\circ$  ( $3.86\text{\AA}$ ). Form IV has two main diffraction peaks at a  $2\theta$  angle of  $20.39^\circ$  ( $4.35\text{\AA}$ ) and  $21.39^\circ$  ( $4.15\text{\AA}$ ). Form V, which is of major interest, shows a very strong sharp peak at

19.36° (4.58 Å) and minor diffractions at 22.31° (3.98 Å), 22.95° (3.87 Å), 23.70° (3.75 Å) and 24.22° (3.67 Å). Finally, Form VI shows a very strong peak at 19.31° (4.59 Å) with other peaks at 21.97° (4.04 Å), 23.01° (3.86 Å) and 24.02° (3.70 Å). This is also summarised in Table 2.2.

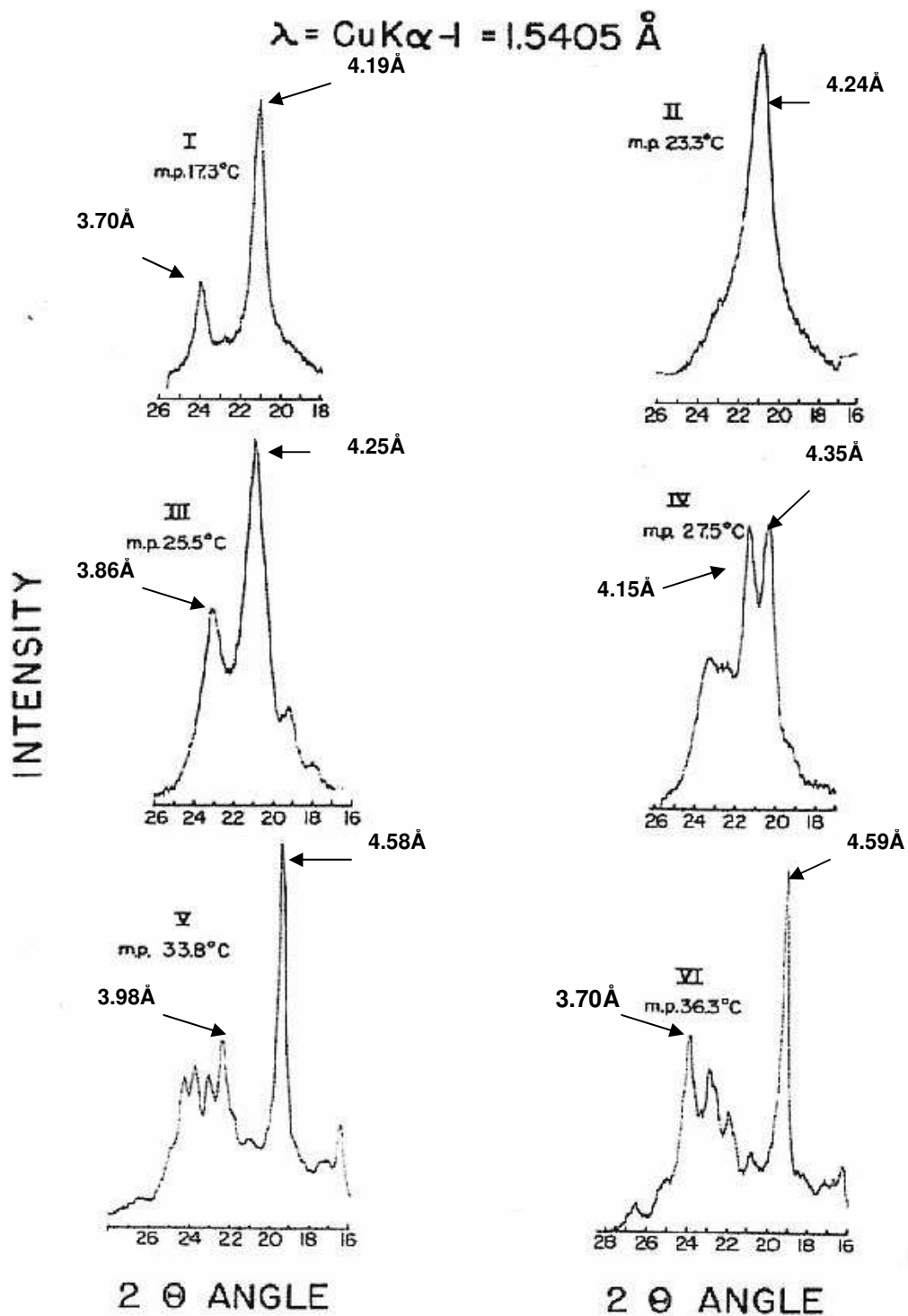


Figure 2.14: X-ray diffraction patterns of the polymorphic forms of cocoa butter. Data take from Wille and Lutton, (1966). Note that the 2 theta angle range is in reverse order.

**Table 2.2: Table showing x-ray diffraction data for the polymorphic forms of cocoa butter**

<b>Polymorphic form</b> (Wille and Lutton, 1966, Larsson, 1994)	<b>Peak at 2<math>\theta</math></b> <b>(Wide angle</b> <b>range)</b>	<b>d- spacing</b> <b>(Å)</b>
Form I ( $\gamma$ form or sub- $\alpha$ )	21.18°	4.19 Å
	24.02°	3.70 Å
Form II ( $\alpha$ )	20.93°	4.24 Å
Form III ( $\beta_2'$ )	20.9°	4.24 Å
	20.88°	4.25 Å
	23.01°	3.86 Å
Form IV ( $\beta_1'$ )	20.39°	4.35 Å
	21.39°	4.15 Å
Form V ( $\beta_2$ )	19.36°	4.58 Å
	22.31°	3.98 Å
	22.95°	3.87 Å
	23.70°	3.75 Å
	24.22°	3.67 Å
Form VI ( $\beta_1$ )	19.31°	4.59 Å
	21.97°	4.04 Å
	23.01°	3.86 Å
	24.02°	3.70 Å

#### 2.5.4 Differential Scanning calorimetry

Differential scanning calorimetry (DSC) is a thermal analysis technique used to measure changes in heat flows associated with material transitions. DSC measurements provide both qualitative and quantitative data on endothermic and exothermic processes. DSC is an important technique for the study of the melting and crystallization behavior of confectionery fats, cocoa butter and pure triacylglycerols and has been extensively used (Adenier, Chaveron and



Ollivon, 1984, Cebula and Smith, 1991, Kellens et al., 1991, Cebula and Smith, 1992, Dimick et al., 1996, Keller et al., 1996, Reddy et al., 1996, Loisel et al., 1998, Stapley, Tewkesbury and Fryer, 1999, Robinson and Sichina, 2000, Spigno, Pagella and De Faveri, 2001, De Graef et al., 2005, Fessas, Signorelli and Schiraldi, 2005) . It provides information on the “quality” of the chocolate, which can be related to processing conditions such as the level of tempering and final cooling rate of the product.

#### 2.5.4.1 Basic principle of the technique

There are two different designs of DSC systems: power compensated and heat flux DSC. These are illustrated in Figure 2.15.

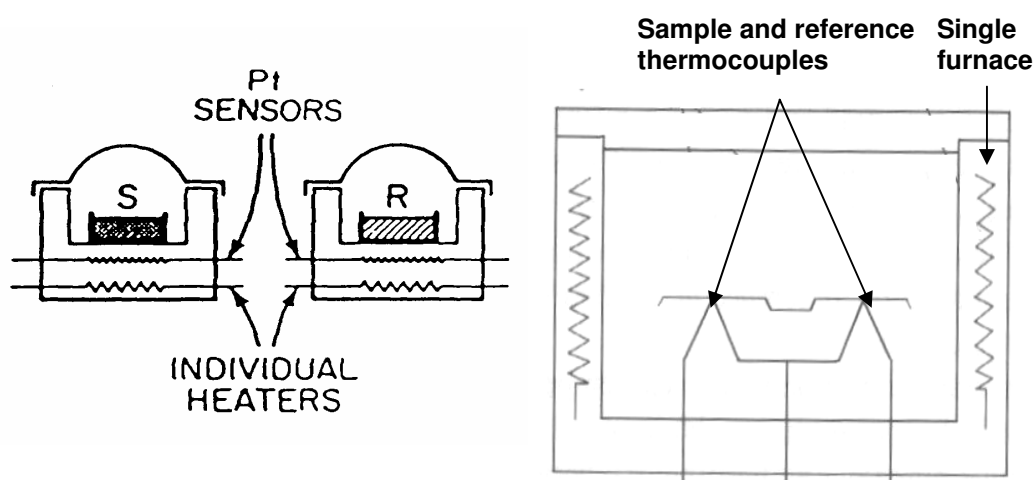


**Figure 2.15: Power compensated DSC (left) and heat flux DSC (right)**

Both designs involve heating a sample pan and a reference pan through a programmable temperature profile. Heat flux DSC uses the same heater to heat both the sample and the reference, determining enthalpy changes through a measurement of the temperature difference between them. Power compensated

DSC has separate furnaces for both sample and reference and enthalpy calculations are made from measurements of the difference in heat input required to keep sample and reference at the same temperature according to equation 2:

$$dQ/dt = dq_s/dt - dq_r/dt \quad \text{Equation 2}$$

Where  $dQ/dt$  is the differential power,  $dq_s/dt$  is the heat input for the sample and  $dq_r/dt$  is the heat input for the reference.

#### *2.5.4.2 Temperature modulated differential scanning calorimetry*

The interpretation of a DSC thermogram is often complex due to various underlying transformations such as melting and recrystallization occurring concurrently during heating. Several weak, broad and overlapping transitions are often seen for chocolate and other foods (De Meuter, Rahier and Van Mele, 1999, Verdonck, Schaap and Thomas, 1999). It has been reported that modulated techniques have the ability to separate thermograms into reversing (melting) and non-reversing (kinetic/ crystallization/ recrystallization) traces.

To increase the sensitivity (i.e. signal-to-noise) for the detection of a weak transition either the sample mass or the scan rate can be increased. To obtain a higher resolution, in order to separate transitions occurring at similar temperatures, either smaller samples are used or the heating rate is decreased. Therefore increased sensitivity is usually at the expense of the resolution and

vice versa (Verdonck, Schaap and Thomas, 1999).

Temperature modulated differential scanning calorimetry (TMDSC) techniques have been developed recently to offer a better understanding of thermal phase transitions particularly in the study of polymers (Sauer et al., 2000) . In contrast to conventional DSC where a linear and constant heating rate is applied, TMDSC uses a periodical temperature modulation over a linear heating or cooling profile and is claimed to be capable of giving accurate heat capacity measurements and separating underlying kinetic and thermodynamic phenomena with better resolution and sensitivity. Two main types of TMDSC have evolved. One uses a sinusoidal wave modulation and the other uses isothermal heat/cool segments, for example, Stepscan DSC (Perkin Elmer Inc).

The theory and principles of TMDSC using sinusoidal modulation can be found in papers by Reading, Schawe and Wunderlich (Reading, Luget and Wilson, 1994, Schawe, 1995, Wunderlich et al., 1997). Reading proposed that the resultant modulated heat flow can be deconvoluted by using a Fourier transform to give reversing and non- reversing components (Reading, Luget and Wilson, 1994). The reversing component is calculated from the periodic part of the heat flow and provides information on events which are thermodynamically reversible in a given time (Gunaratne, Shanks and Amarasinghe, 2004). The non-reversing component is the difference between the underlying heat flow and the reversing component.

The temperature program according to Reading *et al* (Reading, Luget and Wilson, 1994) is expressed as:

$$T = T_0 + bt + B \sin (\omega t) \quad \text{Equation 3}$$

Where  $T_0$  is the starting temperature,  $\omega$  is the angular frequency,  $b$  is the heating rate and  $B$  is the amplitude of temperature modulation.

According to the same authors, assuming the temperature modulation is small and that over the interval of modulation the response of the kinetic process to temperature is approximately linear, the heat flow equation can be written as:

$$dH/dt = C_{p,t}(b + B \cos (\omega t)) + f'(t, T) + C \sin (\omega t) \quad \text{Equation 4}$$

where  $f'(t, T)$  is the average underlying kinetic function once the effect of the sine wave has been subtracted,  $C$  is the amplitude of the kinetic response to the sine wave modulation and  $(b + B \cos (\omega t))$  is the measured quantity  $dT/dt$ .

In temperature modulated experiments using the sine wave function, there are two main methods to analyze the resulting modulated heat flow: the reversing/non-reversing heat flow approach as described by Reading and co-workers (Gill, Sauerbrunn and Reading, 1993) and the complex heat capacity approach proposed by Schawe (1995).

Stepscan™ DSC, as provided by Perkin Elmer, is a simplified version of TMDSC and does not involve complex Fourier transform for the deconvolution of the heat capacity data (Sandor, Bailey and Mathiowitz, 2002). The temperature program consists of periodic short heating rates and isothermal segments. The isothermal holds continue until the heat flow rate falls below a predetermined value (or criterion). The thermodynamic component is the heat flow response to the heating (or cooling) segment and reflects the so-called

reversing changes of the sample. The non-reversing change is obtained from the heat flow at the end of the isothermal segment and is sometimes known as the Iso-K (kinetic) baseline (see Figure 1). The interpretation of results is similar to TMDSC, and the reversing thermodynamic or  $C_p$  signal (reversible under the experimental conditions) and non-reversing (Iso-K baseline, kinetic) contributions can be directly and simply extracted from the data as described in equation 5 (Sandor, Bailey and Mathiowitz, 2002) .

$$dH/dt = C_p( dT/dt) + f(t, T) \quad \text{Equation 5}$$

Where  $dH/dt$  is the overall heat flow,  $C_p$  the heat capacity,  $dT/dt$  the heating rate and  $f(t, T)$  the kinetic response which is a function of time and temperature. Heat capacity on heating is calculated as the heat flow divided by the heating rate:

$$C_p = (dH/dt) / (dT/dt) \quad \text{Equation 6 (Sandor, Bailey and Mathiowitz, 2002)}$$

So far, temperature modulated DSC has not been used in the study of fats with the exception of Singh, Jalali and Alden, (1999). These authors studied the transformations of tristearin by modulated temperature differential scanning calorimetry in order to study the effect of operational parameters on the nature of information obtained from this technique. Their main conclusion was that MTDSC enables overlapping alpha-melting and beta-crystallization events to be separated, thus increasing the information obtained compared to normal

thermal analysis. Their other general conclusions were that observation of reversible processes is strongly influenced by the underlying heating rate with low to moderate heating rates being recommended. They also state that amplitude of modulation has a complicated effect on the phenomenon being studied and that when studying systems that exhibit metastable or polymorphic transitions, it is recommended that a range of amplitudes be tested to enable confirmation of whether an observed recrystallization effect is a new phase or the same phase as the one melting.

## **Chapter 3: Materials and Methods**

*This chapter summarises all the materials, equipment and methods used throughout this study. It first describes the samples used and their preparation. Then it moves on to the equipment description and experimental procedure.*

### 3 Materials and Methods

#### 3.1 Materials

Milk chocolate, Cadbury's dairy milk (CDM), was supplied by Cadbury Trebor Basset (Birmingham, UK). The triacylglycerol profile of this chocolate was determined by high performance liquid chromatography (based on AOAC methods 969.33 and 963.22) carried out by Reading Scientific Services Limited (RSSL, UK). The composition is given in Table 3.1. Cocoa butter (from Ghana) and chocolate fats (a blend of cocoa butter, milk fat, vegetable fats and emulsifiers) were also supplied. Their triacylglycerol compositions are shown in Table 3.2. It is worth mentioning that the composition of the fat phase of chocolate was similar to that of the composition of the chocolate fat mixture. However both of these differed from that of cocoa butter.

**Table 3.1: Composition of the fat phase of milk chocolate**

Triacylglycerol	Percentage (%)
PLO	1.6
PLP	1.1
POO	2.7
PLSt	1.5
POP	26.1
StOO	1.7
StLSt	1.0
POSt	39.8
PPSt	0.5
StOSt	21.0
AOSt	0.6
Others	2.5

**Note:** P = palmitic, O = oleic, St = stearic and A = arachidic and L = linoleic



**Table 3.2: Composition of cocoa butter and chocolate fats**

<b>Cocoa butter</b>		<b>Chocolate fats</b>	
<b>Triacylglycerol</b>	<b>Percentage (%)</b>	<b>Triacylglycerol</b>	<b>Percentage (%)</b>
PLO	0.6	PLO	1.3
POO	0.7	POO	2.0
PLSt	1.1	PLSt	1.3
POP	11.8	POP	24.5
StOO	1.3	StOO	2.0
StLSt	0.7	SLSt	0.9
POSt	52.5	POSt	42.7
PPSt	0.3	PPSt	0.6
StOSt	30.1	SOSSt	23.4
StStP	0.3	AOSSt	0.5
AOSSt	0.5	Unidentified	1.0

**Note: P = palmitic, O = oleic, St = stearic and A = arachidic and L = linoleic**

### **3.2 Tempering**

Since the thermal history of the chocolate and the confectionery fats for example industrial tempering, fluctuation in storage temperature would have had a significant effect on their melting behaviour, prior to any kind of analysis, the samples had to be melted and re-tempered in order to produce samples of known thermal histories and with the desired polymorph, Form V. Tempering was carried out in a purpose built lab scale-tempering machine, the TTM mini temperer© (Figure 3.1), provided by Cadbury-Schweppes, which operates under a continuous shear of  $53 \text{ min}^{-1}$ . 20g of melted chocolate or

confectionery fat were poured into a stainless steel pot and stirred by a U-shaped stainless steel mixer with scraper blades. The continuous shear enables the formation of crystal nuclei and influences the growth and agglomeration of crystals. Continuous mixing also removes the crystallised mass from the cooling surface, thus enabling uniform heat transfer throughout the sample. The steel mixer was driven by a low voltage servo motor.

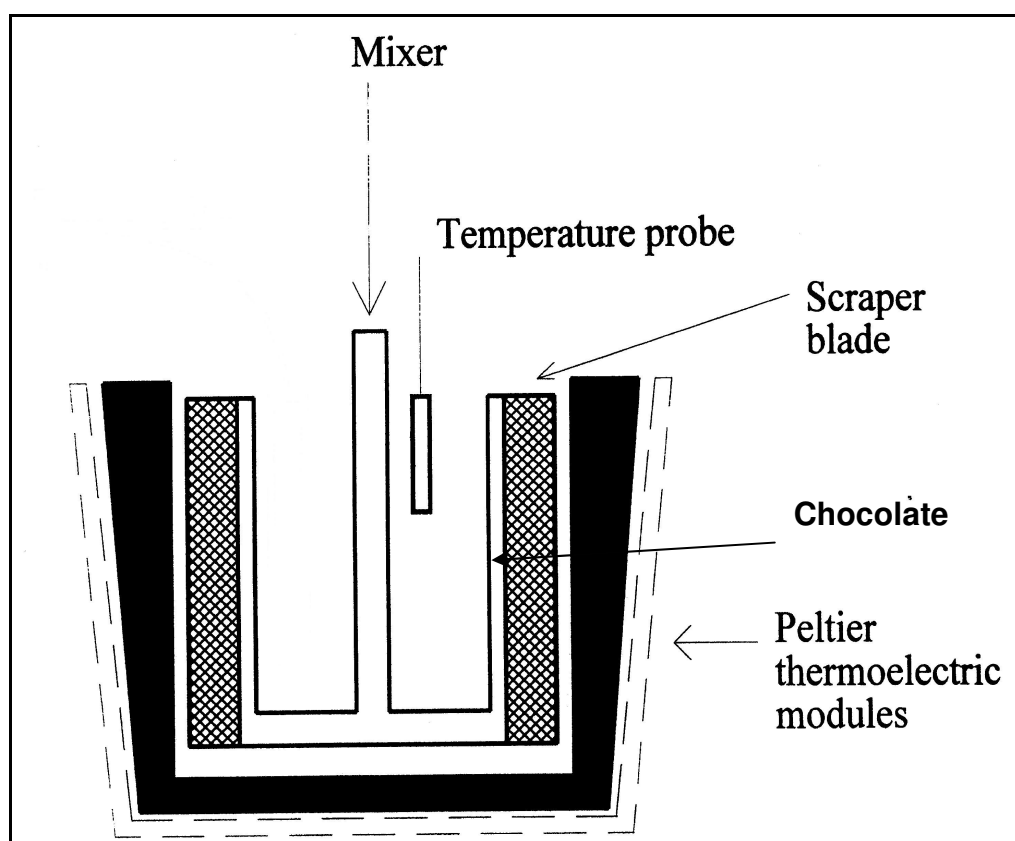


**Figure 3.1 Schematic diagram of lab-scale temperer**

Determination of the appropriate tempering profile for chocolate as well as cocoa butter and chocolate fats will be discussed in more details in Chapter 4. The tempering profile used for chocolate was as follows: melt at 55 °C and maintain under shear for 20 min to melt out all fat crystals. This was followed

by cooling to 22 °C at a rate of  $\sim 2\text{ }^{\circ}\text{C min}^{-1}$  then holding for 8 min to induce crystallisation and finally reheating to 28 °C and holding for 6 min to melt lower melting polymorphs, leaving the mixture with only the high melting polymorph, Form V. The profiles for cocoa butter and chocolate fats are given below:

#### Cocoa butter

Melt at 50 °C for 10min

Crystallise at 25 °C for 20min

Reheat and hold at 30 °C for 12min  
12min

#### Chocolate fats

Melt at 50 °C for 10min

Crystallise at 20 °C for 20min

Reheat and hold at 29.5 °C for

### ***3.2.1 Test of Temper: Use of the Tempermeter***

The degree of temper of chocolate can be assessed by obtaining a temperature-time curve for the chocolate while it is cooling. An instrument called a tempermeter can be used to obtain such curves. Figure 3.2 shows a schematic diagram of a tempermeter. A Grant chocolate temper recorder from Grant instruments (Cambridge, UK) was used to assess the temper of the chocolate samples.

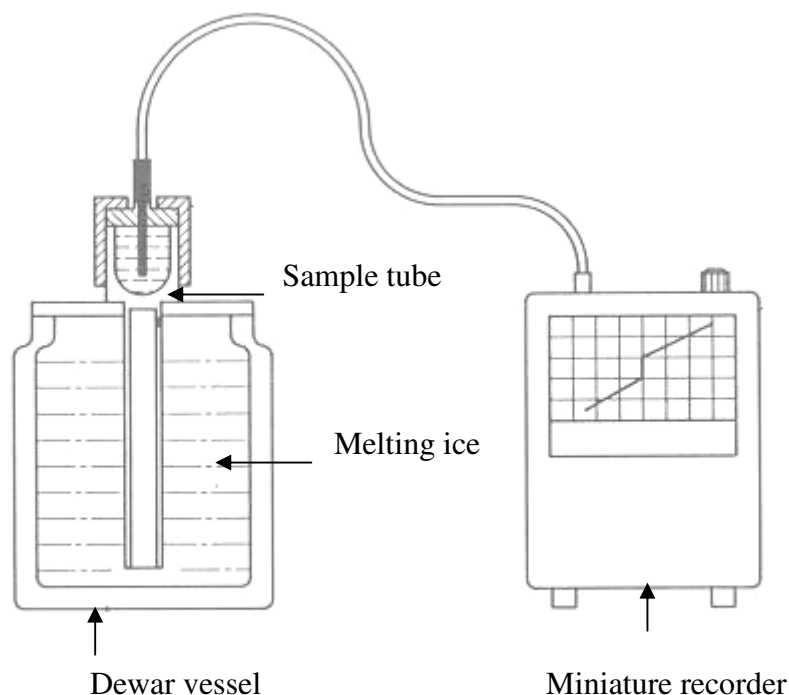


**Figure 3.2: Schematic diagram of the Tempermeter**

The tempermeter basically consists of 2 components, a sample cooling assembly and a temperature recording device. The tempermeter was used as follows: A small sample of chocolate, typically around 10g, was placed in the sample holder. The bottom half of the sample holder was immersed in an ice-water mixture in the vacuum container. During crystallisation, latent heat is released and the temperature of the chocolate sample was measured with a temperature probe and plotted by the recorder to produce a cooling curve. The degree of temper was assessed from the point of inflection and the degree of recalescence. Examples of curves obtained from this instrument are shown in Figure 3.3.

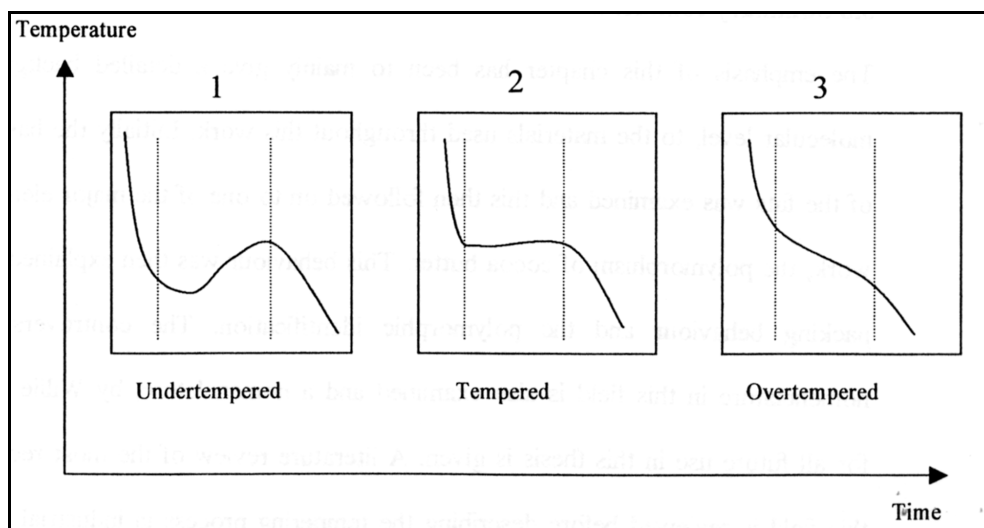


**Figure 3.3: Typical curves used to assess the degree of temper**

The first part of the curves refers to the initial cooling of the tempered chocolate before further crystallisation. The second region is the most important one. As the fat crystallises, it releases heat in the form of the latent heat of crystallisation, which results in an increase of temperature. Undertempered chocolate has insufficient seed crystals and therefore has to undergo a larger amount of crystallisation (Talbot, 1999). In the case of over-tempering, many seeds are present and a larger amount of crystallisation has already taken place, resulting in an overall reduction in bulk temperature. In optimum temper, the amount of heat produced is equal to the amount of heat removed by the cooling water of the tempering unit, so the chocolate temperature shows a constant figure.

### **3.3 Differential Scanning Calorimetry (DSC)**

Thermal analysis was performed using a Perkin Elmer DSC7 and Pyris

Diamond DSC (both from Perkin Elmer, UK). The instruments were calibrated for temperature and enthalpy using indium ( $T_{m, onset} = 156.6^{\circ}\text{C}$  and  $\Delta H = 28.45 \text{ J.g}^{-1}$ ) and cyclohexane ( $T_{m, onset} = 6.7^{\circ}\text{C}$ ). Nitrogen gas was used as a purging agent in both instruments. Cooling was achieved with an intra-cooler allowing a temperature of  $-60^{\circ}\text{C}$  to be reached. Conventional DSC experiments (discusses in Chapters 4 and 5) were performed on both the DSC7 and Pyris Diamond while StepScan experiments (discussed in Chapter 6) were only possible on the Pyris Diamond DSC.

### ***3.3.1 Sample Pan Preparation***

The preparation of the DSC pans was carried out in a temperature-controlled oven big enough to allow preparation of samples inside it, with all instruments (sealing tool, DSC pans, spatulas and tweezers) being maintained at a temperature which would match that of the samples coming out of the temperer. This was done as small amounts of tempered material were being used and these were sensitive to sudden fluctuations in temperature, which could cause the tempered material to lose its state of temper (e.g. if the temperature was higher than that of the melting point of the Form V polymorph present, these would melt and effectively an untempered sample would be produced).

In the case of chocolate the temperature of the incubator oven was set at  $28^{\circ}\text{C}$ , for cocoa butter and chocolate fats, these were  $30^{\circ}\text{C}$  and  $29^{\circ}\text{C}$  respectively. The oven itself was on a moveable trolley such that it could be wheeled as close as possible to the temperer and the DSC. A schematic layout of the oven,

temperer and DSC apparatus is shown in Figure 3.4.

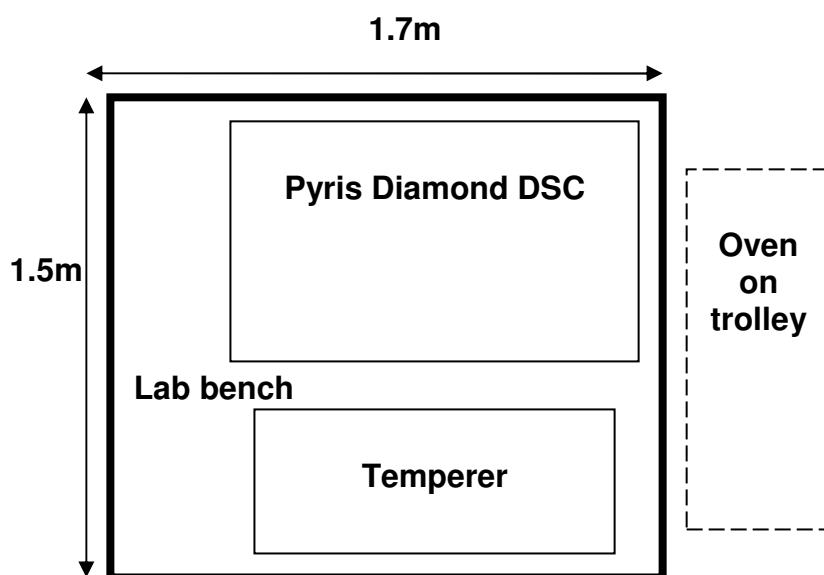


**Figure 3.4: Diagram of arrangement of equipment to minimize tempered samples experiencing fluctuation in temperature during transfer from temperer to DSC machine**

In order to minimise uncontrolled cooling of the samples during the transfer of the sample from the temperer to the DSC apparatus, the sample weight (between 15-25 mg) was determined after the completion of the experiment and used to normalise the heat flow data. The importance of maintaining all the DSC pans and sealing tools in a temperature controlled environment is made clear in the subsequent chapter. It is also to be noted that a substantial amount of time was spent optimizing the layout of the equipment and adjusting the temperature of the oven in order to obtain the best possible results.

*Tempered samples:* For tempered samples, the material was immediately transferred from the temperer, sealed into 50  $\mu$ L aluminium pans and inserted in the calorimeter held at 28  $^{\circ}$ C (for chocolate), 29  $^{\circ}$ C (for

chocolate fats) or 30 °C (for cocoa butter). The entire sample transfer procedure was carried out in less than 60s.

*Untempered samples:* Untempered samples were produced by first melting chocolate, cocoa butter or chocolate fats in DSC pans at 50°C in the calorimeter. Once melted, they were then subjected to the same cooling regimes as tempered ones. Untempered samples were used as controls in order to assess the role of tempering. They were produced in the absence of shear, as the aim was to produce samples that had no nuclei of any polymorph of cocoa butter.

### **3.3.2 Conventional DSC experiments**

#### *3.3.2.1 Effect of cooling and heating rate*

A series of experiments was carried out in order to

- Study the effect of cooling rates on chocolate
- Study the effect of heating rates on chocolate
- Determine the optimum cooling and heating rates that would produce reproducible and good quality data.

Table 3.3 shows each cooling rate used and subsequent heating rates that were applied.

Two types of cooling experiments were carried out

- 1) Cooling in the DSC: Samples were cooled at various rates to -



30 °C as shown in Table 3.3. The samples were then held isothermally at this temperature for 2 min before being heated up.

- 2) Cooling outside the DSC: Samples were crashed cooled in liquid nitrogen before insertion into the DSC machine held at -60 °C

**Table 3.3: List of cooling and heating rates used in the study**

Cooling rates (°C min <sup>-1</sup> )	Heating rates applied
1	2 and 10 °C min <sup>-1</sup>
5	10 °C min <sup>-1</sup>
10	2 and 10 °C min <sup>-1</sup>
20	10 °C min <sup>-1</sup>
Crash cooling in liquid Nitrogen	1, 5, 10 and 30 °C min <sup>-1</sup>

The results of these experiments are discussed in Chapter 5.

### **3.3.3 Stepscan DSC experiments**

#### *3.3.3.1 Optimisation of Stepscan parameters*

Preliminary experiments were carried out to determine the appropriate

Stepscan heating protocol for chocolate. This was done by systematically varying the parameters within the capabilities of the available machine by applying a matrix of conditions based on extreme high and low values for

- 1) The temperature step amplitude (0.5 and 2°)
- 2) The heating rate during the step (10 and 150 °C.min<sup>-1</sup>) and
- 3) The period of isothermal hold (1 and 5 min).

Experiments were carried out on tempered chocolate samples that were first cooled in the DSC at 1 °C.min<sup>-1</sup>.

The matrix of parameters was also applied to 10 mg Tripalmitin (Sigma Aldrich, UK). Tripalmitin (PPP) was used as a simple model system to study the influence of Stepscan parameters. The tripalmitin samples were first melted at 10 °C min<sup>-1</sup> to 80 °C. They were then cooled at 40 °C min<sup>-1</sup> to 30 °C and held isothermally for 2 min. They were then heated in Stepscan mode.

#### *3.3.3.2 Stepscan DSC on tempered and untempered chocolate samples*

Samples were cooled (at either 1 or 10 °C min<sup>-1</sup>) to -30 °C and held isothermally for 2 min. After the isothermal period, they were heated in Stepscan mode between -30 and 50 °C. Following the preliminary experiments described in section 3.3.3.1, it was decided to use the following Stepscan heating profile. The parameters used were :amplitude (step size) of 2 °C, step heating rate of 150 °C.min<sup>-1</sup>, an isothermal time of 5 min and equilibrium criterion (±0.01mW), giving an overall underlying heating rate of approximately 2°C.min<sup>-1</sup>. Figure 3.5 shows an example of a Stepscan DSC

trace which has the temperature vs. time profile superimposed on it.

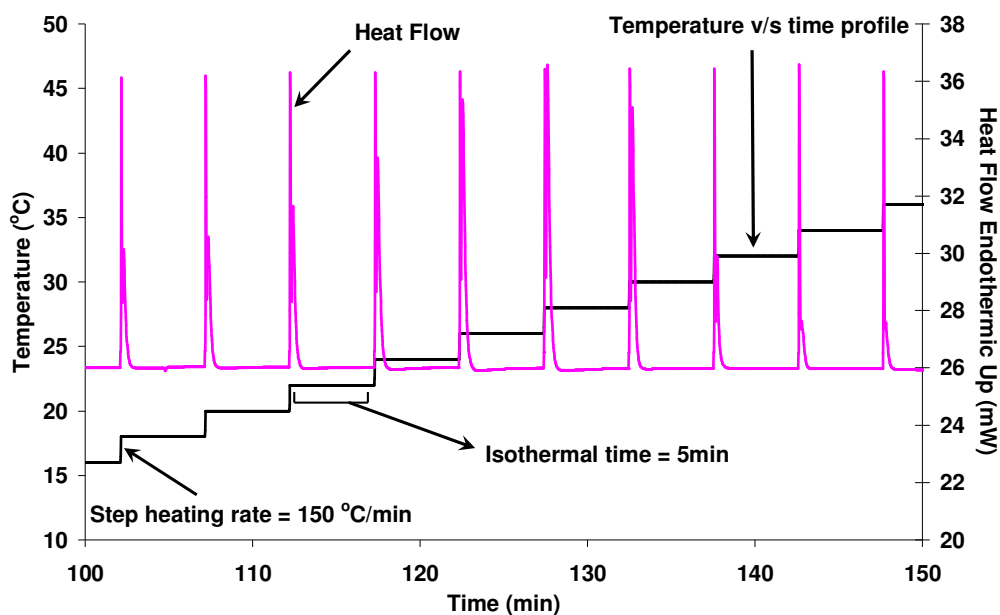


**Figure 3.5: Example of part of a Stepscan DSC profile illustrating the temperature v/s time profile as well as the heat flow during Stepscan heating.**

All DSC data were analysed using Pyris software version 7.0 provided by Perkin Elmer. A minimum of 5 replications was carried out for each variation in cooling or heating rate. The results shown in the following chapters are examples showing typical traces selected from each data set. Whilst the relative magnitude of the endo- and exothermic events observed varied between replications, the number of these events and the temperature at which they occurred were reproducible. This point is further discussed in the individual results section.

### **3.4 X-ray diffraction**

Experiments were carried out on a Bruker D5005 wide-angle X-ray diffractometer equipped with a copper source operating at 40 kV and 30 mA producing a Cu K radiation with a wavelength of 1.54 Å. X-ray diffraction experiments were only carried out on cocoa butter and chocolate fats samples. The reason that chocolate was not used is because the sucrose diffraction patterns are very strong and interfere with any fat diffraction pattern. Even if the sucrose pattern was subtracted from a chocolate pattern, this analysis would not be accurate.

In order to identify polymorphic forms present at a particular temperature, it is of course important to have temperature control on the X-ray. The low temperatures relevant to the Frozen Cone Process should be accessible. An initial objective was therefore to develop and validate a temperature control system for the Bruker X-ray diffractometer.

#### **3.4.1 Development of temperature controlled X-ray**

The existing University X-ray diffractometer (Bruker Siemens AXS D5005) as shown in Figure 3.6 could initially only take measurements at ambient temperature as it did not have a cooling chamber attachment or cooling system attached to the sample holder.

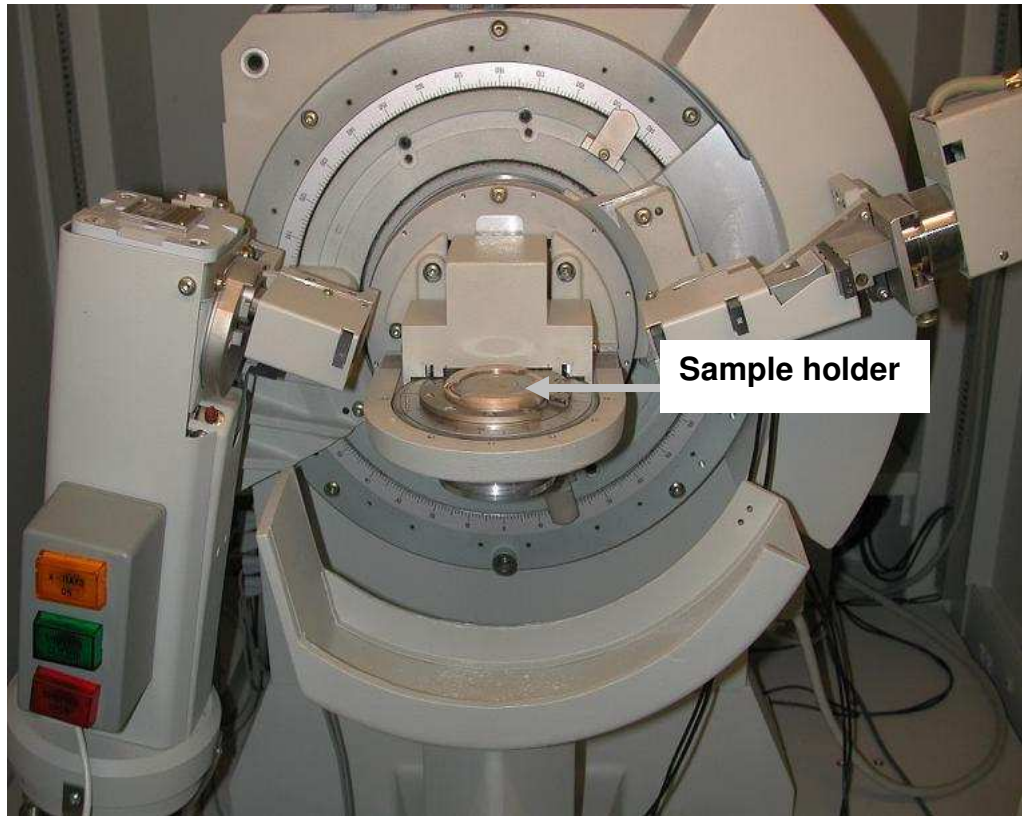


**Figure 3.6: Siemens X-ray diffractometer with rotary sample holder (no temperature control)**

An initial attempt was made to design a cooling attachment that could be fitted onto the sample holder. This attachment had a cryogenic liquid flowing around the base of the sample holder to cool the sample. This attachment was based on the design described by Gray, Lovegren and Mitcham, (1976). However this was unsuccessful as despite the best efforts, there was significant ice formation on the surfaces of the holder and the sample. Further progress was possible because a Philips X-ray diffractometer was acquired from a United Biscuits research facility in High Wycombe. This machine came with an Anton Paar temperature controllable sample chamber and temperature control units. It was decided to modify the Bruker Siemens machine by attaching the cooling units to it such that temperature controlled measurements could be carried out. This

modification to the sample holder and chamber is shown in Figure 3.7.

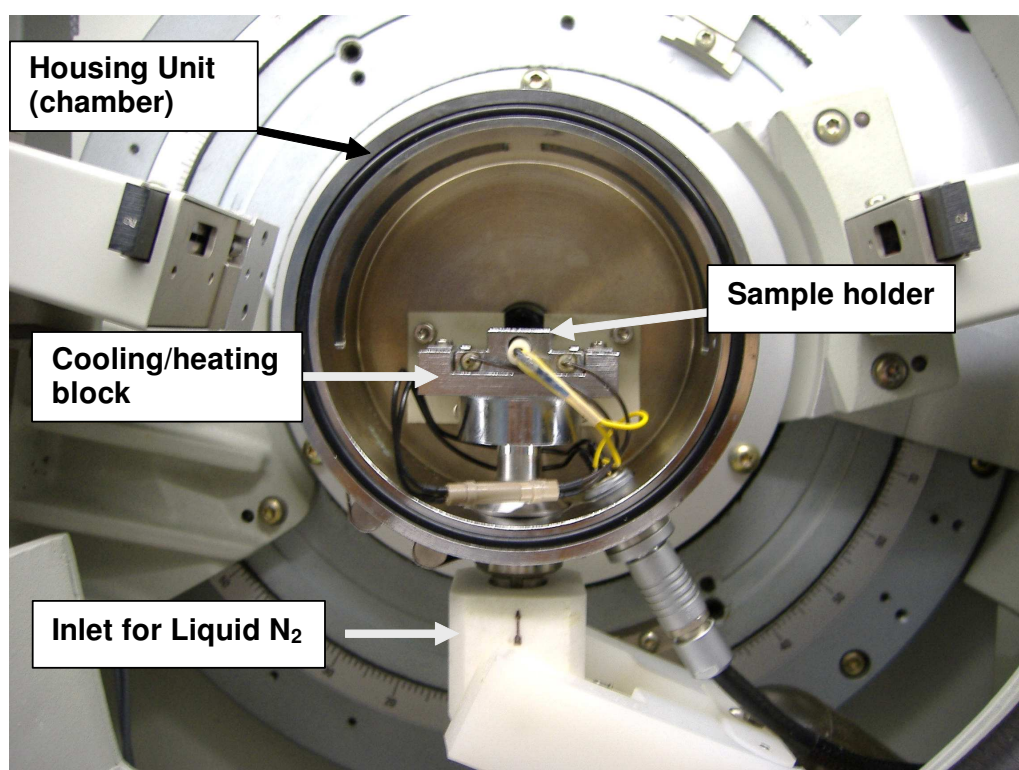


**Figure 3.7: Siemens X-ray fitted with Anton Paar Temperature control chamber TTK 450 (note: the chamber cover is off)**

The alignment of the sample holder was checked using silicon powder as reference material.

### ***3.4.2 Detailed Equipment Description***

As mentioned above, variable cooling and heating was achieved by attaching a low- temperature Anton Paar TTK Temperature chamber (model 25100) to the goniometer. The chamber was connected to an Anton Paar Liquid Nitrogen controller (model 25119) and an Anton Paar TTK-HC Temperature Controller (model 25111). A picture of the cooling chamber with the sample holder is shown in Figure 3.8.

The sample holder is made of nickel-plated copper, providing a good thermal conductivity and high corrosion resistance with a sample volume of 17mm<sup>3</sup>. A Pt 100 temperature sensor is inserted in the sample holder providing exact temperature measurement. A connector for the Pt 100 permits fast and easy exchange of the sample holder. The whole chamber was closed with the chamber cover as shown in Figure 3.9 and was purged with Nitrogen gas in order to maintain a dry atmosphere and prevent condensation during low temperature measurements.

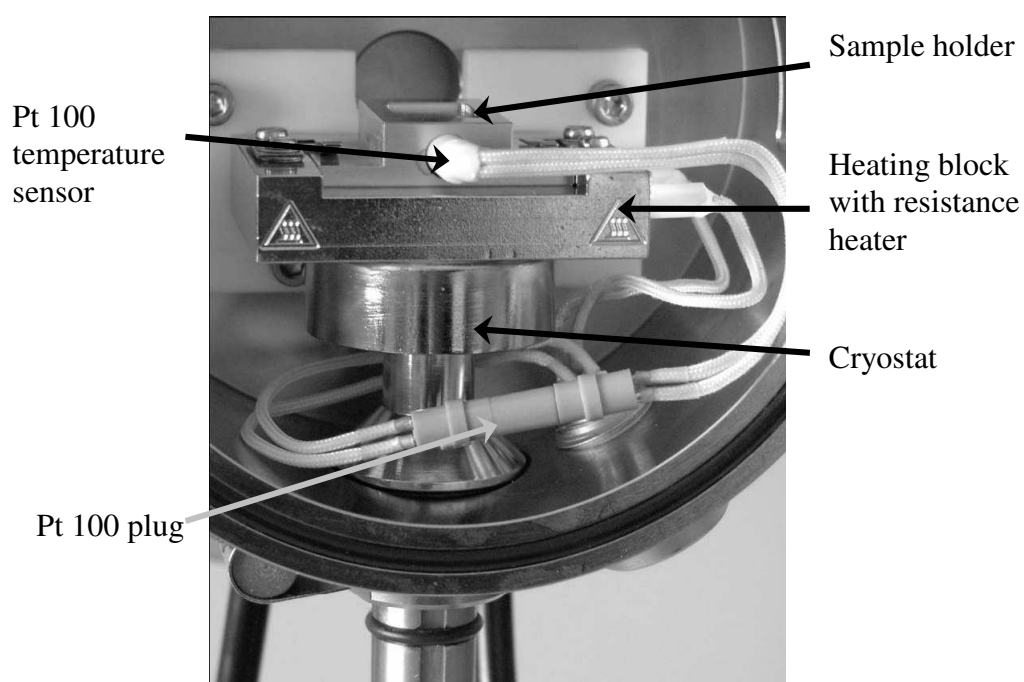


**Figure 3.8: Cooling chamber with sample holder (From Anton Paar Manual)**

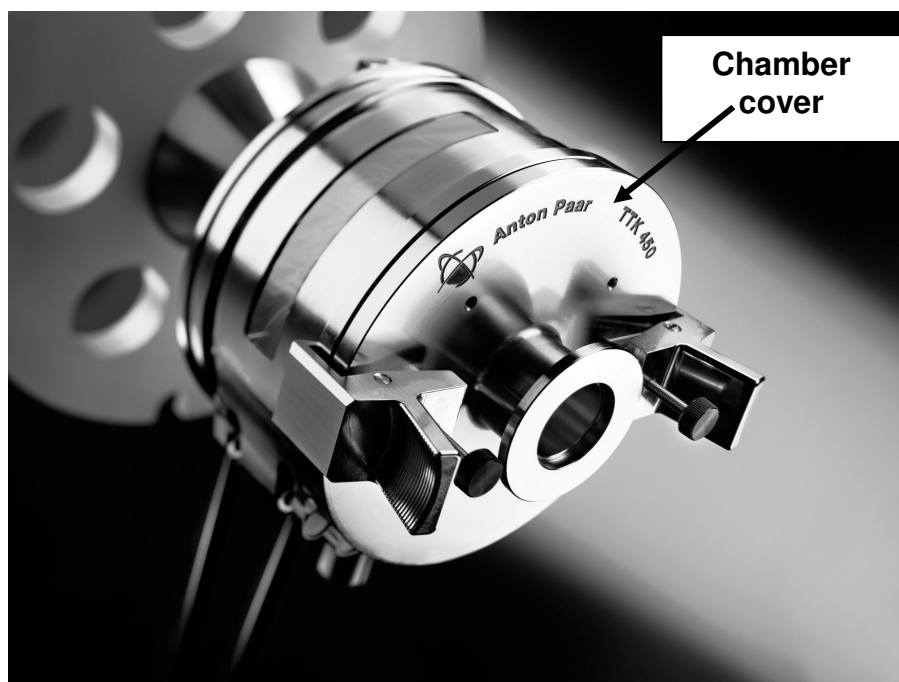


**Figure 3.9: Cooling chamber with cover on**

### **3.4.3 Experimental Procedure**

Two types of cooling experiments were performed on the X-ray

1. Cooling from 29 or 30 °C to -30 °C at predefined rates then warming the samples
2. Direct contact cooling, where the samples were smeared on the sample holder held at temperatures between -30 and 5 °C

#### **3.4.3.1 Cooling warm samples at predefined rates**

Tempered samples of cocoa butter and chocolate fats were smeared onto the sample holder which was held at a temperature corresponding to that of the sample coming out of the temperer (30 °C for cocoa butter and 29 °C for chocolate fats). They were then cooled to -30 °C at rates of 1, 5, 10 and 20 °C min<sup>-1</sup>. Once at -30 °C, an X-ray scan was taken. The samples were then



warmed at 1 and 10 °C min<sup>-1</sup> with scans acquired at every 10 °C interval until 20 °C. Warming rates of 1 and 10 °C min<sup>-1</sup> were chosen to match that of the DSC experiments. Untempered samples were also subjected to the same procedure.

#### *3.4.3.2 Direct contact cooling*

These experiments were carried out to mimic the Frozen cone® process. The sample holder was set at a particular temperature and the sample was smeared onto it. The temperatures used were: -30, -20, -15, -10, -5, 0 and 5 °C. After contact cooling, a scan was acquired and subsequently the sample was warmed at 1 and 10 °Cmin<sup>-1</sup> with scans acquired at every 5 or 10 °C interval until 20 °C. Both tempered and untempered samples were used for these experiments.

All X-ray scans were acquired between 4-35 ° on the 2θ scale with a step size of 0.02 ° and exposure time of 0.25 second. After each run, the diffractogram of the empty holder was subtracted and the data normalised. All runs were done in duplicate.

#### **3.4.4 Identification of polymorphs from X-ray data**

Once each X-ray diffractogram was normalised, polymorph assignment were made by comparing the diffractogram with the patterns identified by (Wille and Lutton, 1966) as shown in Figure 2.14 and using the short spacing data

tabulated in Table 2.2. For example, an X-ray pattern showing strong d-spacing at 4.58, 4.19 and 3.70 Å is interpreted as being a mixture of polymorphic Forms V and I.

## **Chapter 4: Lab-scale tempering and characterisation of chocolate and chocolate fats**

*This chapter details the determination of the tempering profiles of chocolate, cocoa butter and chocolate fats and tests carried out to check for correct temper. Optimisation of experimental conditions, handling and transfer procedure are also described.*

## 4 Lab-scale tempering and characterisation of chocolate and chocolate fats

### 4.1 Introduction

For the purpose of this research work, three types of materials were used, namely, chocolate, cocoa butter and chocolate fats. As mentioned before, the main reason for using cocoa butter and chocolate fats instead of chocolate for X-ray diffraction experiments is because the sucrose peaks in the chocolate interfere strongly with any peaks given by fats and this makes analysis very difficult. This is shown in Figure 4.1 where the X-ray patterns of chocolate, cocoa butter and sucrose are compared.

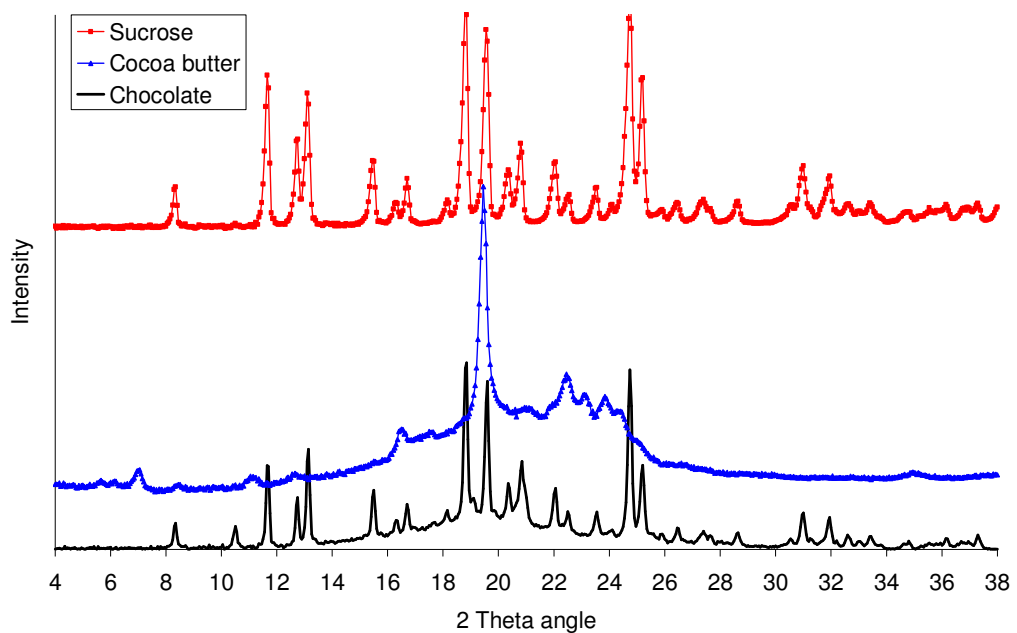


**Figure 4.1: Wide angle X-ray diffraction pattern for chocolate (bottom), cocoa butter (middle) and sucrose (top)**

One of the solutions to this problem could have been washing away the sucrose from the surface of the solid chocolate as described by Adenier et al., (1975)

and , Loisel et al., (1997) ) . However, this was not practical in this case as there was a need for freshly tempered liquid chocolate to be analysed while undergoing rapid or slow cooling in the X-ray. Another solution would have been to produce sucrose free chocolate. The problem here was getting all the ingredients, some of which are confidential, and producing chocolate from scratch in a pilot plant. This would be time consuming and impractical. Therefore, it was decided to use chocolate fats, which would include all the fats in their appropriate ratio found in the chocolate and cocoa butter for comparison for the X-ray experiments. Specific tempering profiles then needed to be determined for them. It was of crucial importance that each material used was tempered appropriately before undergoing any type of experimentation. This optimisation procedure was of crucial importance as if the samples were of incorrect temper, this would have affected all the subsequent results regardless of the analytical technique used. The tempering trials for chocolate are first presented followed by those for cocoa butter and finally chocolate fats.

## **4.2 Determination of tempering profile for chocolate**

The tempering profile of chocolate is normally based on that of cocoa butter. This is shown in Figure 2.10. Essentially, chocolate is first heated to a temperature where no nuclei or thermal memory (Van Malssen et al., 1996, van Langevelde et al., 2001a) remains. Then it is supercooled to induce crystallisation and warmed above the melting point of all unstable  $\alpha$  and  $\beta'$  crystals, i.e., above the melting point of Form IV but below that of Form V. This tempered mass can then be moulded and solidified, further promoting the

growth and stabilisation of the Form V crystals.

Before presenting the results of the tempering trials for chocolate, it is important to point out that it is a well-known fact that optimal tempering profile for milk chocolate differs from that of cocoa butter due mainly to the addition of milk fats (Timms, 1980, Timms and Parekh, 1980, Ali and Dimick, 1994a, Ali and Dimick, 1994b, Dimick et al., 1996, Metin and Hartel, 1996, Reddy et al., 1996) . The same authors also stress on the influence of milk solids with regards to depression of peak melting points of cocoa butter. In this particular chocolate, milk solids (non-fat and fat) make up 24% of the total chocolate, which is much more than that found in an average standard milk chocolate bar (approx 17% total), while the cocoa butter content was only 17%. The chocolate also contained 5 % of vegetable fats (origin confidential) which also contributes to the tempering profile deviating from that of cocoa butter. Hence, a significant amount of time was spent in optimising the temper conditions for this particular type of chocolate as opposed to using existing tempering profiles found in literature for cocoa butter or work carried out by previous researchers.

#### **4.2.1 Optimisation of tempering profiles: variation of insertion and final tempering temperatures**

The initial tempering profile used for chocolate was the one provided by Reading Scientific Services limited (RSSL), who routinely carry out work with Cadbury's chocolate. Molten chocolate (20g) was placed in the mini-temperer

and was tempered as follows: Melt at 55 °C for 20min, cool to 22.5 °C for 8 min and re-heat to 30 °C for 5 min.

A sample of the chocolate was then transferred into 20µl aluminium pans, sealed and inserted into the DSC where it was subsequently cooled and heated up. The insertion temperature into the DSC was 30 °C and the sample was held at this temperature for 3 min before being cooled. A typical result for a sample cooled at 1 °C min<sup>-1</sup> then warmed at 10 °C min<sup>-1</sup> is shown in Figure 4.2

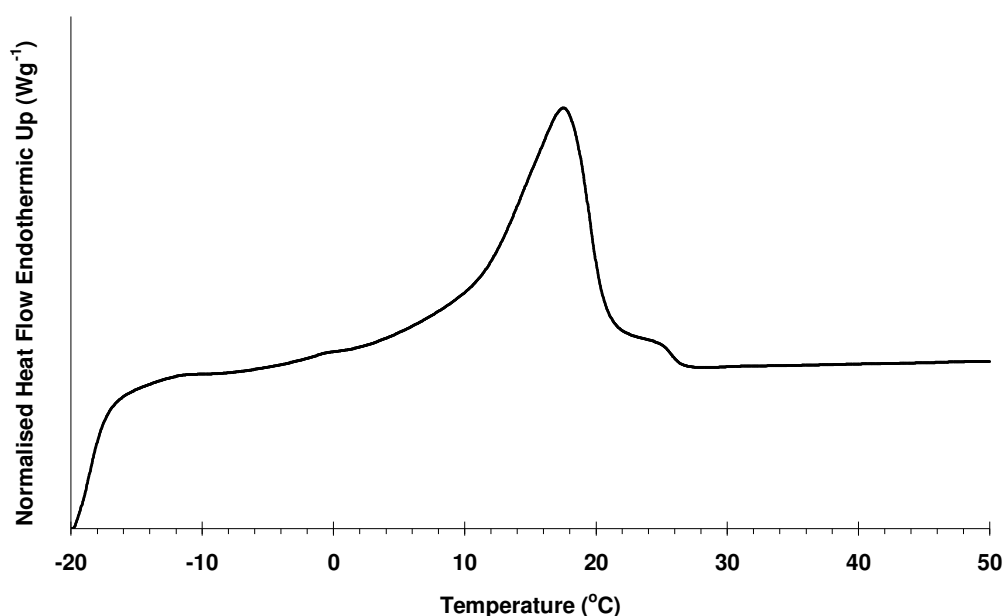


**Figure 4.2: Tempered sample (final tempering and insertion T = 30 °C) cooled at 1 °C min<sup>-1</sup> then warmed at 10 °C min<sup>-1</sup>. Only the heating thermogram is shown.**

As can be seen in Figure 4.2, contrary to what was expected, no higher forms were seen on the reheat. The possible explanations for the results were that

- a) the sample size was too small (the 20µl pans could only hold approx. 5ml of chocolate) hence lessened the chance of seed crystals being

present;

- b) the transfer time between pan preparation and insertion into the DSC apparatus could also rapidly cool the sample hence forming unstable polymorphs;
- c) the final tempering temperature was too high, hence melting any Form V nuclei being formed.

The following improvements were then made to the experimental setup:

- Use of aluminium DSC pans with a bigger sample volume (50  $\mu$ l) instead of the smaller 20 $\mu$ l ones used before: The new pans contained between 15-50mg chocolate
- Use of a temperature controlled oven to maintain the pan and sealing tool at the same temperature as the sample coming out of the temperer
- DSC sealing tools were kept on wooden block to avoid contact with metal floor of oven which could be at higher temperature
- Careful monitoring of the temperature in the oven
- Minimise transfer time by moving temperer and oven closer to the DSC equipment
- Final tempering temperature and insertion temperature were lowered to 29°C

Figure 3.4 in the Materials and Method section shows the layout of the instruments following the changes made above.



The result following the above changes can be seen in Figure 4.3. However despite these changes, the results still showed significant amounts of lower forms being present on the reheat. Higher forms were also seen but in much smaller amounts when compared to the lower forms.

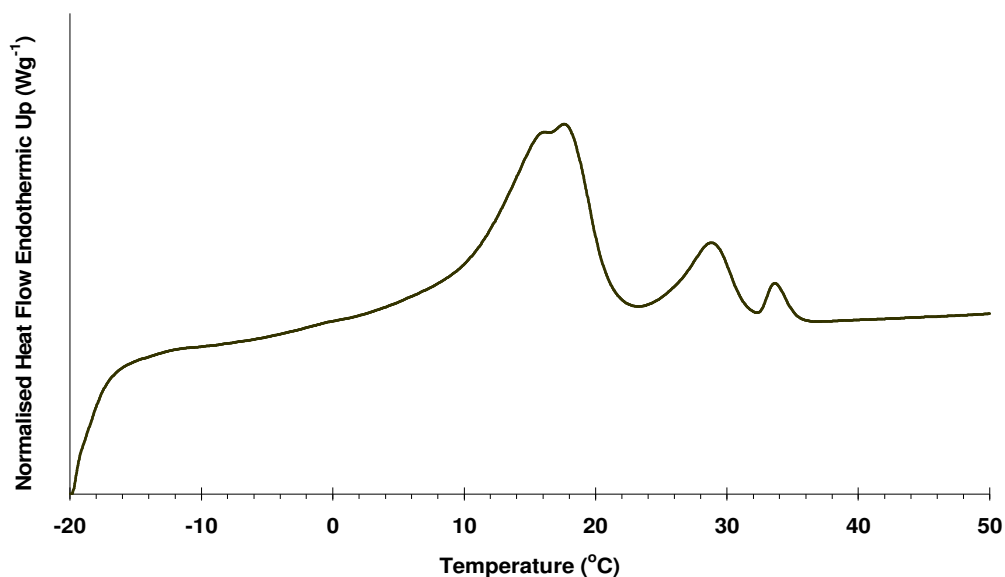


**Figure 4.3: Tempered sample (insertion and final tempering  $T = 29\text{ }^{\circ}\text{C}$ ) cooled at  $1^{\circ}\text{Cmin}^{-1}$  followed by heating at  $10\text{ }^{\circ}\text{Cmin}^{-1}$ . (only heating thermogram is shown)**

Following these results, the final tempering temperature and insertion temperature was further lowered to  $28\text{ }^{\circ}\text{C}$ . The samples were held isothermally for 3 min at  $28\text{ }^{\circ}\text{C}$  then cooled at  $1\text{ }^{\circ}\text{C min}^{-1}$  to  $-30\text{ }^{\circ}\text{C}$ . After a 2 min isothermal hold, they were heated up at  $10\text{ }^{\circ}\text{C min}^{-1}$ . This result is shown in Figure 4.4.

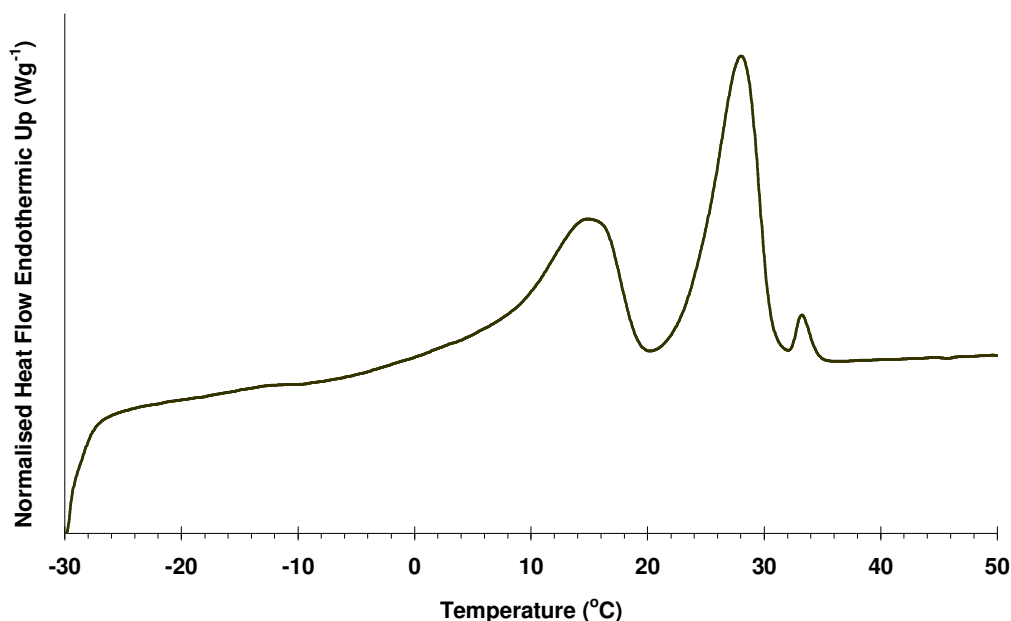


**Figure 4.4: Tempered chocolate cooled (insertion and final tempering  $T=28\text{ }^{\circ}\text{C}$ ) at  $1\text{ }^{\circ}\text{C min}^{-1}$  then heated at  $10\text{ }^{\circ}\text{Cmin}^{-1}$**

Although there was a marked improvement in the result, there was still high proportion of lower forms present on the re-heat. It was then decided to change the tempering regime as well as the insertion temperature of the DSC pans into the apparatus. The new tempering regime was as follows:

- Melt at  $55\text{ }^{\circ}\text{C}$  and maintain under shear for 20 min
- Cool to  $22\text{ }^{\circ}\text{C}$  and hold for 8 min
- Finally reheating to  $28\text{ }^{\circ}\text{C}$  and holding for 6 min

Tempered samples were sealed in the DSC pans, inserted in the apparatus at  $28\text{ }^{\circ}\text{C}$  and cooled at  $1\text{ }^{\circ}\text{C min}^{-1}$  to  $-30\text{ }^{\circ}\text{C}$ . Figure 4.5 shows the result of these changes after the sample was heated up at  $10\text{ }^{\circ}\text{C min}^{-1}$ .

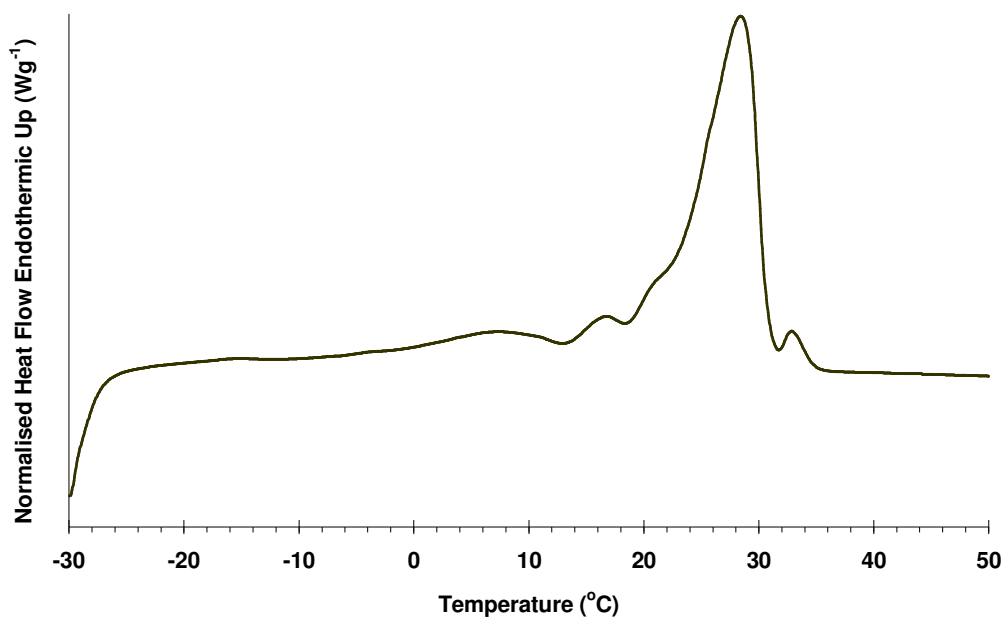


**Figure 4.5: Tempered chocolate using new tempering regime. The sample was cooled at 1 °C min<sup>-1</sup> to -30 °C then heated at 10 °C min<sup>-1</sup>**

As shown in Figure 4.5, a major endotherm is picked up at a peak temperature of 28.4 °C, indicating that the new tempering profile with the lower final tempering T of 28 °C did not melt any high melting nuclei formed during crystallisation. Although the melting temperature of Form V of cocoa butter is reported as 33.8°C (Wille and Lutton, 1966) , this value is usually depressed by the presence of other fats such as milk and vegetable fats (Timms, 1980, Timms and Parekh, 1980, Ali and Dimick, 1994a, Ali and Dimick, 1994b, Reddy et al., 1996) . As mentioned earlier, in this formulation of chocolate, milk fat contributed 7% of the total ingredient list while cocoa butter accounted for only 17% of the total. It is therefore highly likely that the major melting event occurring at a peak temperature of 28.4 °C is that of the Form V polymorph. Other minor melting events are observed at temperatures (peak) of ~7, 17 and 21 °C. These are attributed to low melting point triacylglycerols

present in the fat fraction of chocolate solidifying due to the sample of chocolate being cooled to  $-30^{\circ}\text{C}$ . These triacylglycerols would normally be in the liquid phase at room temperature. A small shoulder at  $33^{\circ}\text{C}$  is also observed. This is attributed to the formation of Form VI. In an industrially tempered sample, this peak is not noticed. Its presence here is probably due to the chocolate tempered in the lab-scale temperer being kept longer (6 min) at the final re-warm temperature of  $28^{\circ}\text{C}$  than it would in an industrial scale temperer (typical holding time 2min) (Martin Wells, Cadbury Schweppes, personal communication). These conditions may favour the formation of the more heat stable Form VI.

#### *4.2.1.1 Checking final tempering temperature*

To determine whether a final tempering T of  $28^{\circ}\text{C}$  was most suitable, the final tempering T was lowered to 26 and  $27^{\circ}\text{C}$ . Chocolate produced by these 2 regimes were cooled and heated up in the DSC as with previous experiments. The results are presented in Figure 4.6. It can be seen that neither of these temperatures resulted in the formation of stable Form V. The explanation for this is that at the re-warm T of 26 and  $27^{\circ}\text{C}$ , there is a significant amount of lower form nuclei present and these temperatures are too low to melt them. Hence, on cooling, the growth of these lower forms is favoured over that of Form V. It was therefore concluded that a final tempering temperature of  $28^{\circ}\text{C}$  was most suitable for use in this case.

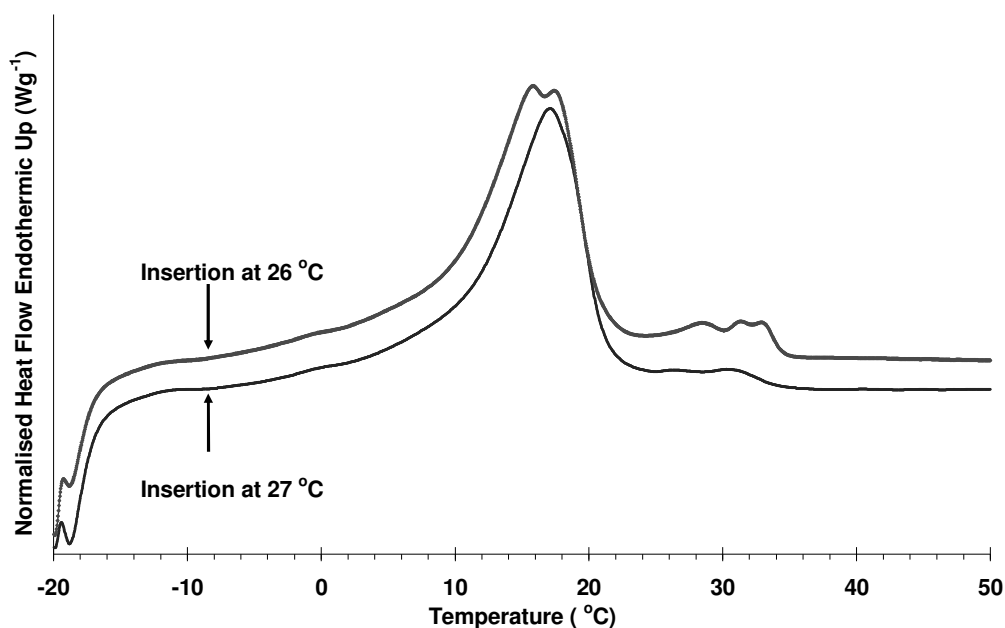


**Figure 4.6: DSC thermogram of chocolate samples with 2 different final tempering temperatures.**

#### **4.2.2 Checking lab-scale tempering against industrial tempering**

Once a lab-tempering profile had been established, it was important to check the result of this tempering with that obtained during industrial tempering. To this effect, tests were carried out on-site at the Cadbury Bournville factory. Samples of freshly tempered chocolate coming out of the industrial temperer were taken and carried in an insulated vessel to minimise uncontrolled cooling to the analytical lab next door, where they were encased in DSC pans and analysed immediately. The analysis consisted of cooling the pans at  $1\text{ }^{\circ}\text{C min}^{-1}$  to  $-30$  and then following a holding period, the sample was warmed at a rate of  $10\text{ }^{\circ}\text{C min}^{-1}$  to  $50\text{ }^{\circ}\text{C}$ . Typical melting profile of such a sample is shown in Figure 4.7. As can be seen the peak melting temperature is  $\sim 28.5\text{ }^{\circ}\text{C}$  which is close to the peak melting value,  $28\text{ }^{\circ}\text{C}$  obtained with the lab-tempered chocolate sample.

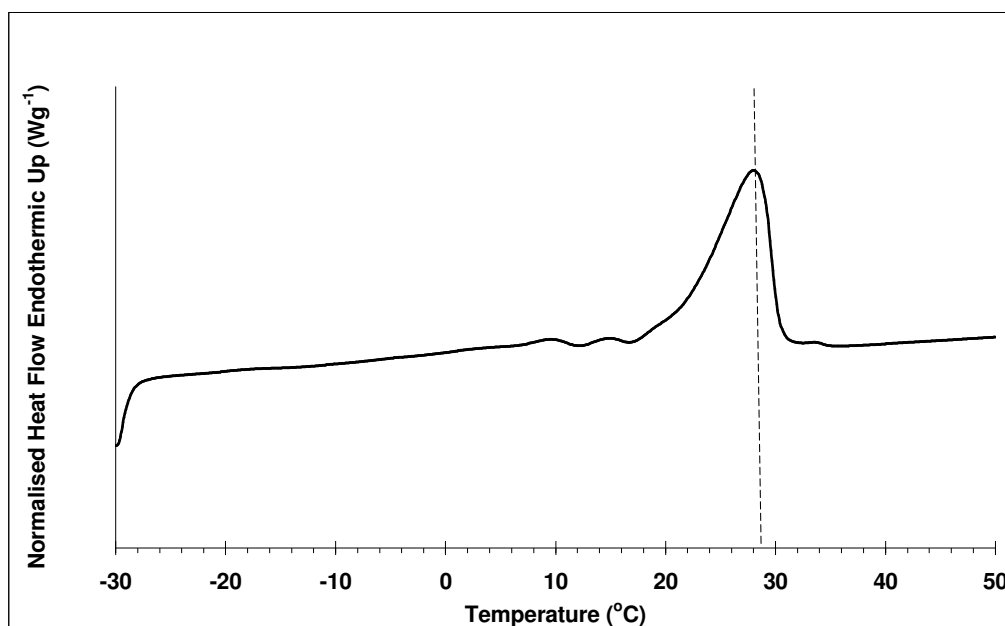


**Figure 4.7: Melting profile (at 10 °C min<sup>-1</sup>) of industrially tempered chocolate sample after being cooled in the DSC at 1 °C min<sup>-1</sup> to -30 °C**

#### **4.2.3 Fresh chocolate versus ‘aged’ chocolate**

Throughout this research work, only freshly tempered samples, i.e., liquid would be used. It was therefore important to compare how the melting characteristic of a freshly cooled sample, cooled within an hour of production, would differ from one that had undergone ageing, i.e. been stored for a while. These checks were made by a combination of DSC, done within the lab and nuclear magnetic resonance (NMR) results supplied by the analytical lab at Cadbury Trebor Basset in Bournville. The NMR results in Figure 4.8 show the evolution of the solid fat content (SFC) of the chocolate with time. It can be seen that as time progressed, the SFC of the chocolate increases, stabilising after 9 days. This increase in the SFC will also have an effect on the melting of the chocolate.

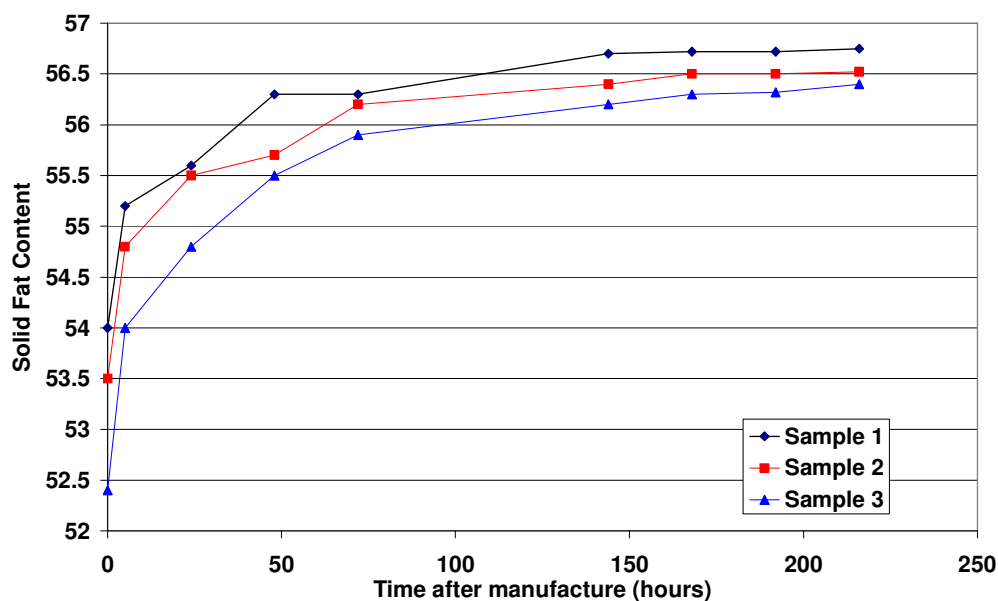


**Figure 4.8: Evolution of solid fat content measured by NMR of 3 chocolate samples taken from the industrial temperer**

DSC experiments were also carried out to show the difference between freshly tempered and cooled chocolate with samples that had been stored for longer periods of time. The DSC results comparing the melting profile of aged chocolate samples and that of a freshly tempered one are shown in Figure 4.9. The explanation for the increase in the peak melting temperature is due to the growth and stabilisation of the Form V crystals within the chocolate upon storage contributing to an overall increase in the SFC. The perfection of the crystals will contribute to the higher melting point as more energy is required to break the lattices down. Upon storage, as shown by sample D in Figure 4.9, eventually the Form V crystals will transform to Form VI, which has a higher melting point of 36.2 °C and heat of crystallisation of 148.2 kJ. kg<sup>-1</sup> (Rudnicki and Niezgódka, 2002)

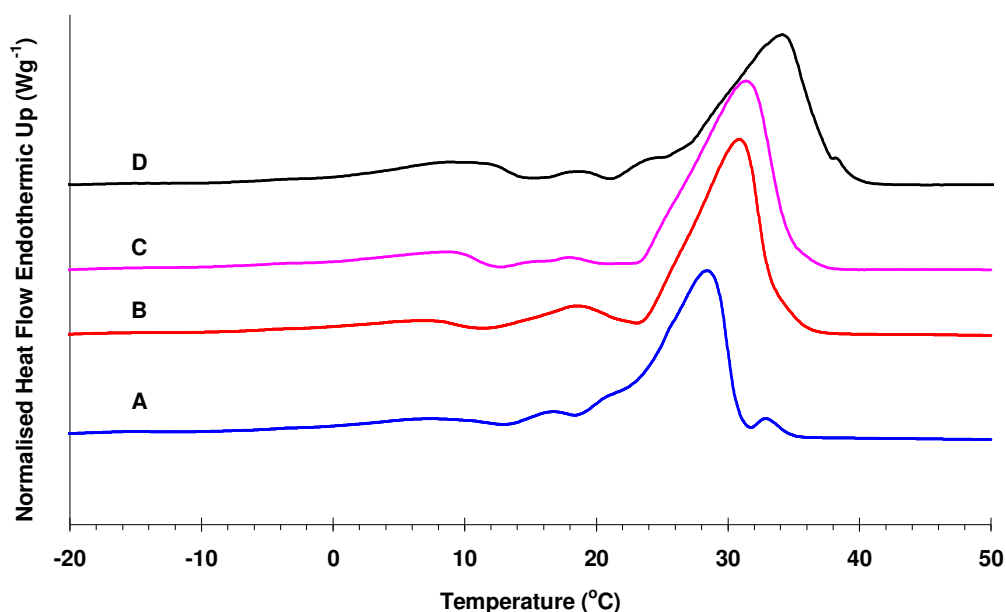


**Figure 4.9: DSC melting profiles of freshly tempered and cooled (at  $1\text{ }^{\circ}\text{C min}^{-1}$ ) sample (A) and aged samples; cooled tempered sample after 24h (B), 3 month old commercial chocolate sample (C) and 1 year old chocolate (D)**

Hence, after these series of optimisation and tests, it was shown that the best tempering profile to be used for future chocolate samples was melting under shear at  $55\text{ }^{\circ}\text{C}$  for 20 min then cooling to  $22\text{ }^{\circ}\text{C}$  and holding for 8 min and finally, reheating to  $28\text{ }^{\circ}\text{C}$  and holding for 6 min.

### 4.3 Tempering of chocolate fats

Having finalised the tempering procedure for chocolate, it was now equally important to determine the correct profile for chocolate fats. The main differences between the chocolate and the chocolate fats were the absence of sugar and cocoa mass in the latter. The absence of sugar meant that the viscosity of the chocolate fats was significantly less than that of chocolate and one of the implications of this was the need of extending the amount of time



the sample was sheared during tempering. One solution to the reduced viscosity was the addition of salt (NaCl) to molten chocolate fats. Salt would not interfere with either DSC or X-ray diffraction patterns analysis because its melting point (800.8 °C) is much higher than the temperature range studied (-30 to 50 °C) and the diffraction patterns given by salt crystals do not interfere with the fats in the range used (4- 35° 2 $\theta$ ).

#### **4.3.1 Tempering with salt**

The first tempering profile used for chocolate fats was the one determined for chocolate. The profile was as follows:

Melt under shear with salt at 55 °C for 20 min

Cool to 22 °C and hold for 8 min and finally,

Reheat to 28 °C and hold for 6 min.

5g of salt (NaCl) was added to the molten chocolate fats mixture prior to tempering. A sample was taken from the temperer, sealed into a DSC pan, inserted in the DSC at 28 °C and cooled in the DSC at 1 °C min<sup>-1</sup>, followed by heating at 10 °C min<sup>-1</sup>. This result is shown in Figure 4.10. As shown by the results, this profile did not result in the formation of Form V crystals, which would have had a melting point of ~ 28 °C but instead favoured the formation of lower melting polymorphs.

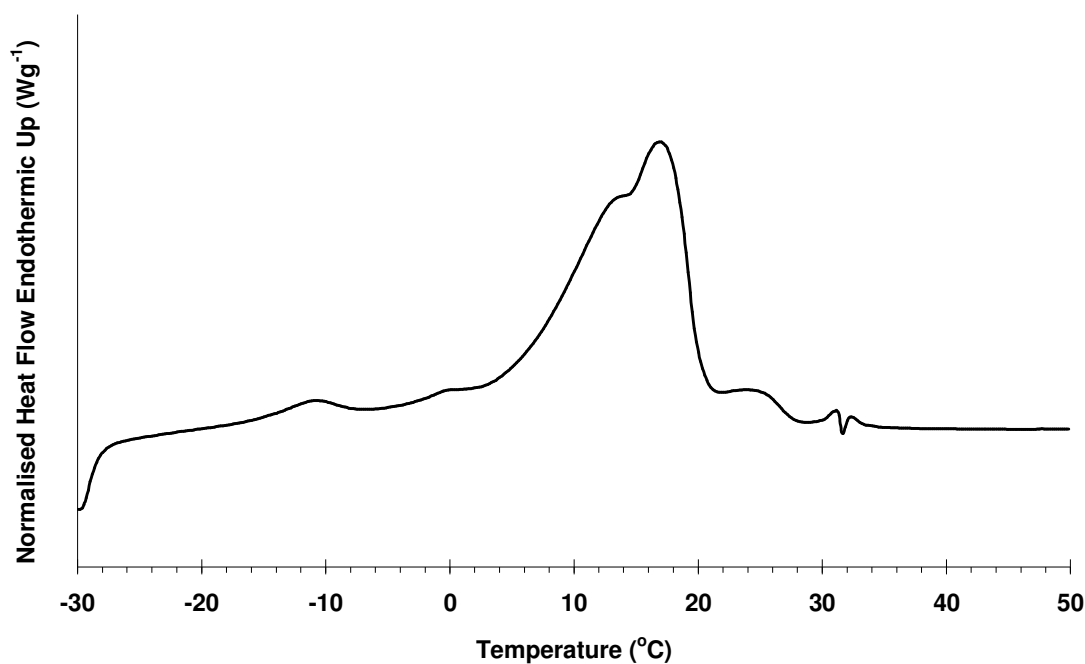


**Figure 4.10: DSC melting profile of chocolate fats tempered using chocolate profile. The sample was cooled at  $1\text{ }^{\circ}\text{C min}^{-1}$  prior to melting.**

The tempering profile was then modified. The initial melting temperature was lowered to  $50\text{ }^{\circ}\text{C}$  for 10 min. This was followed by cooling to  $20\text{ }^{\circ}\text{C}$  for 20 min and finally, reheating to  $29.5\text{ }^{\circ}\text{C}$  for 12 min. This produced a viscous yellowish material. A sample was then cooled at  $1\text{ }^{\circ}\text{C min}^{-1}$  in the DSC and heated at  $10\text{ }^{\circ}\text{C min}^{-1}$  to test for temper. This result is shown in Figure 4.11. It can be seen that the major melting event has a peak melting temperature of  $\sim 29\text{ }^{\circ}\text{C}$ , with a minor peak at  $\sim 9\text{ }^{\circ}\text{C}$  and a small shoulder occurring between  $32$  and  $36\text{ }^{\circ}\text{C}$ . This result suggested that the sample was tempered with sufficient Form V nuclei being generated.

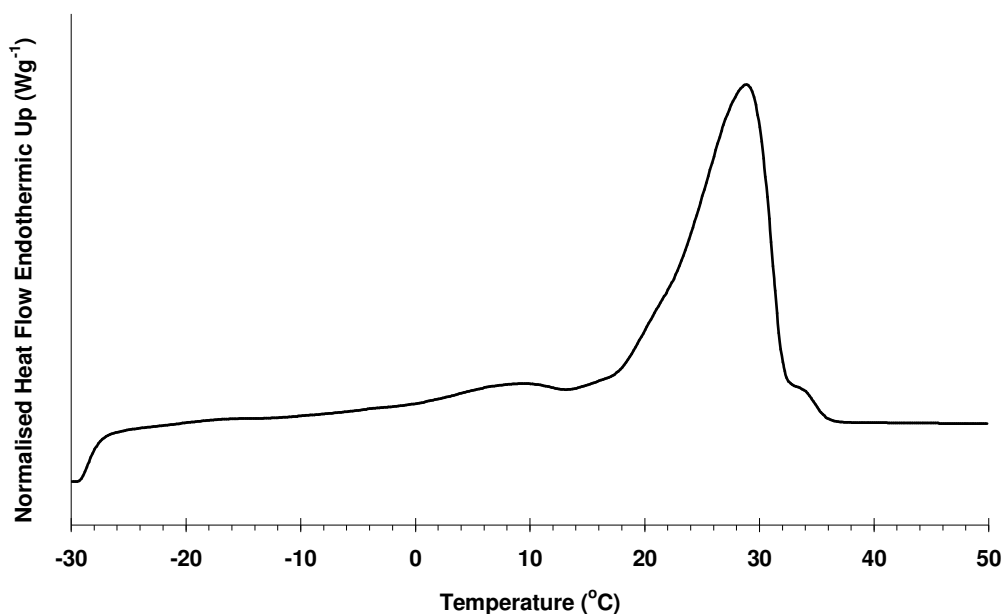


**Figure 4.11: Melting profile of chocolate fats sample tempered with the modified profile. The sample was cooled at  $1\text{ }^{\circ}\text{C min}^{-1}$  prior melting**

A sample of this material was also analysed in the X-ray. The sample was spread onto the holder which was held at  $29.5\text{ }^{\circ}\text{C}$  and the X-ray pattern was acquired. This pattern is shown (bottom) in Figure 4.12 together with the X-ray pattern of a solidified tempered chocolate fat sample stored at room temperature ( $20\text{ }^{\circ}\text{C}$ ) for 24h (top). As can be seen, the freshly tempered chocolate fats sample has a significant proportion of liquid and only a very small amount of crystalline material as shown by the d-spacing at  $4.58\text{ }\text{\AA}$  (Wille and Lutton, 1966) , indicating the presence of Form V crystals. Upon cooling and storage, the liquid proportion decreases and the proportion of crystalline material (Form V) significantly increases. This proves that the tempering profile was appropriate for the chocolate fat mixture.

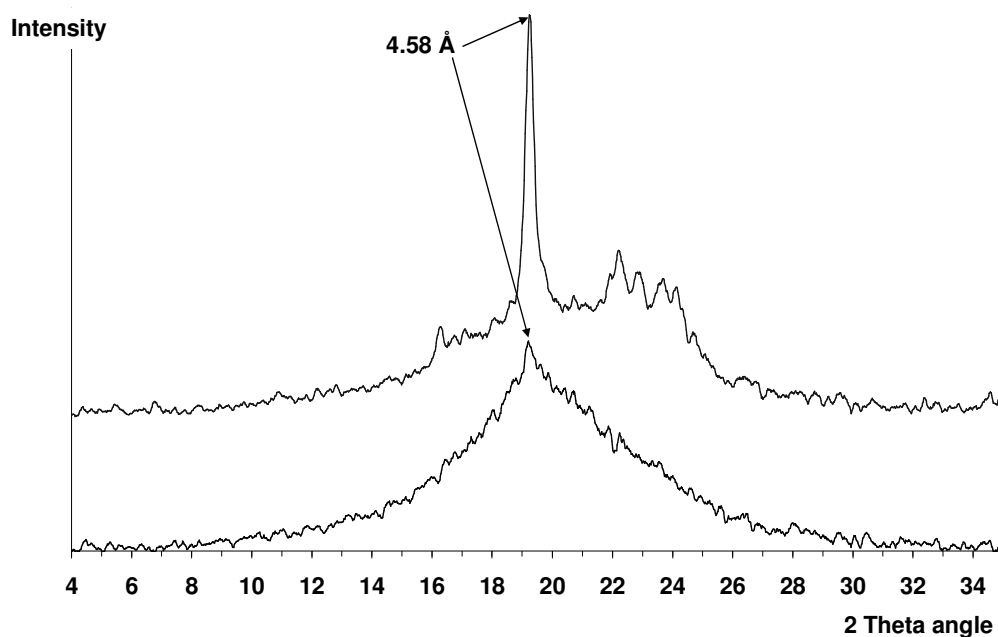


**Figure 4.12: X-ray diffraction pattern of freshly tempered chocolate fats (bottom) and solidified tempered chocolate fats stored at room temperature for 24 h (top)**

#### **4.3.2 Tempering without addition of salt**

Having determined the appropriate tempering conditions for the chocolate fats, it was decided to try tempering without the addition of salt and note any differences this made. The melting DSC thermogram of such sample is presented in Figure 4.13 together with one that was tempered with salt. As can be seen, the 2 traces are almost identical with both having a peak melting temperature of  $\sim 29^{\circ}\text{C}$  and it was therefore decided not to include salt in the future sample preparations.

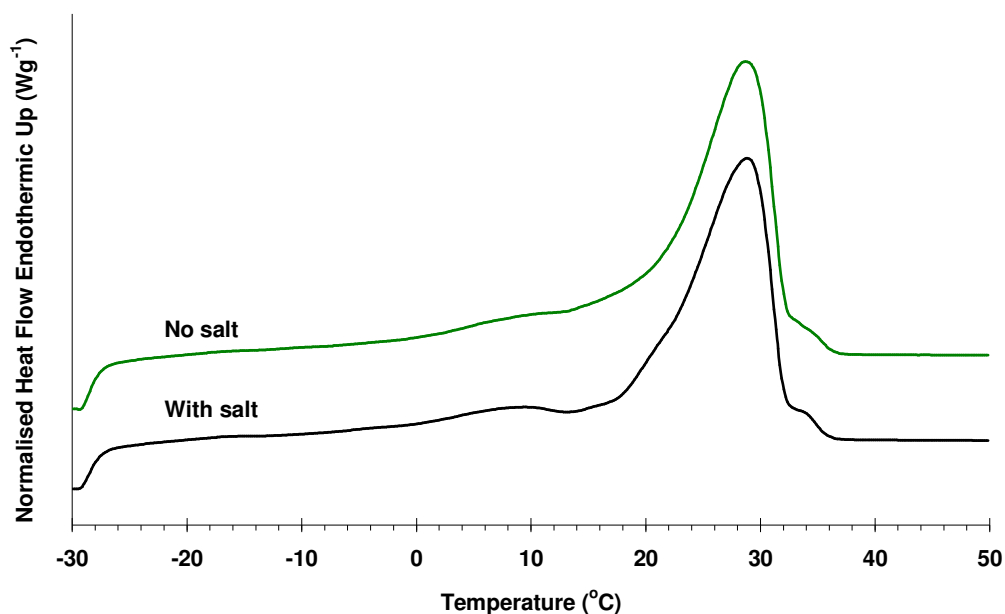


**Figure 4.13: Comparison of DSC melting thermograms for chocolate fats tempered with salt (bottom) and without salt (top). Note that the samples were cooled to  $1\text{ }^{\circ}\text{C min}^{-1}$  prior to heating**

#### **4.4 Tempering of cocoa butter**

Tempering of cocoa butter was more straightforward than for the chocolate and the fats mixture. The tempering profile used was one supplied by RSSL and was deemed most suitable for this particular type of cocoa butter supplied. The profile used was: melt for 10 min at  $55\text{ }^{\circ}\text{C}$ , cool for 20 min at  $25\text{ }^{\circ}\text{C}$  and reheat at  $31\text{ }^{\circ}\text{C}$  for 8 min. A sample was then examined in the DSC and the result is shown in Figure 4.14. Although the DSC thermogram showed the presence of some lower forms and possibly lower melting point triacylglycerols, indicated by peaks at  $13$  and  $28\text{ }^{\circ}\text{C}$ , the sample was mostly in the Form V state. X-ray diffraction, carried out at  $31\text{ }^{\circ}\text{C}$  on this sample, in Figure 4.15 also shows that despite being mostly amorphous in nature, the sample did possess Form V

crystals and no lower forms could be picked up on the X-ray trace. This suggests that the amount of lower forms may be significantly less than that of Form V and hence would not interfere significantly with any future results. Another explanation for the presence of lower melting point polymorphs could be the absence of a holding period prior to scanning in the DSC. Had this sample been held isothermally at around 25 °C prior to heating, only Form V would have been obtained. However, as the sample was scanned immediately after cooling, this allowed other lower melting polymorphs to be formed as well.

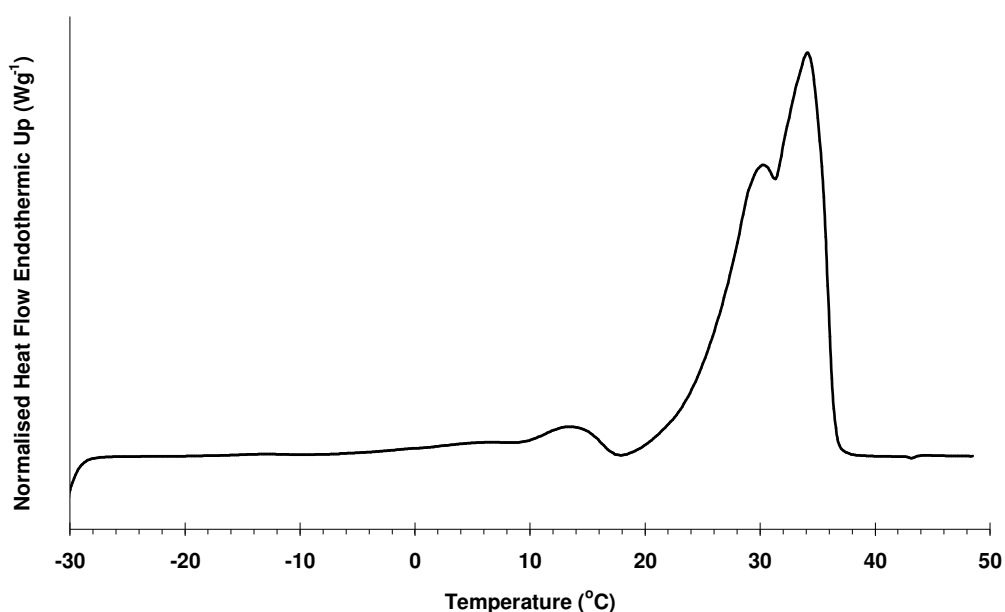


**Figure 4.14: DSC melting profile of a tempered cocoa butter sample**

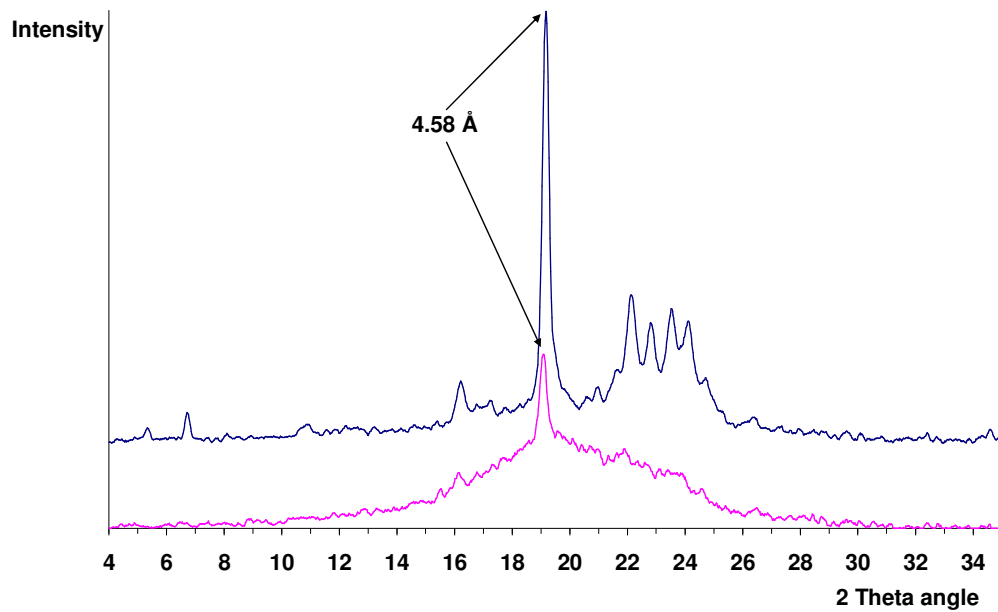


**Figure 4.15: X-ray pattern of freshly tempered cocoa butter (bottom) and the same sample stored at 20 °C for 24h (top)**

## 4.5 Conclusions

This chapter looked at the various tempering trials and tests carried out in order to determine the tempering profile most suitable for the chocolate being studied. Although this proved to be a lengthy set of trial, it was of crucial importance as the level of temper of the chocolate would have significant influence on subsequent results obtained using different experimental techniques. Having found the appropriate tempering profile for chocolate, it was then easier to determine one for chocolate fats and indeed for cocoa butter, this process was more straightforward.

## **Chapter 5: Effect of the rate of cooling and heating on the phase behaviour of chocolate using differential scanning calorimetry**

*This chapter uses conventional DSC to study the effect of cooling and heating rates on melting and crystallisation of chocolate. Comparison between tempered and untempered samples is made. Effect of cooling rate on cocoa butter and chocolate fats is also discussed*



## **5 Effect of the rate of cooling and heating on the phase behaviour of chocolate using DSC**

### **5.1 Introduction**

As previously discussed in the introduction and literature review, it is a well recognised fact that the polymorphic forms of cocoa butter obtained on cooling chocolate is dependent on the cooling rate. The previous generally accepted view that rapid cooling leads to unstable lower polymorphic forms in the final chocolate has been questioned partly as a result of the success of the Frozen Cone Process. The observation of high melting polymorphic forms in a process such as this could result not only from formation of the high melting point forms on cooling but also possible transformation of lower melting polymorphs upon reheating.

Two techniques were used to investigate the changes in polymorphic forms of chocolate during both cooling and subsequent heating.

1. DSC (results presented in this chapter): this identifies the temperature of phase transitions and the magnitude of these. Since the temperature of a melting transition depends on the polymorph present, the technique can provide some evidence as to which forms are present
2. X-ray diffraction (results in the next chapter): In contrast to DSC this technique is not well suited to measuring melting transitions; however, it can provide identification of which form is present at a particular

temperature.

For this work, three different fat systems were used namely chocolate, cocoa butter and chocolate fats. The majority of the DSC experiments were carried out on chocolate as this was the main subject of the investigation while experiments using the two other materials were done for confirmatory purposes.

## **5.2 Effect of slow cooling on tempered chocolate**

As mentioned in the literature review, slow cooling is deemed to induce the formation of Form V crystals in tempered chocolate. It is important to stress that it is only upon melting the sample that any change induced by cooling can be detected. Experimental results showing a typical melting thermogram of lab-tempered chocolate cooled at  $1^{\circ}\text{C}.\text{min}^{-1}$  are shown in Figure 5.1.

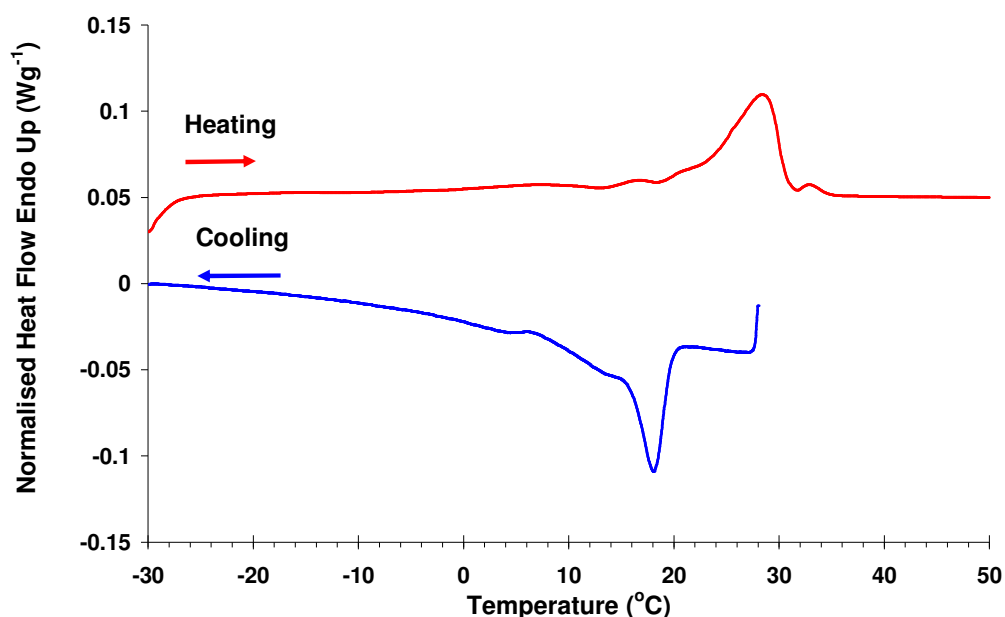


**Figure 5.1: Tempered chocolate cooled at 1 °C min<sup>-1</sup> to -30 °C then heated at 10°Cmin<sup>-1</sup> (For clarity the heating rate has been normalised to a rate of 1 °C.min<sup>-1</sup>)**

It can be seen from the cooling curve that the major crystallisation event takes places at 18 °C. This event relates to the crystallisation of Form V nuclei, which were formed during the tempering process. The other minor crystallisation events after the major one are believed to be due to the triacylglycerols in milk fat crystallising as well. Upon heating this sample, a major endotherm is seen at a peak temperature of 28.4 °C, which is attributed to the melting of Form V crystals. As mentioned in Chapter 4, the lower peak melting point of Form V (28.4 °C) as opposed to 33.8 °C for pure cocoa butter is assumed to be due to the presence of milk and vegetable fats depressing the melting point of Form V in the chocolate mixture. The thermogram indicates that for tempered chocolate at a low cooling rate, the thermodynamics favour the growth of Form V rather than the nucleation and growth of lower forms. This is in agreement with current manufacturing practice. The minor

endotherms occurring at temperatures of ~7, 17 and 21 °C on heating are believed to be due to the melting of milk fat triacylglycerols which solidified during the cooling process.

### 5.3 Effect of rapid cooling on tempered chocolate

In order to assess the impact of rapid cooling, tempered chocolate was cooled in the calorimeter at a rate of 10, 20 and 30 °C.min<sup>-1</sup>. Cooling at these rates would be expected to lead to the formation of lower melting temperature polymorphs (Hagemann, 1988) . It is worth noting however that the melting response of the rapid cooled chocolate exhibited a high degree of variability at higher heating rates. Two types of behaviour were observed and are illustrated in Figure 5.2.

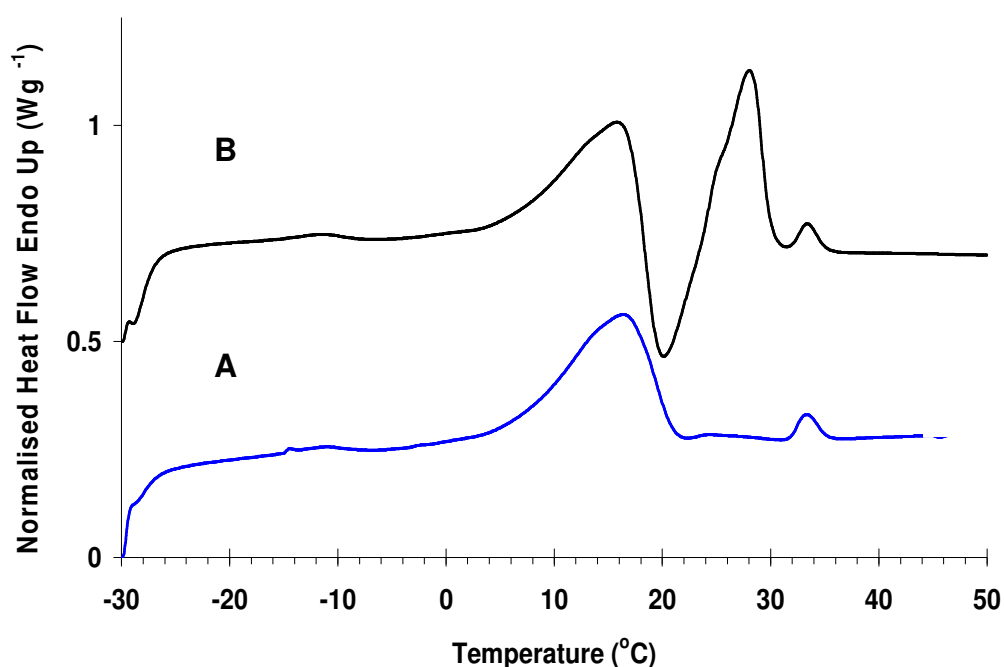


**Figure 5.2: The two different type of behaviour observed upon melting of rapidly cooled tempered chocolate; melting profile similar to untempered chocolate (A) and pronounced recrystallisation behaviour (B). Both thermograms were obtained after cooling a tempered chocolate sample at a rate of 10°C.min<sup>-1</sup>**

Thermogram A, obtained after cooling a tempered chocolate at  $10^{\circ}\text{C}.\text{min}^{-1}$ , shows melting behaviour similar to that of untempered chocolate with a peak temperature of  $\sim 16.7^{\circ}\text{C}$  and a minor endotherm at  $\sim 33.5^{\circ}\text{C}$ . The second behaviour, as shown by B also obtained following cooling a tempered sample at  $10^{\circ}\text{C}.\text{min}^{-1}$ , shows melting at a peak temperature of  $\sim 16.5^{\circ}\text{C}$  followed by recrystallisation at  $20.4^{\circ}\text{C}$  and finally melting at a peak of  $28.4^{\circ}\text{C}$ . The term recrystallisation is used here as this crystallisation behaviour is being picked up following a melting event and is occurring during the heating of the sample. The pronounced recrystallisation exotherms were observed in approximately 1 sample out of 3 at rates greater than  $10^{\circ}\text{C}.\text{min}^{-1}$  in conventional DSC runs. Table 5.1 shows data on the number of runs at different cooling rates and the proportion of samples showing this recrystallisation exotherm. These samples were all then subjected to a heating rate of  $10^{\circ}\text{C}.\text{min}^{-1}$ .

**Table 5.1: Number of experiments carried out at different cooling rates showing recrystallisation exotherm upon melting. All the experiments were subjected to a heating rate of  $10^{\circ}\text{C}.\text{min}^{-1}$ .**

Cooling rate	Number of experiments done	Number of experiments showing exotherms	% of experiments showing recrystallisation exotherm on heating
<b><math>1.0^{\circ}\text{C}.\text{min}^{-1}</math></b>	40	0	0 %
<b><math>10^{\circ}\text{C}.\text{min}^{-1}</math></b>	25	14	56 %
<b><math>20^{\circ}\text{C}.\text{min}^{-1}</math></b>	20	7	35 %
<b><math>30^{\circ}\text{C}.\text{min}^{-1}</math></b>	20	5	25 %
<b>Quenching in liquid nitrogen</b>	20	4	20 %

This variability is unlikely to be due to variation in the initial degree of temper of the chocolate since the samples were uniformly sheared in the temperer in order to evenly distribute Form V nuclei throughout the sample. Furthermore, increasing sample size to increase the number of nuclei in a given DSC pan and address potential heterogeneity in nuclei had no significant impact. A more likely explanation therefore is the inverse relationship between heating rate and time being allowed for recrystallization events to proceed. A lower heating rate would allow more time for the system to convert to higher forms over a wider temperature range. This is addressed further in Chapter 6 with the use of Stepscan DSC which allows a lower heating rate and a longer isothermal hold time during the melting phase. For comparison, a typical Stepscan DSC experiment lasts on average 4 hours compared with 1.5 hours for a conventional DSC run.

The type of behaviour shown on thermogram B in Figure 5.2 is believed to be representative of what happens industrially during the Frozen Cone process and subsequent processing steps leading to the final chocolate shell. Therefore the remainder of the DSC results for rapidly cooled chocolate will focus on those which upon heating exhibit the recrystallisation exotherm which leads to the formation of a higher polymorph.

A typical DSC result for cooling at  $10\text{ }^{\circ}\text{C}.\text{min}^{-1}$  is shown in Figure 5.3

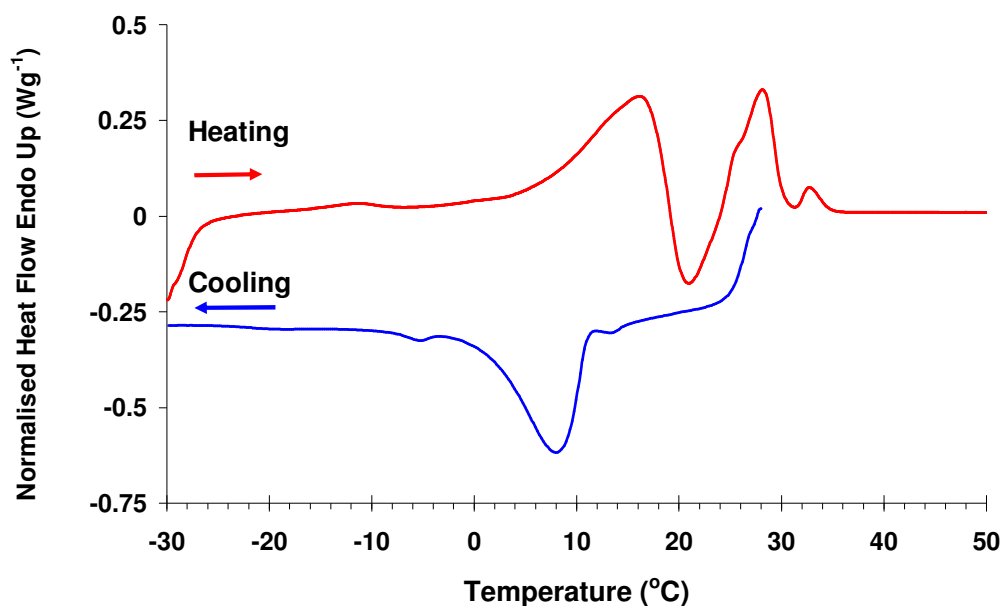


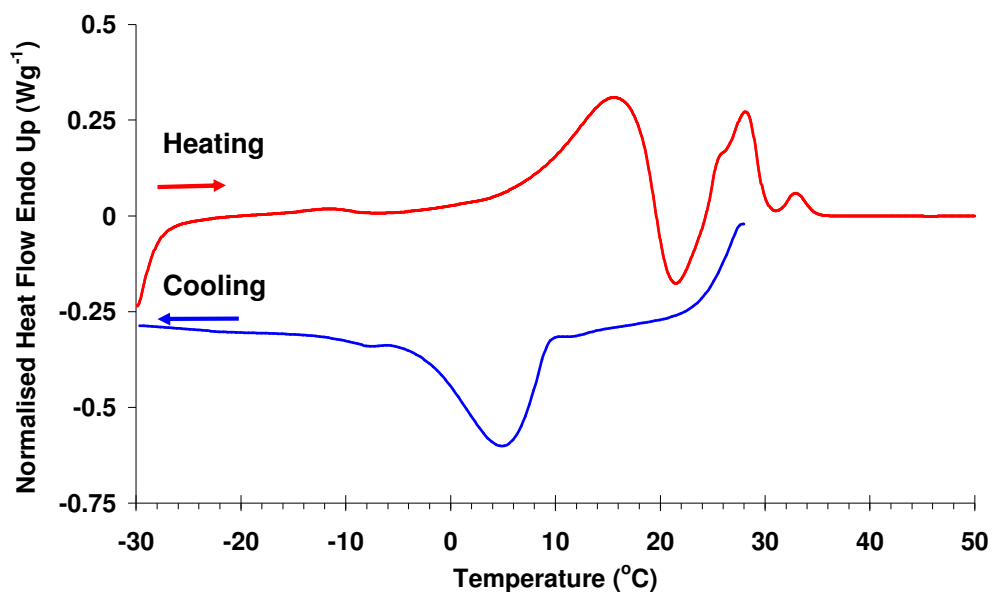
**Figure 5.3 : DSC thermogram for a tempered chocolate initially cooled at  $10^{\circ}\text{C.min}^{-1}$  to  $-30^{\circ}\text{C}$  followed by heating at  $10^{\circ}\text{C.min}^{-1}$  to  $50^{\circ}\text{C}$ .**

In comparison to chocolate cooled at  $1^{\circ}\text{C.min}^{-1}$  (Figure 5.1), the major exotherm upon rapid cooling is seen at a temperature of  $8^{\circ}\text{C}$  and not at  $18^{\circ}\text{C}$  as seen when cooling at  $1^{\circ}\text{C.min}^{-1}$ . The melting thermogram of this rapidly cooled tempered chocolate shows the presence of an endotherm at  $\sim 16^{\circ}\text{C}$ , followed by an exotherm centred at  $\sim 20.5^{\circ}\text{C}$ . This recrystallisation is immediately followed by another major endotherm, having a peak temperature of  $28.4^{\circ}\text{C}$ . This pattern suggests that at a cooling rate of  $10^{\circ}\text{C.min}^{-1}$ , a significant fraction of chocolate crystallized into low melting point polymorphs, which melted on heating and subsequently recrystallised into higher melting temperature ones. These then melted at temperatures comparable to those of the higher melting temperature polymorphs obtained on slow cooling (Figure 5.1). As with the chocolate cooled at  $1^{\circ}\text{C.min}^{-1}$ , there is evidence for a small amount of a higher melting point polymorph ( $\sim 33^{\circ}\text{C}$ )

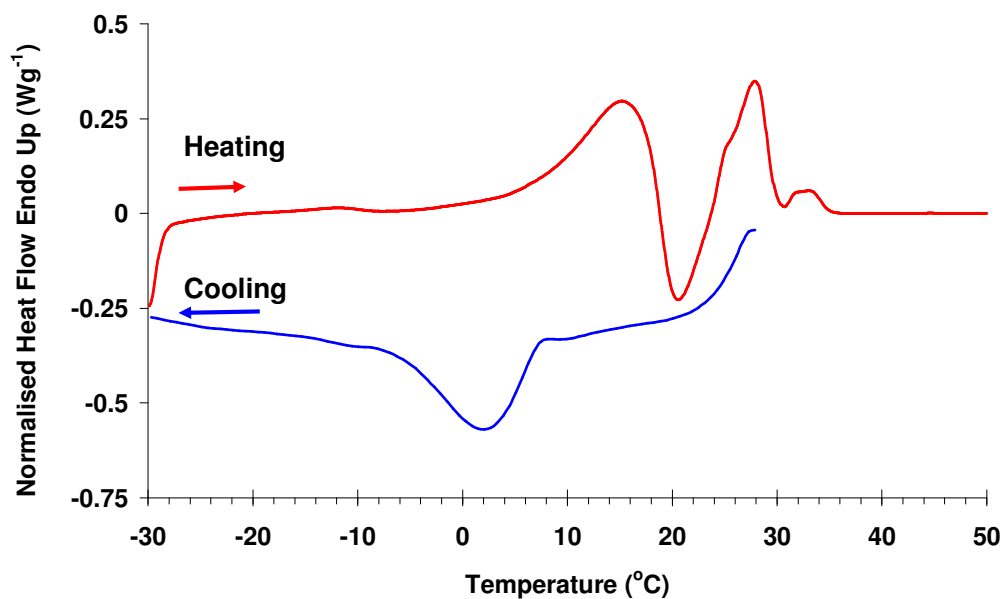
which is believed to be Form VI.

Figure 5.4 and Figure 5.5 show the results of cooling tempered chocolate at a rate of 20 and 30 °C.min<sup>-1</sup> respectively.. The major exotherm on cooling moves to a lower temperature (5° C for cooling at 20°C.min<sup>-1</sup> and 2° C for cooling at 30°C.min<sup>-1</sup>). An explanation for this could be that the faster the cooling rate, the lower the temperature at which the polymorphs crystallise or that different polymorphs are formed depending on the cooling rate utilised. These results also indicate that at the higher cooling rates, the kinetics favour the formation of lower polymorphs than found at rates of 1 °C.min<sup>-1</sup>. This will be further discussed in light of the X-ray data. The heating response is similar to that seen following cooling at 10 °C.min<sup>-1</sup>. First, a major endotherm is seen with a peak temperature of ~16° C (15.6° for cooling at 30 °C.min<sup>-1</sup>), with the recrystallisation event occurring at ~21.8° C (21° C for cooling at 30 °C.min<sup>-1</sup>). This is followed by melting at a peak of 28.4° C in both cases. A small shoulder at ~26° (25.4° C for cooling at 30 °C.min<sup>-1</sup>) is also observed on this endotherm. This could be due to either some Form IV forming during the recrystallisation exotherm or could also be attributed to the melting of milk fat triacylglycerols that also could have been formed during the recrystallisation exotherm. These results seem to suggest that the rate of rapid cooling does not have an effect on the endotherms and recrystallisation exotherm formed during heating of the rapidly cooled sample.





**Figure 5.4: DSC thermogram for a tempered chocolate initially cooled at 20°C.min<sup>-1</sup> to -30 °C followed by heating at 10 °C.min<sup>-1</sup> to 50°C.**



**Figure 5.5: DSC thermogram for a tempered chocolate initially cooled at 30°C.min<sup>-1</sup> to -30 °C followed by heating at 10 °C.min<sup>-1</sup> to 50°C.**

### 5.3.1 Quench-cooling chocolate samples in liquid nitrogen

Very rapid cooling was achieved by immersing sealed DSC pans containing

tempered chocolate into liquid nitrogen and immediately inserting them into the calorimeter to minimise ice formation on the outside of the pans. The subsequent heating profiles at rates of 10, 5 and 1 °C.min<sup>-1</sup> are shown in Figure 5.6 to Figure 5.8 respectively. The essential features of the heating curve seen for the samples conventionally cooled at rates of 10 to 30 °C.min<sup>-1</sup> are retained. Minor presence of ice formation is picked up at ~ 0 °C. Essentially, quench cooling in liquid nitrogen results in the formation of 2 major endotherms, separated by a recrystallisation event. It is of some interest to note that the temperature of the recrystallisation exotherm does not appear to be strongly dependent on the heating rate with it occurring at ~21.8° for heating at 10 °C.min<sup>-1</sup>, 21.5° for 5 °C.min<sup>-1</sup> and 18.8° for heating at 1°C.min<sup>-1</sup>. This suggests that the recrystallisation is a very rapid process. It is worth mentioning that these results also showed a lot of variation like the previous rapidly cooled experiments. Only 20 % of runs for quench-cooled samples showed the pronounced recrystallisation exotherm upon heating, regardless of the heating rate used. The difference in the temperatures between the lower and higher rates of heating can be explained by the effect of thermal lag caused by the higher heating rates (Cebula and Smith, 1991) . As found by the same authors (Cebula and Smith, 1991) , a lower heating rate (Figure 5.8) also sharpens the transitions observed with a higher heating rate broadening both endo- and exotherms observed upon heating. The result of slow heating (Figure 5.8) also suggests that the lower heating rate favours the formation of more stable (higher melting) polymorphs as evidenced by the higher magnitude of the second endotherm (peak of ~28.4 °C) compared to the first one (peak of ~16 °C). At the higher heating rates (Figure 5.6 and Figure 5.7), more lower

melting polymorphs are formed. However, although resolution is improved by a lower scanning rate, sensitivity is better with a higher one ( $10\text{ }^{\circ}\text{C.min}^{-1}$ ), hence it was decided to use a heating rate of  $10\text{ }^{\circ}\text{C.min}^{-1}$  for all DSC experiments, except for Stepscan DSC which will be further discussed in Chapter 7. It is also important to stress that the heating rate will not influence the state of the cooled chocolate, i.e., the heating rate will not affect the type of polymorph the material is set in when it was cooled at a particular rate. The comparison of heating rates only is only showing the differences in the polymorphs during melting.

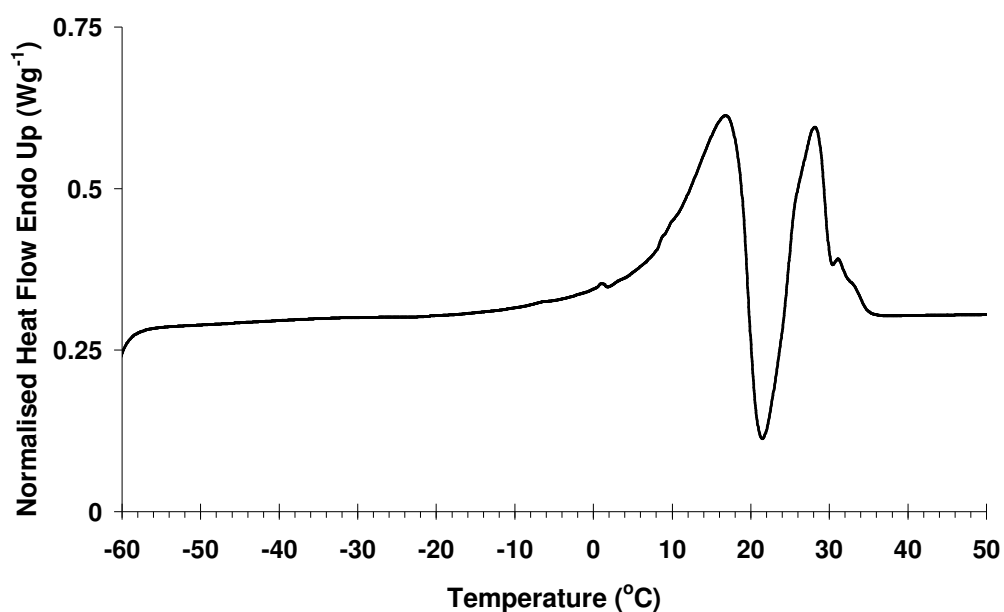


**Figure 5.6: Tempered chocolate quenched in liquid nitrogen and warmed at  $10\text{ }^{\circ}\text{C.min}^{-1}$  from  $-65$  to  $50\text{ }^{\circ}\text{C}$**

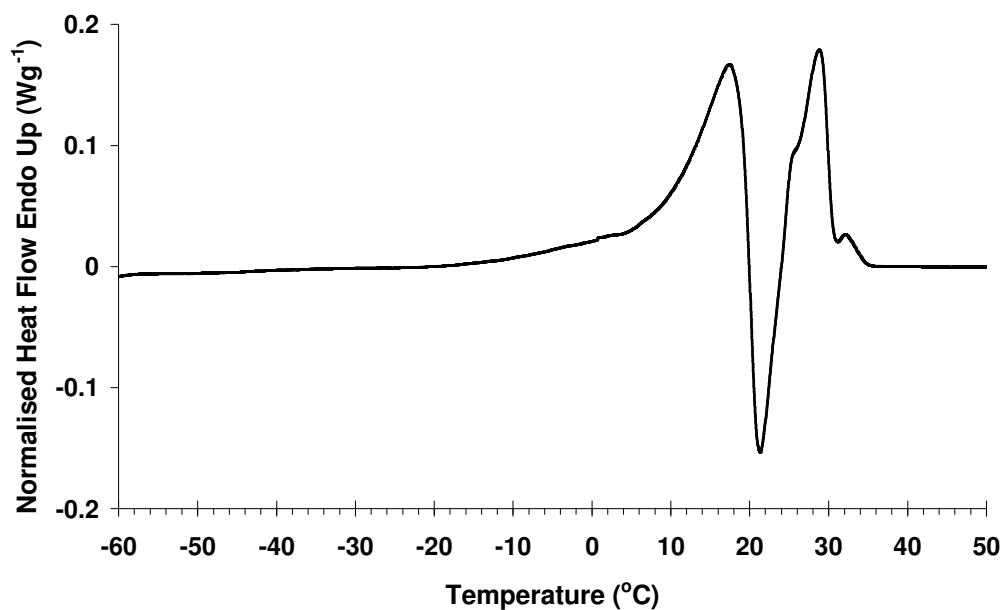


**Figure 5.7: DSC thermogram of tempered chocolate quenched in liquid nitrogen and warmed at 5 °C.min<sup>-1</sup>**

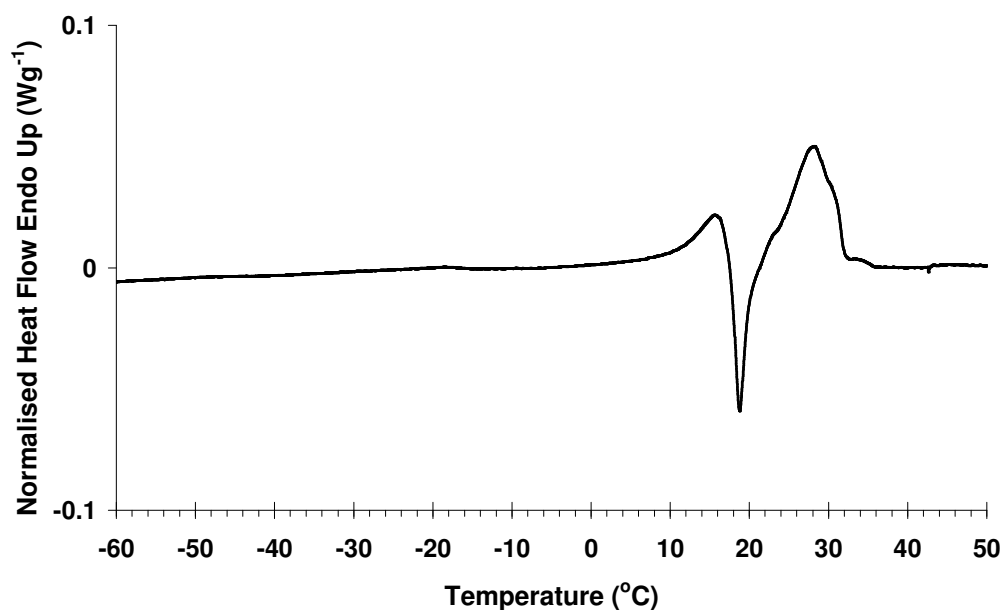


**Figure 5.8: DSC thermogram of tempered chocolate quenched in liquid nitrogen and warmed at 1 °C.min<sup>-1</sup>**

#### **5.4 Effect of cooling rate on untempered chocolate**

It is of interest to compare the effect of cooling rate on crystallisation processes in untempered chocolate. Figure 5.9 shows the results of slow cooling. As

would be expected when this is compared with Figure 5.1, crystallisation of lower melting polymorphs results. On subsequent heating, these have a peak melting temperature of  $\sim 18\text{ }^{\circ}\text{C}$  compared with  $28.4\text{ }^{\circ}\text{C}$  observed for tempered chocolate. On the cooling curve for the untempered chocolate, a small exotherm is observed between  $15$  and  $21\text{ }^{\circ}\text{C}$ . This could be attributed to the crystallisation of the remnants of the incomplete melting of Form V or VI crystals in the chocolate or due to the  $\beta$ -memory effect of cocoa butter as described by Van Malssen et al., (1996), van Langevelde et al., (2001a), and van Langevelde et al., (2001b) . Since the sample was completely melted at  $80\text{ }^{\circ}\text{C}$ , it is also possible that these minor crystallisation events are due to the presence of high melting milk fat triacylglycerols solidifying upon cooling and subsequently melting. If any Form V nuclei had been present; there would have been a peak indicative of their melting at  $\sim 28.4\text{ }^{\circ}\text{C}$  on the subsequent melting curve. However, this is not the case as no such peak is seen on Figure 5.9., hence the small shoulder seen in the melting thermograms is attributed to high melting milk fat TAGs.

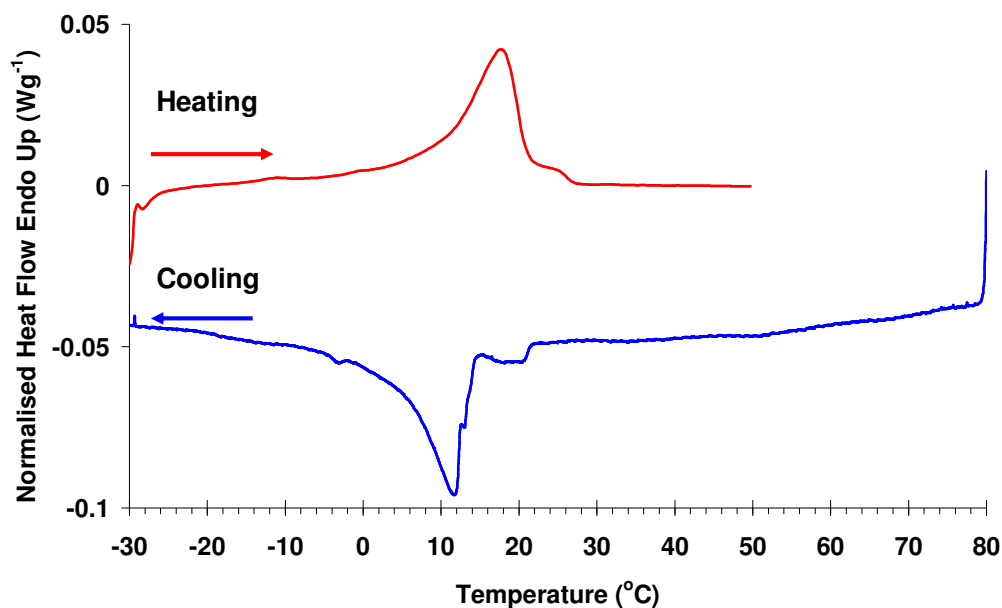


**Figure 5.9: Untempered chocolate cooled at 1 °C.min<sup>-1</sup> then heated up at 10°C.min<sup>-1</sup> (For clarity the heating rate has been normalised to a rate of 1 °C.min<sup>-1</sup>)**

There is suggestion from the Mars patent (Willcocks et al., 2002) that rapid cooling according to the method described in the patent can be carried out on ultra-low and even non tempered chocolate and still result in a stable finished chocolate product. The data in Figure 5.10 and Figure 5.11 does not support this view. For untempered chocolate, the characteristic recrystallisation exotherm is not observed for any of the samples examined whether the chocolate is cooled at 10°C.min<sup>-1</sup> or quenched in liquid nitrogen, hence there is no Form V polymorph being formed in the final product.

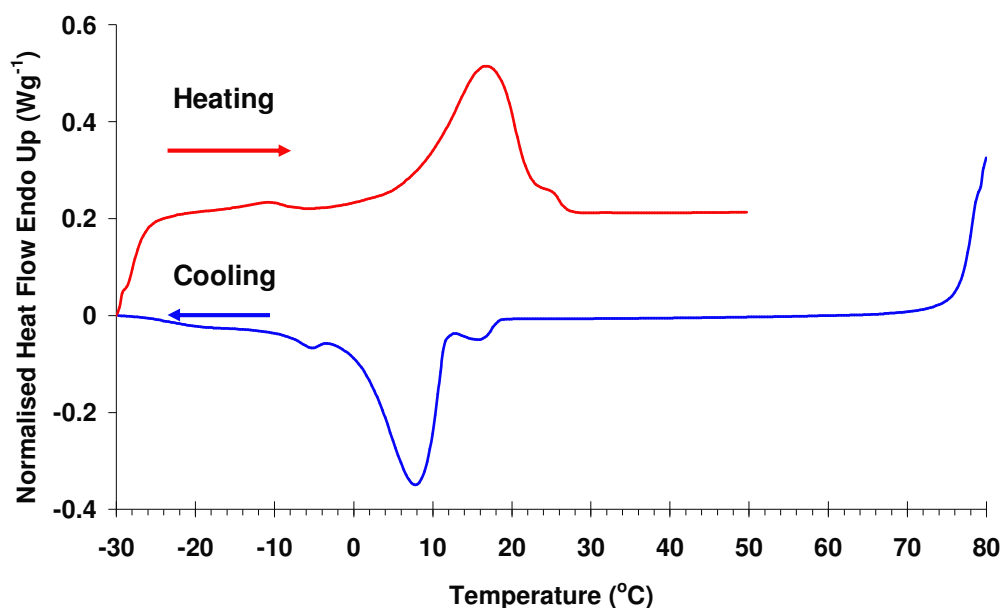


**Figure 5.10: Untempered chocolate cooled at 10 °C.min<sup>-1</sup> then heated up at 10°C.min<sup>-1</sup>**

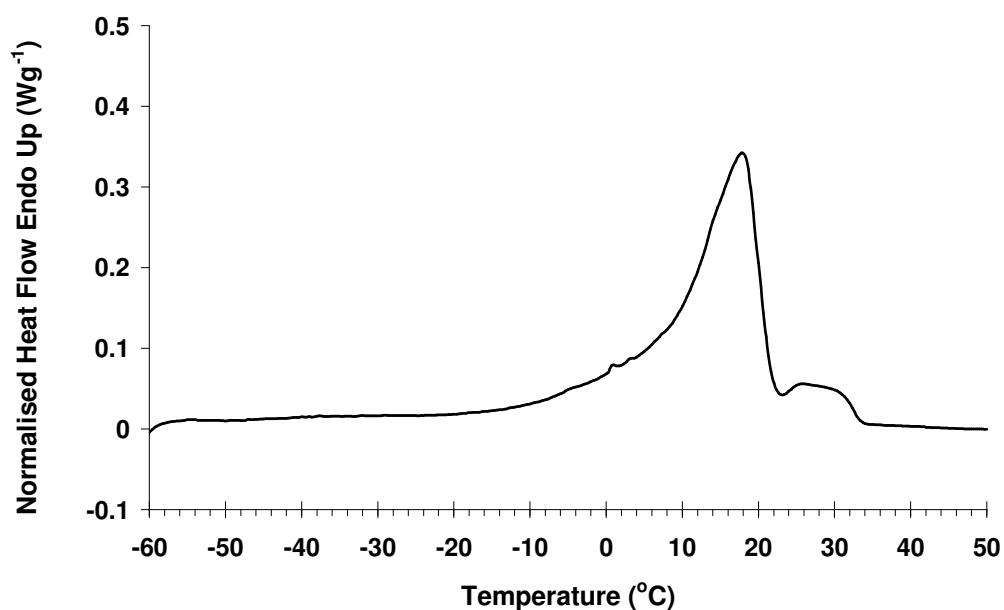


**Figure 5.11: Untempered chocolate quenched in liquid nitrogen followed by heating at 10 °C.min<sup>-1</sup>**

In Figure 5.10 to Figure 5.11, the major endotherm has a peak melting temperature of 18 °C. Only in Figure 5.11 is another minor endotherm observed between 23 and 33 °C. As mentioned previously, this could either be

due to the memory effect of cocoa butter or incomplete melting of Form V crystals in the chocolate. A quench cooled sample of untempered chocolate was also heated at a rate of  $1\text{ }^{\circ}\text{C}\cdot\text{min}^{-1}$  and the result is shown in Figure 5.12. At a lower heating rate, a double peak is seen more clearly with peaks at  $\sim 18.3$  and  $21\text{ }^{\circ}\text{C}$ . This shows the slower heating rate allows separation and formation of 2 different types of polymorphs as opposed to heating at  $10\text{ }^{\circ}\text{C}\cdot\text{min}^{-1}$  where only a single broad peak at  $18\text{ }^{\circ}\text{C}$  is seen. This illustrates the difference between sensitivity and resolution.

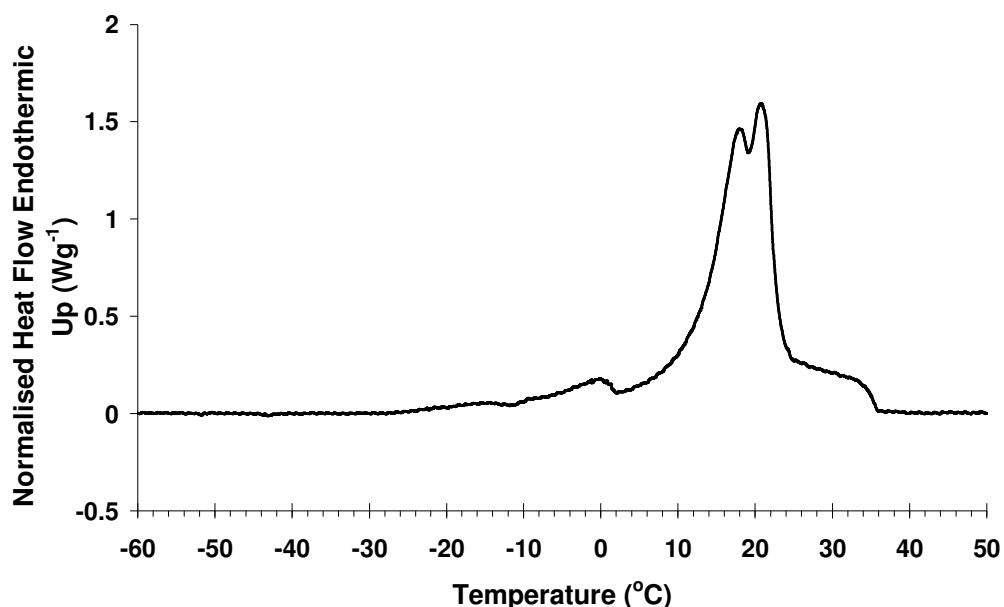


**Figure 5.12: Untempered chocolate quenched in liquid nitrogen followed by heating at  $1\text{ }^{\circ}\text{C}\cdot\text{min}^{-1}$**

### 5.5 Hypothesis developed from DSC results

The DSC results suggest the following hypothesis for the development of different polymorphs upon cooling and subsequent cooling. This is schematically illustrated in Figure 5.13 and Figure 5.14. Upon slow cooling of



tempered chocolate as shown in Figure 5.13, the Form V nuclei generated during tempering grow at the expense of any unstable lower melting polymorph as at this rate the thermodynamics favour its growth. At the end of the cooling process, the product is composed of only Form V crystals. These crystals further mature and stabilise upon storage. Rapid cooling however, as shown in Figure 5.14 favours the growth of lower melting polymorphs at the expense of Form V nuclei, although a tempered material is used during this process. At the end of the rapid cooling process, the matrix is mainly made up of lower polymorphs. After contact cooling and subsequent warming of the product (e.g. while the chocolate shells are being filled, during solidification of the centre and wrapping), the thermodynamics change in favour of the Form V nuclei initially formed. The lower melting polymorphs eventually transform into Form V and hence a product composed of only Form V crystals is obtained.

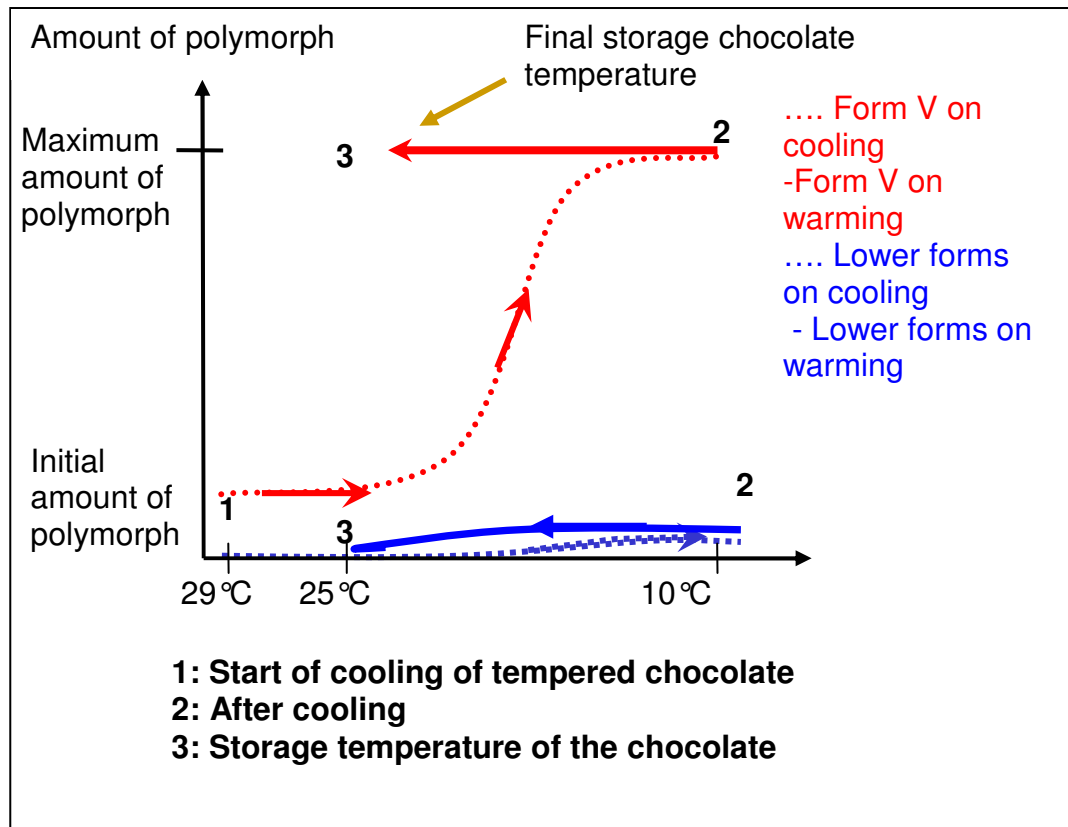


**Figure 5.13: Graphical representation of cooling ( $1\text{ }^{\circ}\text{C}\cdot\text{min}^{-1}$ ) and storage of chocolate and the types of polymorph present during these processes. Dotted red line represents growth of Form V polymorph upon cooling and the solid red line, Form V upon heating. The solid blue line represents growth of lower polymorphic forms upon heating.**

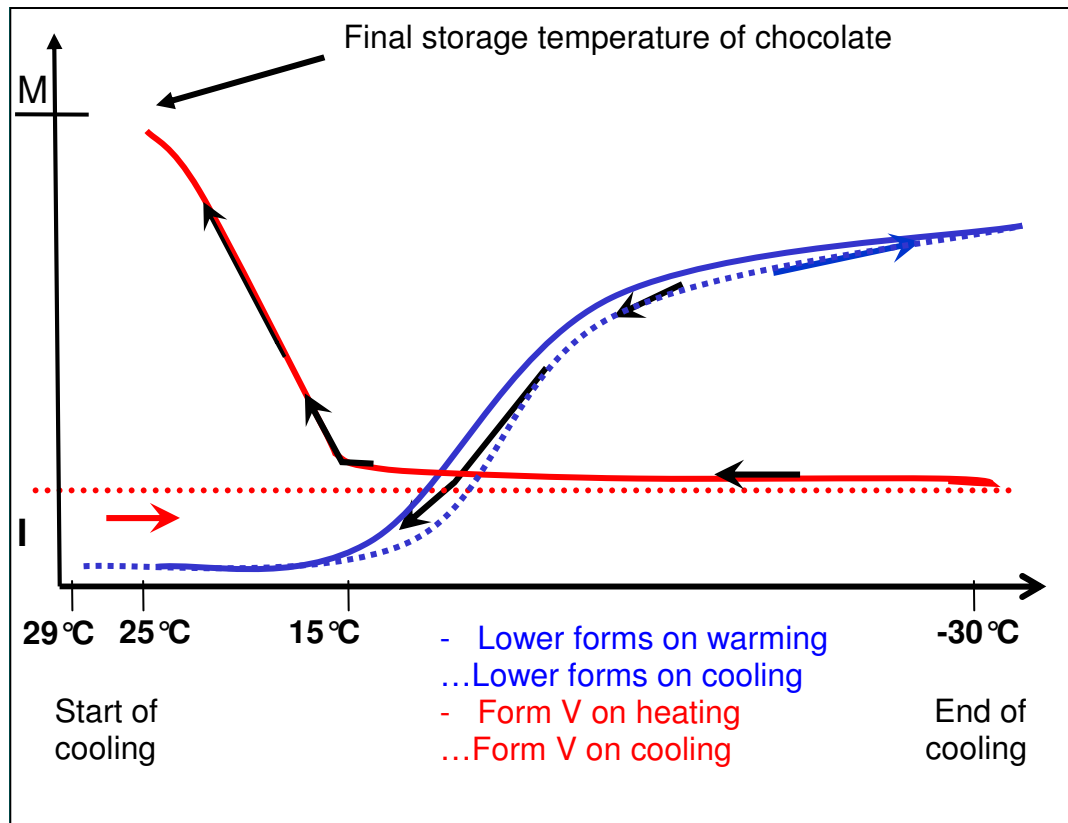
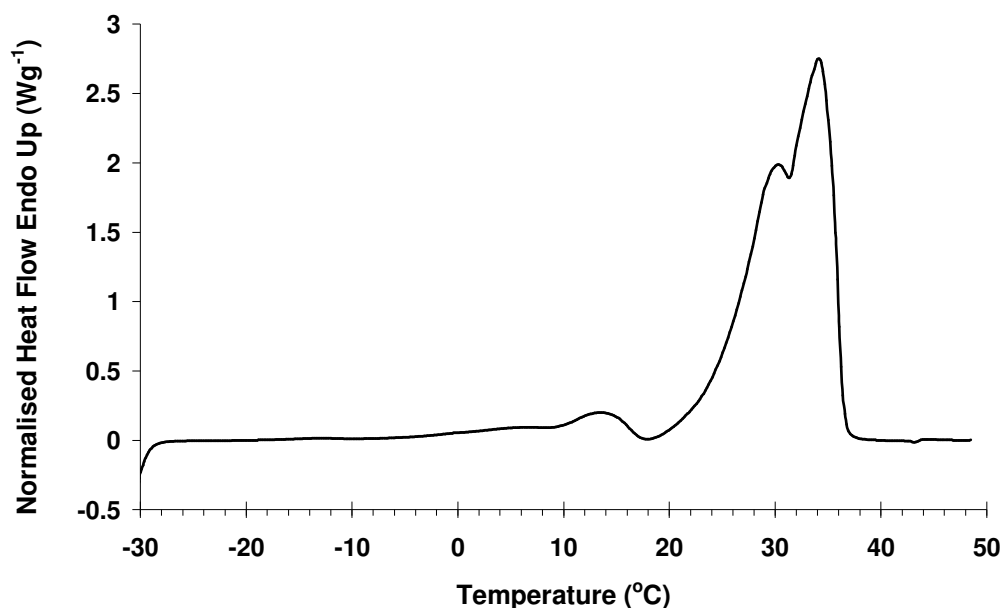


**Figure 5.14: Graphical representation of rapidly cooled chocolate (e.g. 10 °C.min<sup>-1</sup>) and behaviour of polymorphs during cooling and subsequent warming to storage temperature. M= maximum amount of polymorph, I= initial amount of polymorph present. Dotted red line represents growth of Form V polymorph upon cooling and the solid red line, Form V upon heating. The dotted blue line represents growth of lower polymorphic forms upon cooling while the solid blue line represents growth of lower polymorphic forms upon heating.**

Prior to looking at the X-ray results to confirm whether the above hypothesis holds true, it is of interest to determine whether the same results are obtained with cocoa butter and chocolate fats.

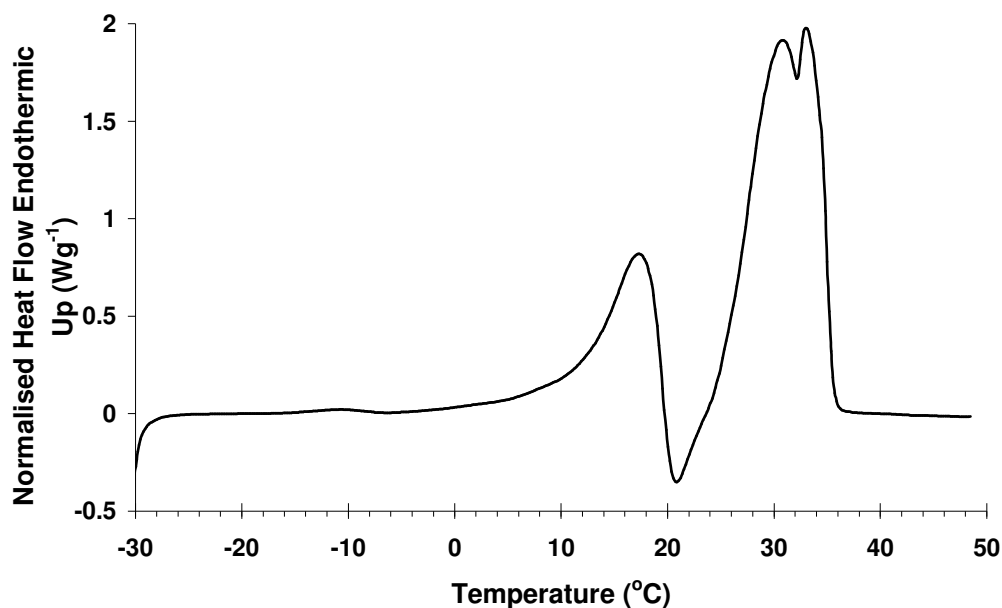
## 5.6 Confirmation of results: experiments using cocoa butter and chocolate fats

Figure 5.15 shows the result of cooling a tempered sample of cocoa butter at a rate of  $1^{\circ}\text{C}.\text{min}^{-1}$ . The endotherms observed are at peak temperatures of  $\sim 14$ ,  $30.5$  and  $34.1^{\circ}\text{C}$ . These peaks would correspond to mixtures of polymorphic Form I and V. Had this sample been held isothermally at around  $25^{\circ}\text{C}$  prior to heating, only Form V would have been obtained. However, as the sample was scanned immediately after cooling, this allowed other lower melting polymorphs to be formed as well. The double peak for Form V might indicate separation of some of the triacylglycerols of cocoa butter. This is a more likely explanation as opposed to formation of Form IV as the temperature of the first double peak is at  $30.5$  which is higher than the peak temperature for Form IV which is reported as  $27.5^{\circ}\text{C}$  (Vaeck, 1951, Vaeck, 1960, Wille and Lutton, 1966, Rudnicki and Niezgódka, 2002). There is also a small amount of recrystallisation occurring at  $\sim 18^{\circ}\text{C}$ . This indicates that upon heating the thermodynamics shifted in favour of the formation of higher polymorphs, hence, the polymorph that melted at a peak of  $14^{\circ}\text{C}$  transformed into a higher form.



**Figure 5.15: DSC thermogram of tempered cocoa butter cooled at 1 °C.min<sup>-1</sup> and heated at 10 °C.min<sup>-1</sup> (only melting thermogram shown)**

The effect of rapid cooling on cocoa butter is shown in Figure 5.16. As observed for chocolate, first there is melting of a lower form at ~17.5 °C followed by a major recrystallisation exotherm at 21 °C upon warming of the sample, and finally the melting of higher polymorphs, which is shown as a double peak with peak temperatures of 31.1 and 33.1 °C. This result was found to be reproducible in all runs carried out. From literature values (Vaeck, 1951, Wille and Lutton, 1966, Rudnicki and Niezgódka, 2002) , the first endotherm corresponds to melting of Form I while the other major endotherm appears to be composed of mainly Form V. This implies that rapid cooling favours the formation of Form I at the expense of Form V. Upon heating, Form I transforms to Form V. It is possible that this transformation goes through other polymorphic forms before finally ending up as the Form V but this can only be verified by X-ray diffraction which will be discussed later on.



**Figure 5.16: DSC thermogram of tempered cocoa butter cooled at 10 °C.min<sup>-1</sup> and heated at 10 °C.min<sup>-1</sup> (only melting thermogram shown)**

The effect of slow cooling on a tempered sample of chocolate fats is shown in Figure 5.17. This result is similar to that obtained with slow cooled tempered chocolate (Figure 5.1). As with tempered chocolate, chocolate fats show a major endotherm with a peak temperature of 29 °C (slightly higher than that for chocolate, 28.4 °C), indicative of the presence of Form V. There is also the small shoulder as observed with tempered chocolate which was attributed to small amounts of Form VI being formed as well. Rapid cooling of tempered chocolate fats, Figure 5.18, also shows similar results to that of rapidly cooled chocolate. Melting of lower polymorphic forms is observed at 15.3 °C, the recrystallisation exotherm is at ~21 °C and finally melting of the higher polymorph at a peak temperature of 28.9 °C. As all these observations were consistent with those obtained with chocolate, data for untempered material is not shown.

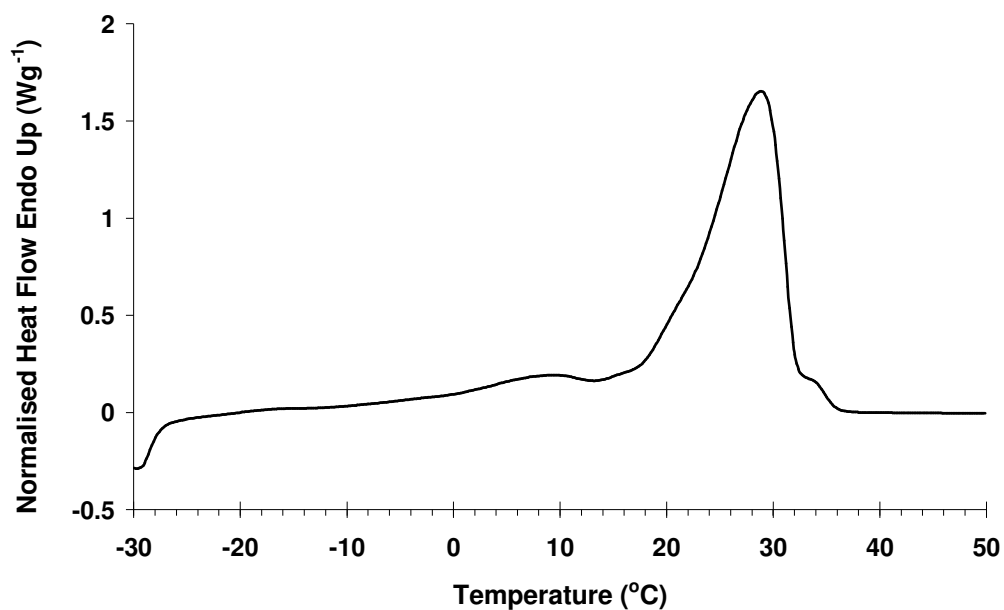


**Figure 5.17: DSC thermogram of tempered chocolate fats cooled at 1 °C.min<sup>-1</sup> and heated at 10 °C.min<sup>-1</sup> (only melting thermogram shown)**

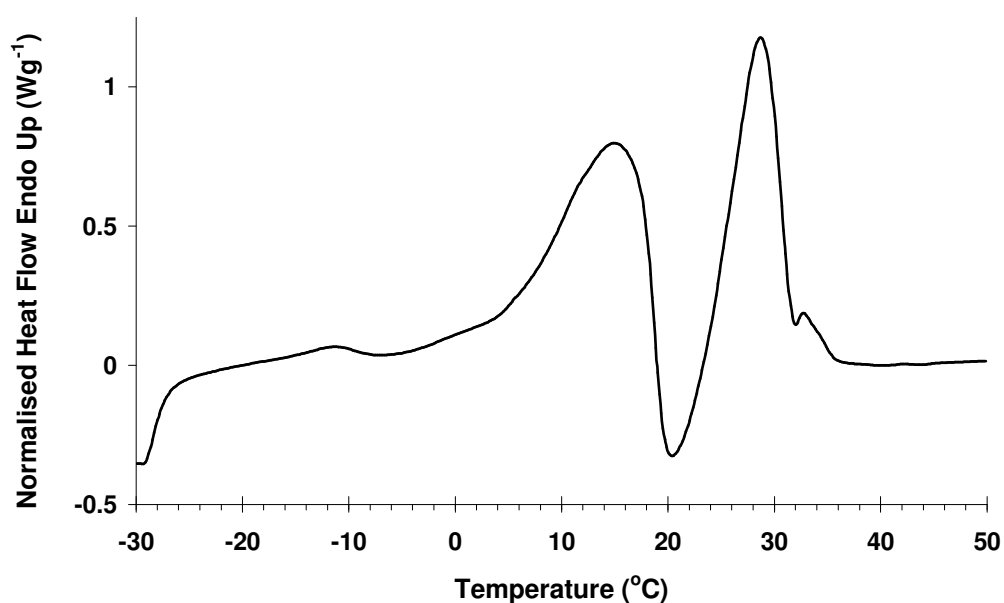


**Figure 5.18: DSC thermogram of tempered chocolate fats cooled at 10 °C.min<sup>-1</sup> and heated at 10 °C.min<sup>-1</sup> (only melting thermogram shown)**

## 5.7 Conclusion

This chapter looked at the effect of slow and rapid cooling on both tempered and untempered chocolate, with confirmatory results done on cocoa butter and

chocolate fats. Slow cooling of tempered chocolate favoured as expected the growth of Form V nuclei generated during tempering. This was seen as an endothermic event occurring at  $\sim 28.4^{\circ}\text{C}$ . The results of rapid cooling on tempered chocolate resulted in the growth of lower melting point (undesirable) polymorphic forms at the expense of Form V nuclei generated upon tempering. Upon heating, however, these lower melting polymorphs undergo melting and a recrystallisation event is seen where they transform to the more stable Form V. Concurrently, as these rapidly cooled samples are warmed, the thermodynamics of the system also shift in favour of Form V and nuclei generated upon tempering start growing.

This recrystallisation event upon rapid cooling was also found to be time dependent with the slower the heating rate during the melting phase, the more time is allowed for the system consisting of unstable polymorphs to convert to higher forms over a wider temperature range. The results also showed that tempering is essential prior to rapid cooling for the formation of Form V during the reheating phase. This was proved by the fact that neither untempered chocolate nor untempered chocolate fats showed the recrystallisation event following rapid cooling.



## **Chapter 6: Temperature controlled X-ray study of polymorphic transitions in cocoa butter and chocolate fats during cooling and heating.**

*Wide angle temperature- controlled X-Ray is used to study polymorphic transitions occurring on variation of cooling rates on chocolate fats and cocoa butter and the results are presented in this chapter.*

## **6 Temperature controlled X-ray study of polymorphic transitions in cocoa butter and chocolate fats during cooling and heating.**

Having discussed the DSC results, we can now move on to the X-ray diffraction results to see whether the hypothesis formed in the light of the DSC results holds true. At this point, it should be stated that the X-ray diffraction results were obtained much later than the DSC results due to numerous difficulties encountered with instrumentation (as mentioned in the Materials and Method section).

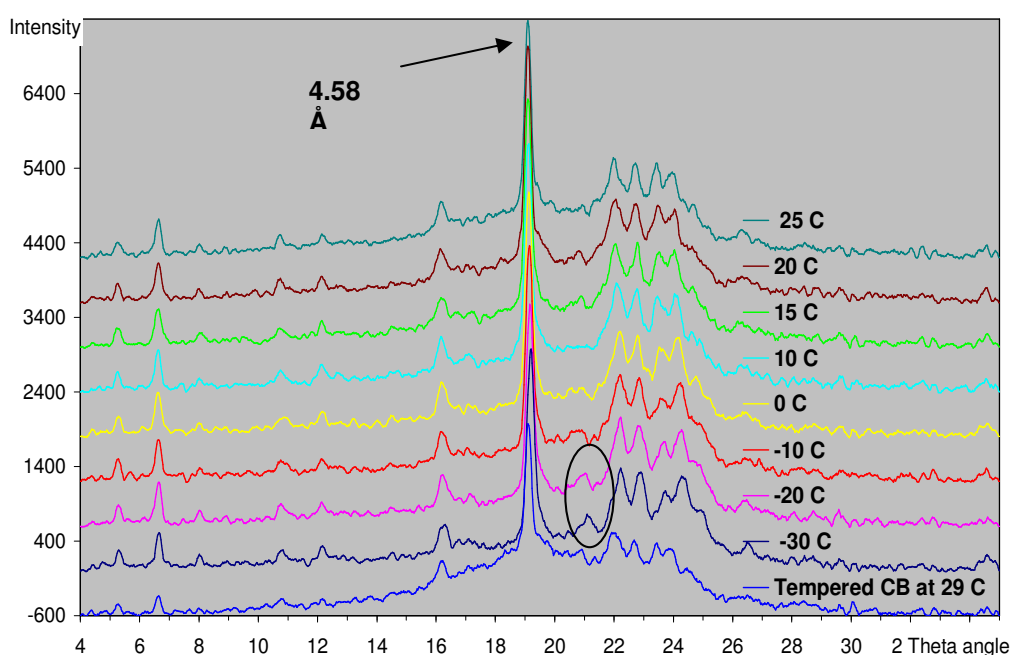
It also worth mentioning again that due to interference from sucrose the crystallisation pattern, X-ray work was confined to cocoa butter and chocolate fats. To illustrate this point a comparison of diffraction patterns given by chocolate, sucrose and cocoa butter is shown in Figure 4.1

### **6.1 Effect of slow cooling**

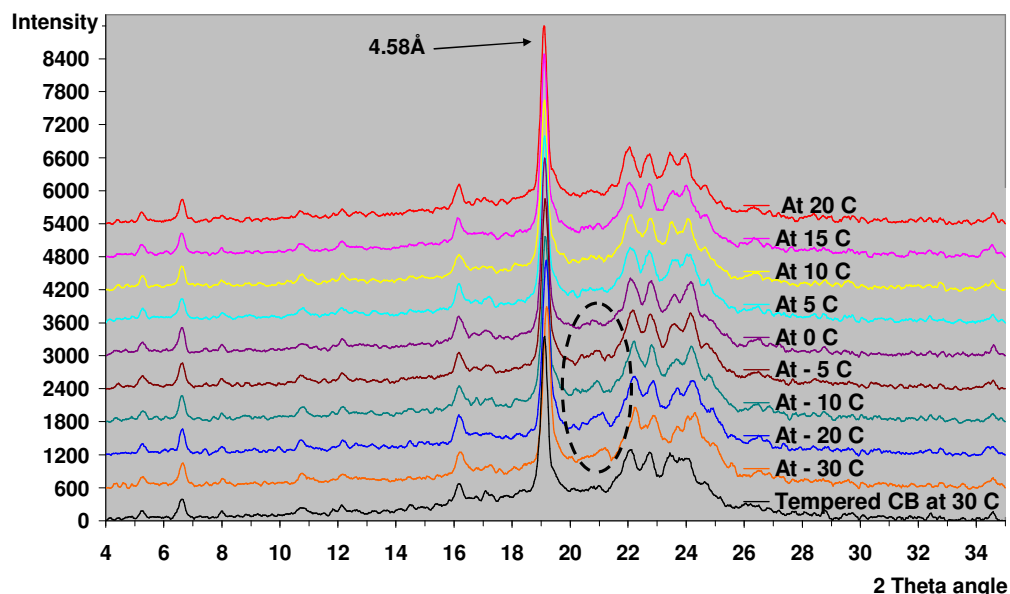
#### **6.1.1 Slow cooling on tempered cocoa butter**

Figure 6.1 shows the X-ray diffraction pattern of tempered cocoa butter cooled at  $1\text{ }^{\circ}\text{C}\cdot\text{min}^{-1}$  to  $-30\text{ }^{\circ}\text{C}$  in the X-ray sample holder. The sample was first evenly spread onto the holder, forming a 1mm thick layer and a scan was immediately acquired to determine whether or not it was tempered. Then cooling was carried out at  $1\text{ }^{\circ}\text{C}\cdot\text{min}^{-1}$  to  $-30\text{ }^{\circ}\text{C}$ . Once at  $-30\text{ }^{\circ}\text{C}$ , another scan was acquired. Then the sample was warmed at  $1\text{ }^{\circ}\text{C}\cdot\text{min}^{-1}$ , with scans acquired at every 5-10

°C interval until 20 °C. Figure 6.2 shows the data for slow cooled tempered cocoa butter but warmed at a rate of 10 °C.min<sup>-1</sup>. The reason for using these 2 rates was to match the heating rate used in the DSC experiments. 1 °C.min<sup>-1</sup> was used to match the heating rate for Stepscan DSC and also simulate industrial conditions where chocolate is slowly warmed to room temperature. 10 °C.min<sup>-1</sup> was used to match the conventional DSC heating rate.



**Figure 6.1: Tempered cocoa butter (CB) cooled at 1 °C.min<sup>-1</sup> to -30 °C then warmed at 1 °C.min<sup>-1</sup> with scans acquired at every 5-10 °C interval up to 25 °C. The first scan is of the tempered material as soon as it comes out of the temperer and prior to cooling. The area circled shows the presence of a small proportion of Form I being formed upon slow cooling. This melts upon warming of the sample.**



**Figure 6.2: Tempered cocoa butter (CB) cooled at  $1\text{ }^{\circ}\text{C.min}^{-1}$  to  $-30\text{ }^{\circ}\text{C}$  then warmed at  $10\text{ }^{\circ}\text{C.min}^{-1}$  with scans acquired at every  $5\text{--}10\text{ }^{\circ}\text{C}$  interval up to  $20\text{ }^{\circ}\text{C}$ . The area circled shows the presence of a small proportion of Form I being formed upon slow cooling. This melts upon warming of the sample.**

On both graphs it can be seen that the molten sample of tempered cocoa butter shows evidence of being heavily tempered with a strong Form V diffraction pattern being seen. Upon cooling, the sample loses its mostly liquid nature as it solidifies and Form V crystals grow and perfect themselves as shown by intensification of the diffraction peaks as the sample is warmed. A very small proportion of Form I is also seen at  $2\theta$  angle of  $21.18^{\circ}$  but this disappears as the sample is warmed to room temperature (Figure 6.1 and Figure 6.2). The presence of this form has also been observed in data obtained by van Langevelde et al., 2001a, Marangoni and McGauley, (2003), who mention that this metastable form quickly transforms to the  $\alpha$  form (Form II) upon warming. It is interesting to note that these researchers however did not use tempered cocoa butter as a starting point of their X-ray analysis. The only difference

between the heating rates of 1 and 10 °C.min<sup>-1</sup> is that slightly broader peaks were obtained at the higher heating rate. This is explained according to Cebula and Smith, (1990) that at the higher heating rate the sample experiences a wider temperature range during the minimum exposure time to the X-ray.

### 6.1.2 Slow cooling on tempered chocolate fats

Figure 6.3 shows the scans obtained upon cooling tempered chocolate fats at 1 °C.min<sup>-1</sup> and warming the sample at 1 °C.min<sup>-1</sup> with scans acquired at every 5-10 °C interval.

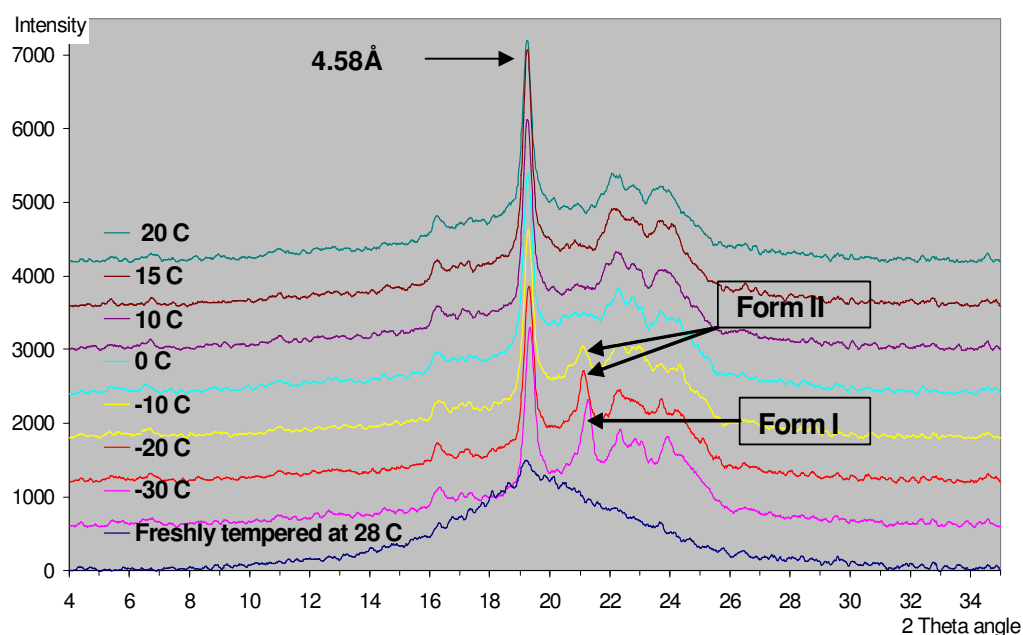


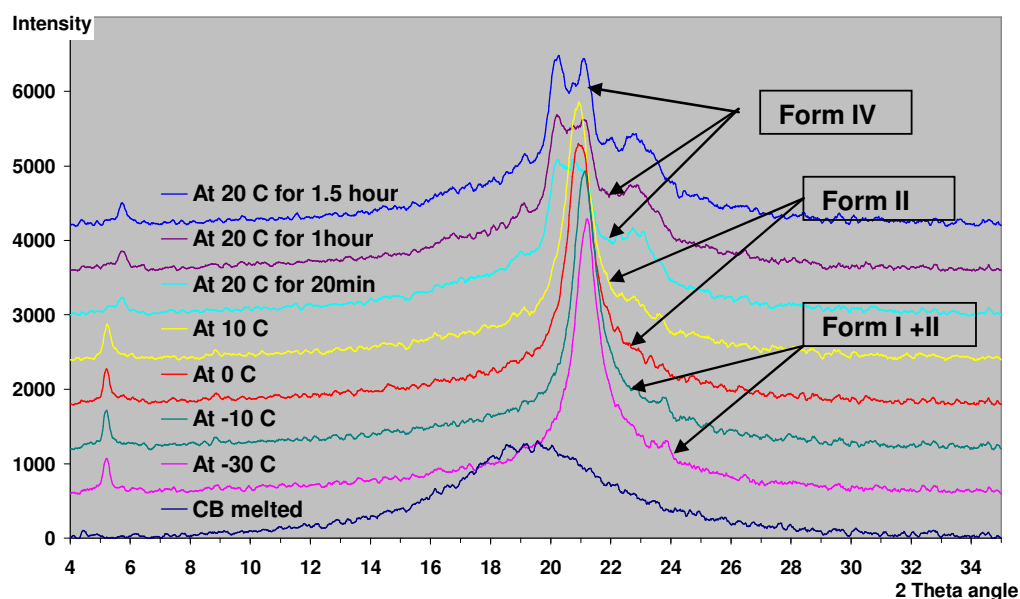
**Figure 6.3: Tempered chocolate fats (CF) cooled at 1 °C.min<sup>-1</sup> to -30 °C then warmed at 1 °C.min<sup>-1</sup> with scans acquired at every 5-10 °C interval up to 20 °C**

It is interesting to note that a freshly tempered sample of chocolate fats appears to be largely liquid in nature with a small proportion of Form V present in the mixture. After being cooled at 1°C.min<sup>-1</sup> to -30 °C, the sample shows presence

of Form V as well as a proportion of Form I polymorph. Upon warming, Form I disappears and at 10 °C there seems to be none of it left in the sample. The final polymorphic form present at 20 °C in the sample is Form V. A similar result was seen when a slow cooled chocolate fats sample was warmed at 10 °C.min<sup>-1</sup> (not shown here). Compared with the results obtained with slow cooling of tempered cocoa butter, the crystals formed during the slow cooling of chocolate fats appear to be less perfect than that of cocoa butter. This is indicated by the broader, less defined peaks obtained at diffraction peaks of 4.58 Å, 3.98 Å, 3.87 Å, 3.75 Å and 3.67 Å on Figure 6.3 compared to those in Figure 6.2.

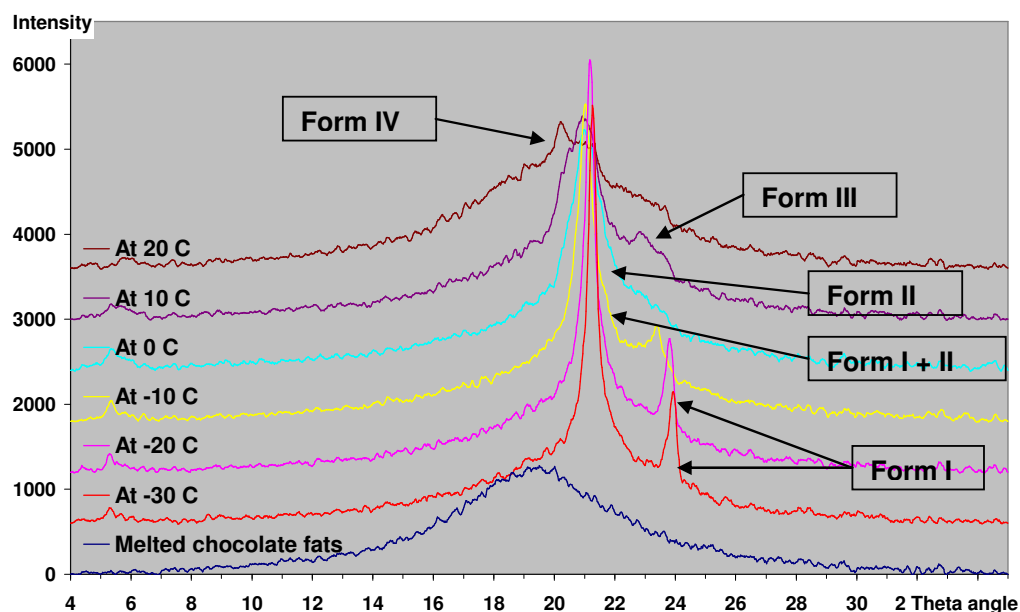
### **6.1.3 Slow cooling on untempered cocoa butter and chocolate fats**

Figure 6.4 and Figure 6.5 show the results of untempered cocoa butter and chocolate fats respectively being cooled at 1 °C.min<sup>-1</sup> followed by warming at 1 °C.min<sup>-1</sup>. Slow cooled untempered cocoa butter solidifies into a mixture of Form I and Form II. The scan at -30 °C is actually dominated by the X-ray pattern of Form II, indicating that only a very small amount of Form I is produced. Upon warming any Form I transforms to Form II, which is shown by the broadening of the peak at ~21°. Form II then eventually transforms to Form IV.



**Figure 6.4: Untempered cocoa butter cooled at 1 °C.min<sup>-1</sup> to -30 °C then warmed at 1 °C.min<sup>-1</sup> to 20 °C**

For untempered chocolate fats (Figure 6.5), slow cooling results in the formation of Form I crystals. Upon warming this transforms to Form II with a mixture of the two Forms being present at -10 °C. At 0 °C only Form II is seen, at 10 °C Form III is present and eventually Form IV is formed at 20 °C. It would appear that for chocolate fats, the presence of milk and vegetable fats, acting as impurities and crystal precursors lower the temperature at which Form I crystals nucleate, hence the presence of Form I in the mixture. In the ‘pure’ system of untempered cocoa butter, due to the absence of these precursors, the kinetics of slow cooling favour the formation of Form II at the expense of Form I, hence only a very small amount of the latter is present at -30 °C.



**Figure 6.5:** Untempered chocolate fats cooled at  $1\text{ }^{\circ}\text{C.min}^{-1}$  to  $-30\text{ }^{\circ}\text{C}$  then warmed at  $1\text{ }^{\circ}\text{C.min}^{-1}$  with scans acquired at every  $10\text{ }^{\circ}\text{C}$  interval up to  $20\text{ }^{\circ}\text{C}$ .

## 6.2 Effect of rapid cooling

### 6.2.1 Rapid cooling of tempered cocoa butter

Having seen the results of slow cooling on the two types of fats, the results of rapid cooling are now presented. Figure 6.6 to Figure 6.8 show tempered cocoa butter being cooled at rates of  $5$ ,  $10$  and  $20\text{ }^{\circ}\text{C.min}^{-1}$  respectively to  $-30\text{ }^{\circ}\text{C}$ . Once at  $-30\text{ }^{\circ}\text{C}$ , the samples were warmed at  $1\text{ }^{\circ}\text{C.min}^{-1}$  to room temperature, with scans acquired every  $5$ - $10\text{ }^{\circ}\text{C}$  interval. Cooling at rates of  $5$  (Figure 6.6) and  $10\text{ }^{\circ}\text{C.min}^{-1}$  (Figure 6.7) show very similar results; at  $-30\text{ }^{\circ}\text{C}$ , the sample is mostly in the Form V configuration with a very small proportion of Form I being present. On Figure 6.6 to Figure 6.8, at  $-30\text{ }^{\circ}\text{C}$ , Form V is present together with a very small proportion of Form I. Form I then disappears as heating progresses and eventually the sample is only in polymorphic Form V.



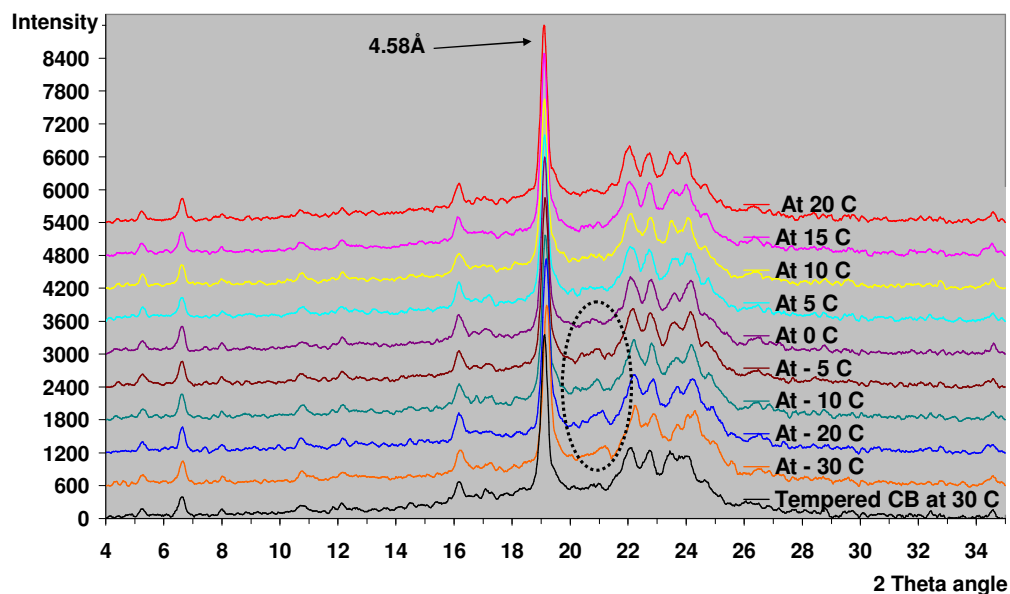


**Figure 6.6:** Tempered cocoa butter (CB) cooled at  $5\text{ }^{\circ}\text{C}\cdot\text{min}^{-1}$  to  $-30\text{ }^{\circ}\text{C}$  then warmed at  $1\text{ }^{\circ}\text{C}\cdot\text{min}^{-1}$  with scans acquired at every  $5\text{--}10\text{ }^{\circ}\text{C}$  interval up to  $20\text{ }^{\circ}\text{C}$ . The area circled shows the presence of a small proportion of Form I being formed upon slow cooling. This melts upon warming of the sample.

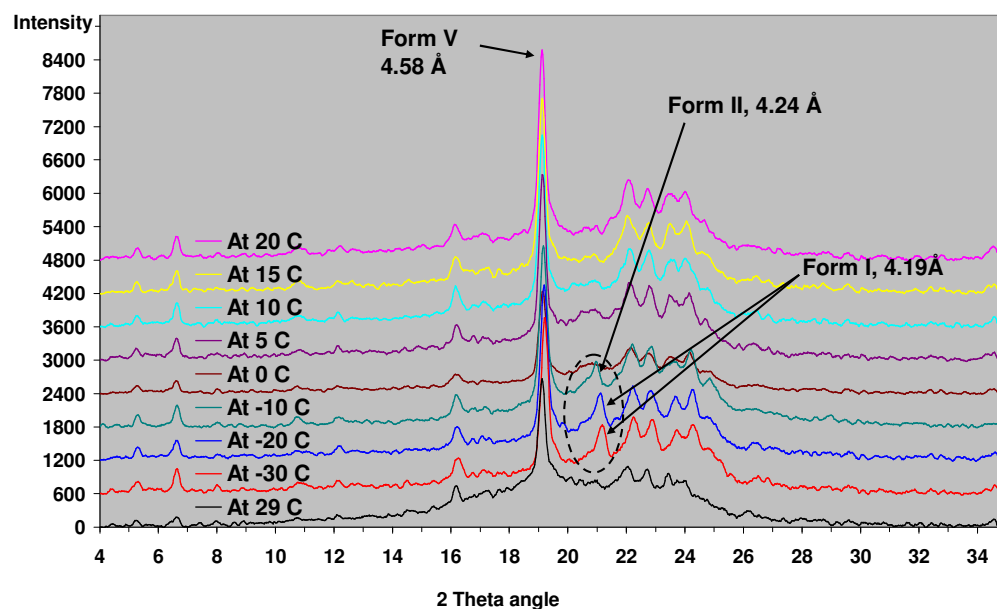


**Figure 6.7:** Tempered cocoa butter (CB) cooled at  $10\text{ }^{\circ}\text{C}\cdot\text{min}^{-1}$  to  $-30\text{ }^{\circ}\text{C}$  then warmed at  $1\text{ }^{\circ}\text{C}\cdot\text{min}^{-1}$  with scans acquired at every  $5\text{--}10\text{ }^{\circ}\text{C}$  interval up to  $20\text{ }^{\circ}\text{C}$ . The area circled shows the presence of a small proportion of Form I being formed upon slow cooling. This melts upon warming of the sample.

Rapid cooling at  $20\text{ }^{\circ}\text{C}\cdot\text{min}^{-1}$  (Figure 6.8) produces a significant proportion of Form I. Under these conditions, there is no growth of any Form V nuclei formed during cooling. It is observed that the intensity of the peak at  $19.36^{\circ}$  for Form V remains the same until  $10\text{ }^{\circ}\text{C}$ , after which the intensity of the peak increases indicating growth of this polymorph. This event coincides with the eventual disappearance of Form II, which was formed through transformation of Form I after  $-20\text{ }^{\circ}\text{C}$  upon heating of the sample. This transformation of Form I to Form II is very clearly seen after cooling at  $20\text{ }^{\circ}\text{C}\cdot\text{min}^{-1}$ . At  $20\text{ }^{\circ}\text{C}$ , there seems to be no sign of Form II present in the mixture. This temperature actually corresponds to the recrystallisation exotherm seen on the DSC graphs when chocolate is cooled at rates of  $10\text{ }^{\circ}\text{C}\cdot\text{min}^{-1}$  or higher (Figure 5.3).

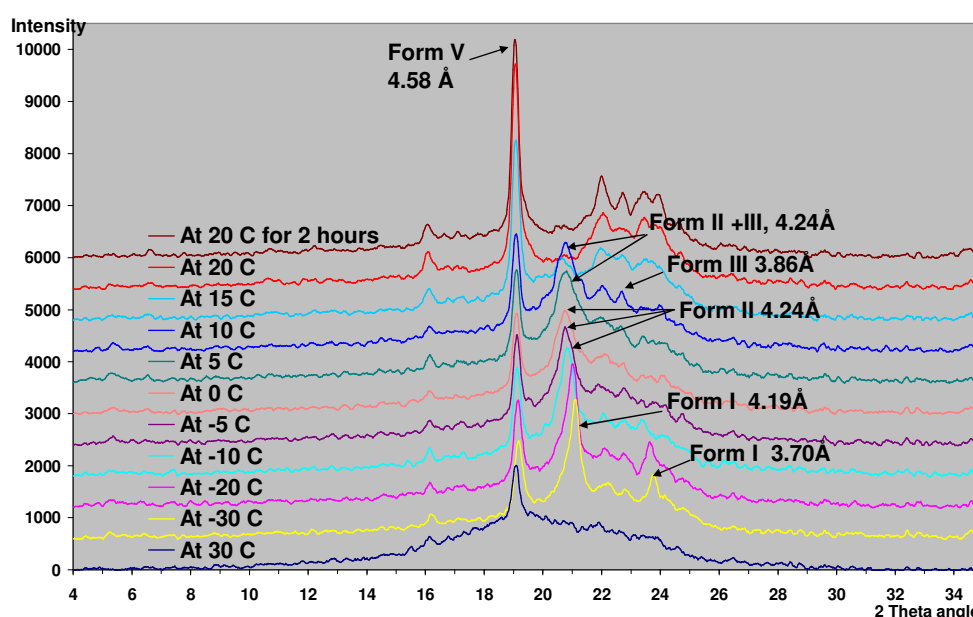


**Figure 6.8:** Tempered cocoa butter (CB) cooled at  $20\text{ }^{\circ}\text{C}\cdot\text{min}^{-1}$  to  $-30\text{ }^{\circ}\text{C}$  then warmed at  $1\text{ }^{\circ}\text{C}\cdot\text{min}^{-1}$  with scans acquired at every  $5\text{--}10\text{ }^{\circ}\text{C}$  interval up to  $20\text{ }^{\circ}\text{C}$

From these results, it can be deduced that the first melting endotherm in Figure 5.3 corresponds to melting of Forms I and II and that the recrystallisation

exotherm represents transformation of Form II into Form V. The formation of Form I upon rapid cooling has also been observed by other researchers (Loisel et al., 1998, Marangoni and McGauley, 2003) . These researchers also refer to Form I as  $\gamma$ -form or sub- $\alpha$  form. (Marangoni and McGauley, 2003) also report that this metastable form seems to co-exist with a species corresponding to the characteristic of the  $\alpha$ -form (Form II) at temperatures below -15 °C. This is also observed with our results of cooling cocoa butter at 20 °C.min<sup>-1</sup> (Figure 6.8) where Form II is present together with Form I at -20 °C. Marangoni and McGauley, (2003) also report that between -15 and 20 °C the material nucleated initially into  $\alpha$ -form (Form II) and then gradually transformed into more stable phases. From the experiments carried out on rapid cooling of cocoa butter, Form II is still present at 15 °C but not at 20 °C and its disappearance coincides with the growth and stabilisation of Form V. These results were also obtained by Loisel et al., (1998) .

### **6.2.2 Rapid cooling of tempered chocolate fats**

The results of rapid cooling on tempered chocolate fats are presented below in Figure 6.9 to Figure 6.11

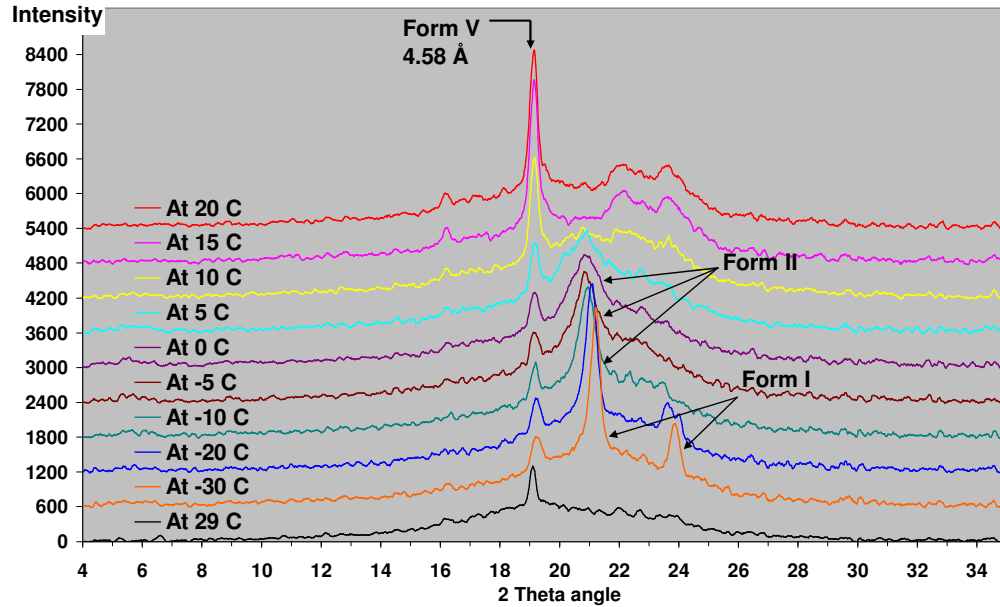


**Figure 6.9: Tempered chocolate fats cooled at 5 °C.min<sup>-1</sup> to -30 °C then warmed at 1 °C.min<sup>-1</sup> with scans acquired at every 5-10 °C interval up to 20 °C**

For chocolate fats, the different cooling rates seem to produce the same result as tempered cocoa butter. At -30 °C, there is a significant proportion of Form I present in the matrix. This eventually transforms to Form II on reaching a temperature greater than -20 °C. Form II only disappears completely after 15 °C with the final sample being composed of Form V crystals only. The small amount of Form V initially formed during tempering does not grow at all until after a temperature of 0 °C is reached and its growth accelerates with the disappearance of Form II. While a cooling rate of 5 and 20 °C.min<sup>-1</sup> seem to produce similar results, cooling at a rate of 10 °C.min<sup>-1</sup> (Figure 6.10) appears different. The proportion of Form V is higher than that of Form V at -30 °C, indicating that during cooling the thermodynamics seemed to have favoured the growth of Form V nuclei and as a consequence, a much smaller proportion of Form I was produced. This is difficult to explain since if there is cooling rate dependence of formation of Form I at the higher cooling rates, it would be

expected that there would be a continuous increase in the proportion of Form I with increased cooling rate. It is possible that this reflects a higher degree of temper in the sample cooled at  $10\text{ }^{\circ}\text{C}\cdot\text{min}^{-1}$ , but this observation could merit further investigation.

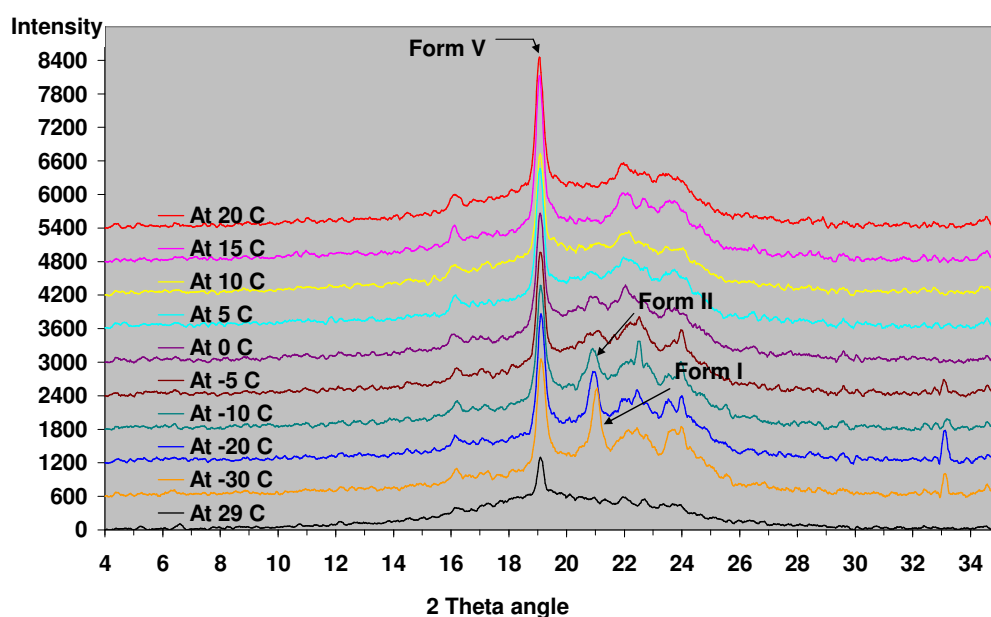


**Figure 6.10:** Tempered chocolate fats cooled at  $10\text{ }^{\circ}\text{C}\cdot\text{min}^{-1}$  to  $-30\text{ }^{\circ}\text{C}$  then warmed at  $1\text{ }^{\circ}\text{C}\cdot\text{min}^{-1}$  with scans acquired at every  $5\text{--}10\text{ }^{\circ}\text{C}$  interval up to  $20\text{ }^{\circ}\text{C}$

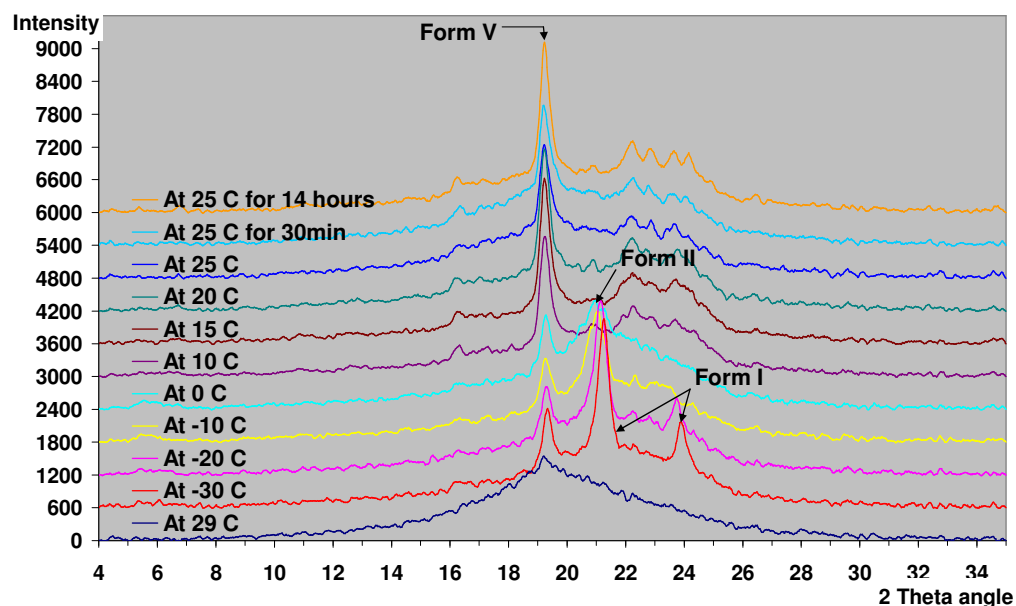


**Figure 6.11:** Tempered chocolate fats cooled at  $20\text{ }^{\circ}\text{C}\cdot\text{min}^{-1}$  to  $-30\text{ }^{\circ}\text{C}$  then warmed at  $1\text{ }^{\circ}\text{C}\cdot\text{min}^{-1}$  with scans acquired at every  $5\text{--}10\text{ }^{\circ}\text{C}$  interval up to  $25\text{ }^{\circ}\text{C}$  up to  $20\text{ }^{\circ}\text{C}$

### 6.2.3 Effect of rapid cooling on untempered samples

The results of rapid cooling at  $20\text{ }^{\circ}\text{C}\cdot\text{min}^{-1}$  on untempered cocoa butter and chocolate fats are shown in Figure 6.12 and Figure 6.13 respectively. Rapid cooling of untempered cocoa butter leads to the formation of Form I, which is as expected as it is the form that is the most kinetically favoured under these conditions and temperature. No Form V is formed, confirming the DSC results. For untempered cocoa butter, the Form I eventually turns to Form II then Form III and at a temperature of  $20\text{ }^{\circ}\text{C}$ , the matrix is composed of Form IV polymorph.

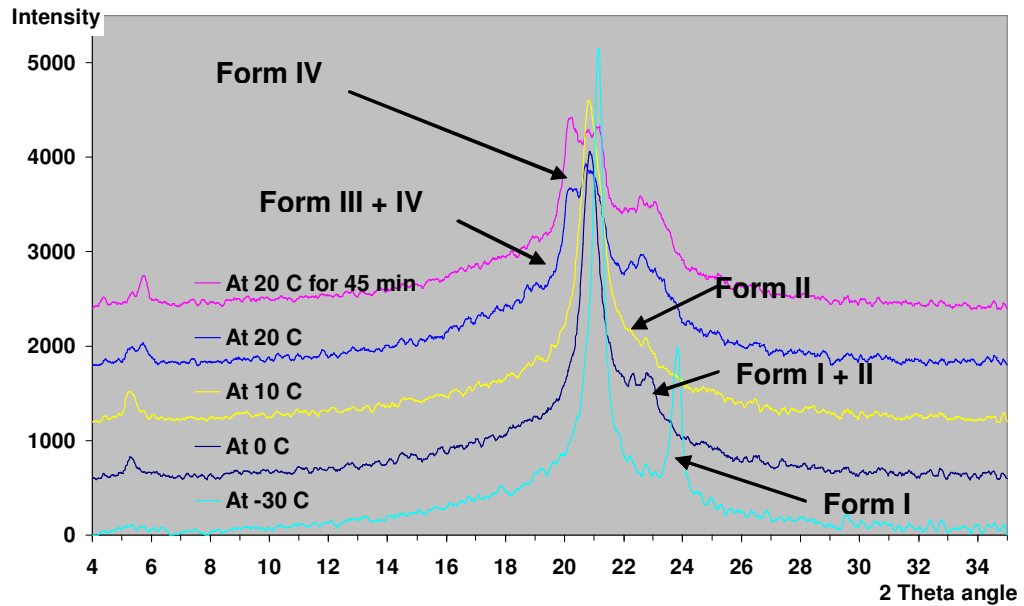


**Figure 6.12: Untempered cocoa butter cooled at 20 °C.min<sup>-1</sup> to -30 °C then warmed at 1 °C.min<sup>-1</sup> to 20 °C. Form I is initially created and eventually transforms to Forms III and IV.**

Untempered chocolate fats (Figure 6.13) seem to stabilise in the Form I upon rapid cooling which upon heating transform to Form II. At 20 °C, it also appears that Form IV is produced after the formation of Form III at 10 °C. Again as with untempered CB, Form V is neither seen at -30 °C nor formed during eventual re-warming.

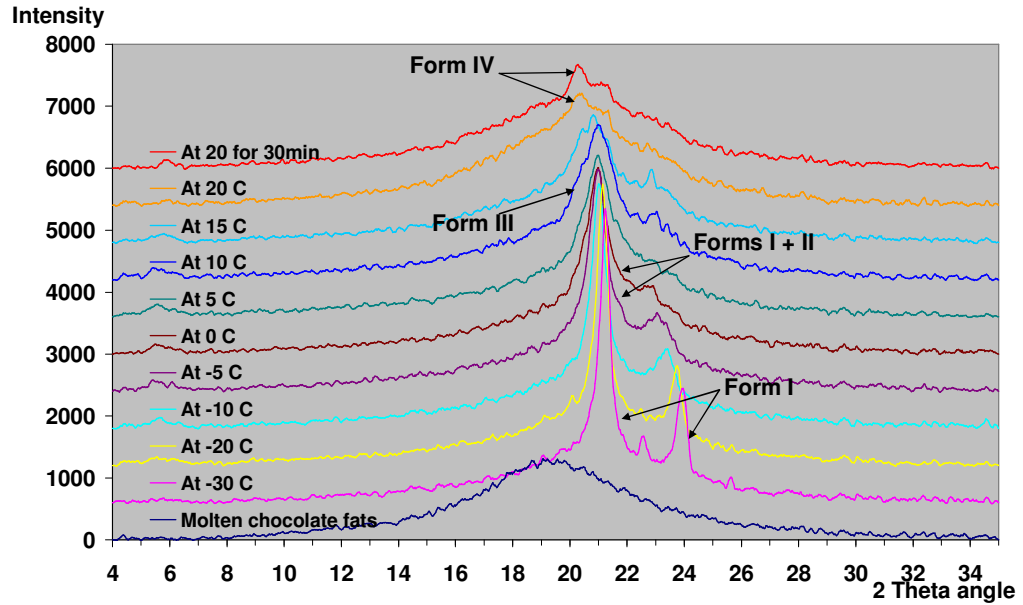


**Figure 6.13: Untempered chocolate fats cooled at 20 °C.min<sup>-1</sup> to -30 °C then warmed at 1 °C.min<sup>-1</sup> with scans acquired at every 5-10 C interval up to 20 °C. Form I is initially created and eventually transforms to Forms III and IV.**

### 6.3 Conclusions from slow and rapid cooling of cocoa butter and chocolate fats

The X-ray results are consistent with the hypothesis from the DSC data. What the X-ray results bring is identification of the lower melting polymorphs formed upon rapid cooling. Figure 6.14 summarises the effect of slow and rapid cooling of tempered material. Slow cooling favours growth of existing Form V nuclei formed during tempering while rapid cooling produces Form I together with Form V. On warming, Form I melts and Form V growth is promoted.



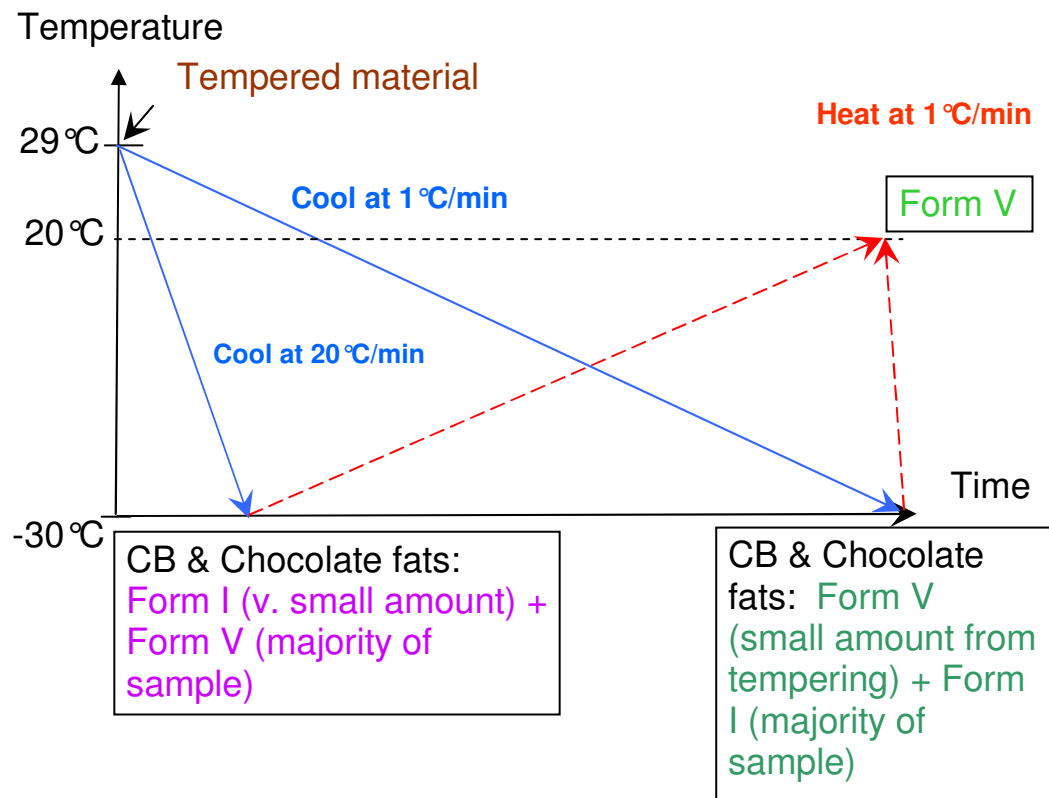


**Figure 6.14: Graphical summary of effect of cooling on tempered cocoa butter and tempered chocolate fats.**

The summary for the result of cooling on untempered cocoa butter is illustrated in Figure 6.15. Both slow and rapid cooling result in the formation of Form I which eventually transforms upon heating to Form IV. For untempered chocolate fats, as shown in Figure 6.16, Form I is also generated upon slow and rapid cooling. This transforms to Form III and some Form IV upon heating. This sample has a very high proportion of liquid.

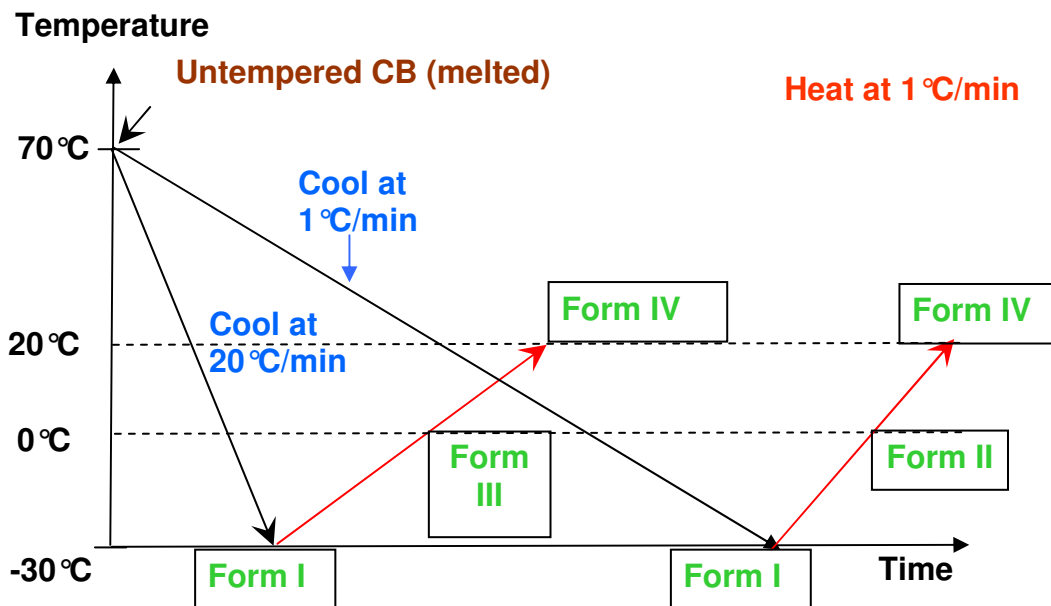


Figure 6.15: Graphical summary of effect of cooling on untempered cocoa butter.

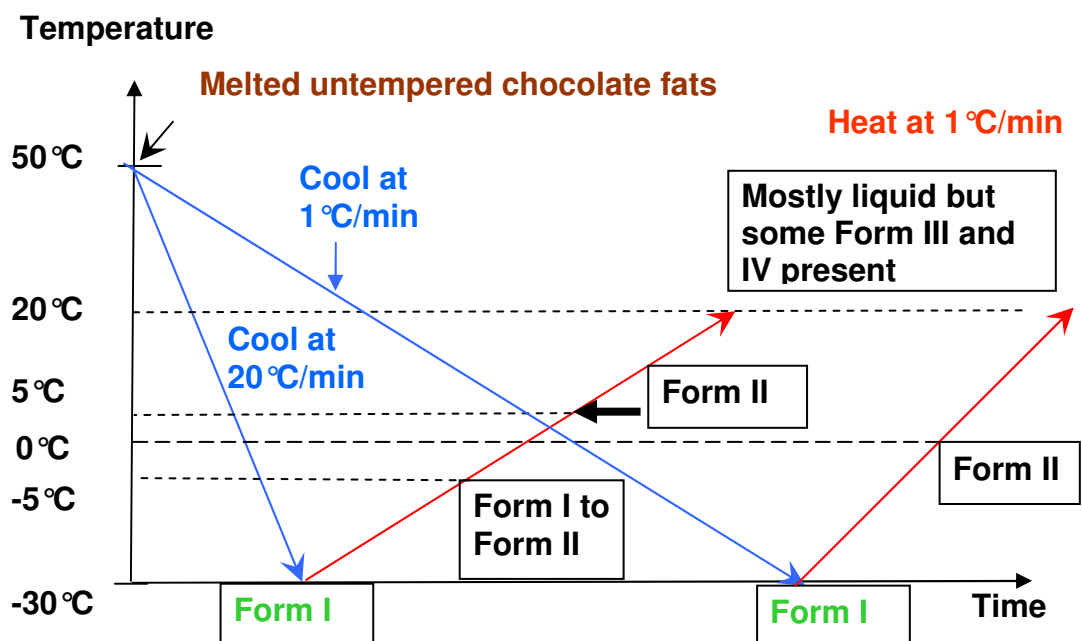


Figure 6.16: Graphical summary of effect of cooling on untempered chocolate fats

#### 6.4 Direct contact cooling

So far all the X-ray results were obtained on cooling the samples in the holder

during the run of the experiment. It would be of interest to mimic the Frozen cone process. The manufacturing process involves deposition of chocolate into a mould and this is immediately cold pressed by a chilled plunger. Although the exact design of the Frozen cone process could not be exactly reproduced in the laboratory environment, the process could still be investigated by X-ray diffraction by quickly smearing samples onto the sample holder held at predefined temperatures and scanning them immediately after 'deposition' to observe the state into which the material was solidified. These samples were then warmed to observe any structural changes taking place inside them.

A range of contact temperatures from -30 to 5 °C was used for this series of experiments. It has been noticed industrially that above a temperature of 5 °C, the Frozen cone process does not work well, with chocolate sticking to the cold plunger resulting in deformation of the chocolate shell. Hence it would be of interest to observe at which temperature this 'stickiness' occurs and which polymorphic form is responsible. For the lab experiments, stickiness was said to occur when the material smeared onto the holder would stick to the spatula with which it was spread or remained stuck to X-ray sample holder. Good release was said to occur when the spread material could be removed from the holder without it sticking to the surfaces (hence good de-moulding properties) or when it did not stick to the spatula after being spread onto the X-ray holder.

#### **6.4.1 Contact cooling of tempered cocoa butter**

Figure 6.17 shows the result of contact cooling of tempered cocoa butter at -30

°C and subsequent warming of this sample at 1 °C.min<sup>-1</sup>. The sample was then held at 10 °C for 1 hour to mimic the industrial process whereby the chocolate shells are filled and the centre is allowed to cool before they are wrapped. An X-ray scan was taken at every 10 minute interval during this holding period in order to observe any changes occurring within the sample. It can be seen that upon contact cooling with the cold surface, the material solidifies with a significant proportion of Form I being formed. This transforms to Form II and completely disappears after 0 °C. Form V nuclei formed during tempering do not growth until after being held at 10 °C for 50 minutes. Its growth is promoted not only by the increase in temperature but also by the disappearance of Form II, eventually leaving the material with only Form V polymorph which stabilises and matures upon storage. Good release of the sample is also observed at -30 °C.

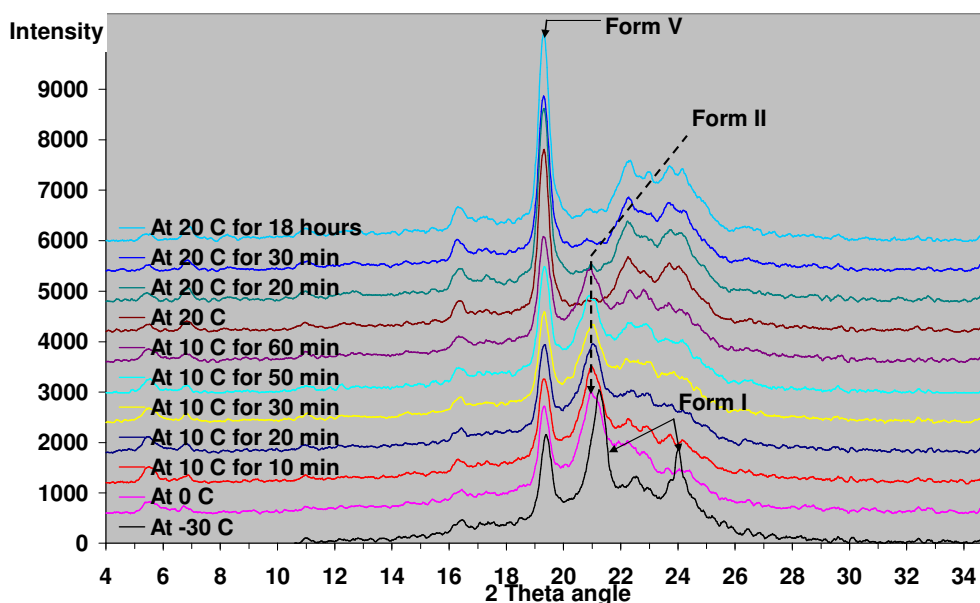


**Figure 6.17: Tempered cocoa butter contact cooled at -30 °C then warmed at 1°C.min<sup>-1</sup> to 20 °C.**

Similar results are observed when tempered cocoa butter is contact cooled at -25 and -20 °C (not shown here). Slight stickiness was observed at a contact temperature of -15 °C and this stickiness increased further as the contact temperature was increased. It is to be noted that the forms present upon contact cooling were still Form V and Form I although the proportion of Form I in the sample decreased steadily.

Eventually, upon contact cooling at 0 °C, no Form I was formed upon contact and the scan is shown in Figure 6.18. The polymorphs present at the point of contact, i.e. when the material solidifies upon contact with the cold surface, were Forms II and V. This sample was very sticky and could not be removed from the sample holder without it sticking to the surfaces. It was also observed that the initial amount of Form V nuclei produced during tempering did not start growing until after a temperature of 10 °C was reached. This is shown by comparing the intensity of the peak at 19.36°.

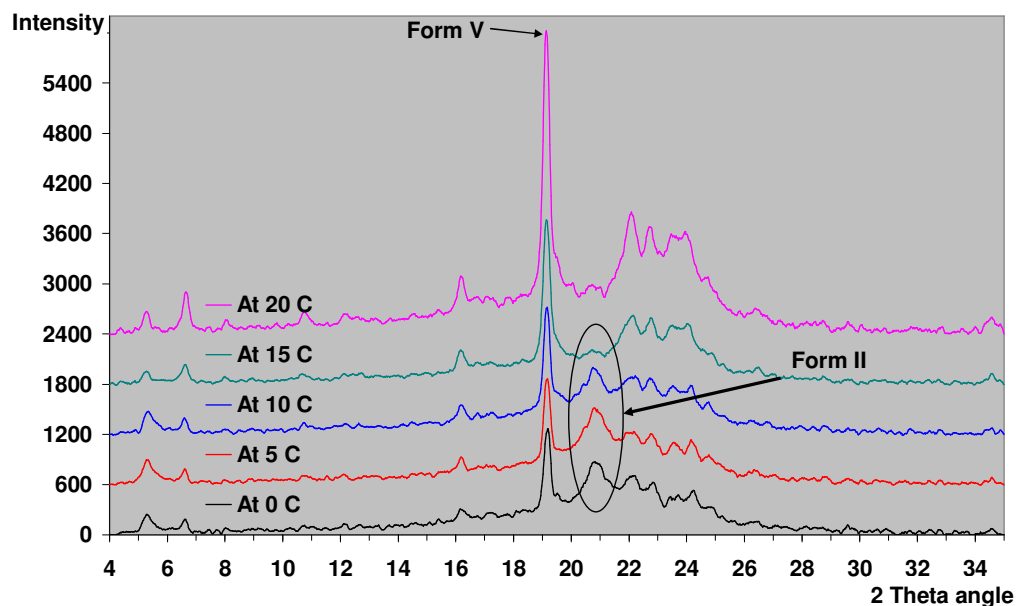


**Figure 6.18: Tempered cocoa butter contact cooled at 0 °C then warmed at 1 °C.min<sup>-1</sup> to 20 °C.**

At 5 °C, this stickiness and failure to de-mould was even more apparent. The scan taken at this temperature is shown in Figure 6.19. As expected, at this temperature, no Form I was present. The material was composed of mainly Forms II and V. As can be seen, upon warming, Form II progressively melts. Form V is also seen to grow as shown by the growing intensity of the peak at 19.36°.

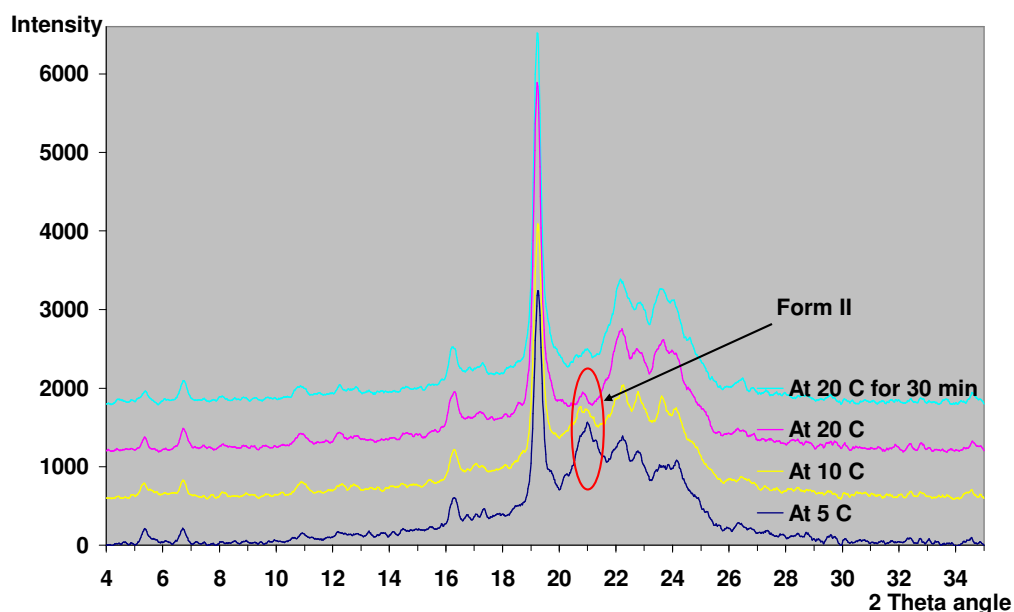


**Figure 6.19: Tempered cocoa butter contact cooled at 5 °C then warmed at 1 °C.min<sup>-1</sup> to 20 °C.**

#### **6.4.2 Contact cooling of untempered cocoa butter**

The results of contact cooling of untempered cocoa butter at -30 and 5 °C are shown in Figure 6.20 and Figure 6.21 respectively. At -30 °C, when the sample was in Form I, the sample exhibited good release from the holder. Results on warming showed that Form I eventually transformed to Form II and eventually Form IV. At 5 °C, poor release was observed. At this temperature, the sample was found to be in Form II. These results seem to suggest that the polymorphic form created upon contact seems to determine the type of release obtained, with Form I producing good release and Form II resulting in stickiness.

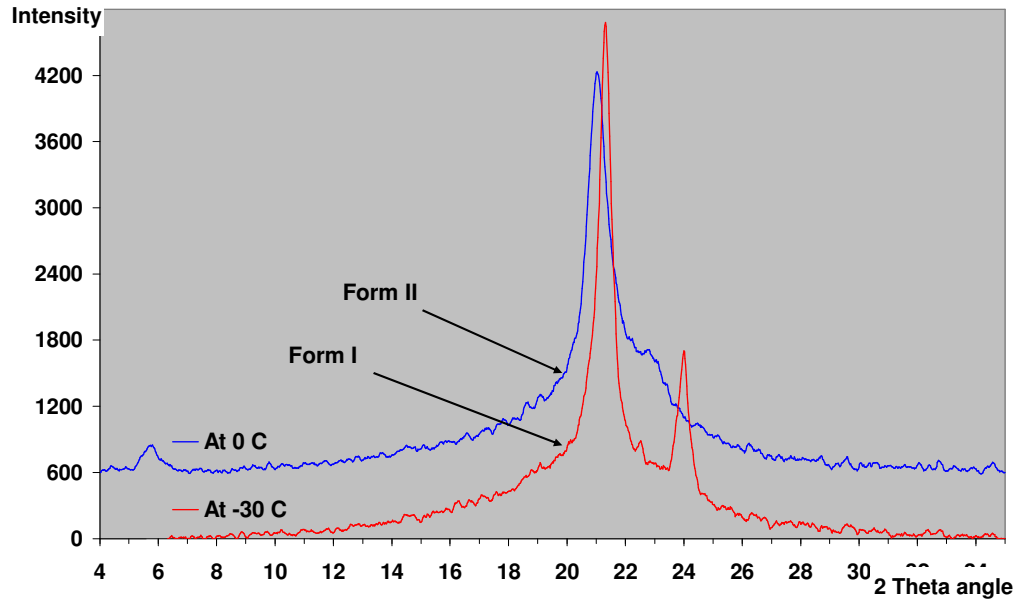


**Figure 6.20:** Untempered cocoa butter contact cooled at  $-30\text{ }^{\circ}\text{C}$  then warmed at  $1\text{ }^{\circ}\text{C.min}^{-1}$ . Form I is created and then transforms to Form II. No further heating was carried out after a temperature of  $0^{\circ}\text{C}$  was reached.

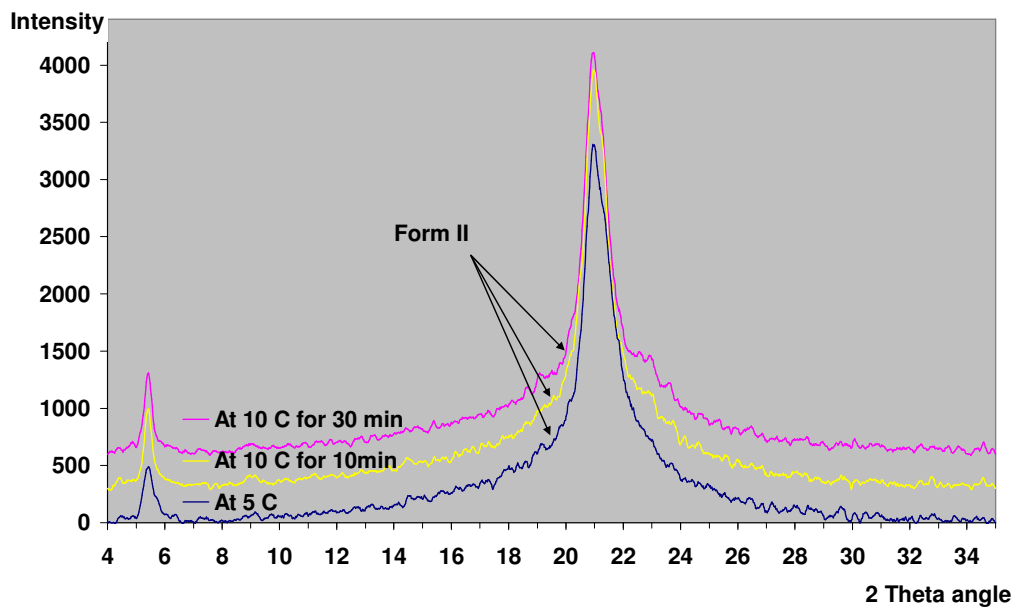


**Figure 6.21:** Untempered cocoa butter contact cooled at  $5\text{ }^{\circ}\text{C}$  then warmed at  $1\text{ }^{\circ}\text{C.min}^{-1}$ . No further heating was carried out after a temperature of  $10\text{ }^{\circ}\text{C}$  was reached. Only Form II is formed.

#### 6.4.3 Contact cooling of tempered chocolate fats

The results of contact cooling for tempered chocolate fats are shown in Figure



6.22 to Figure 6.25. At -30 and -25 °C, good release is observed from the holder. At these temperatures, the material is composed of Forms I and V polymorphs. As in previous cases, Form I eventually transforms to Form II, which subsequently disappears with the kinetics favouring the growth of Form V nuclei generated during tempering.

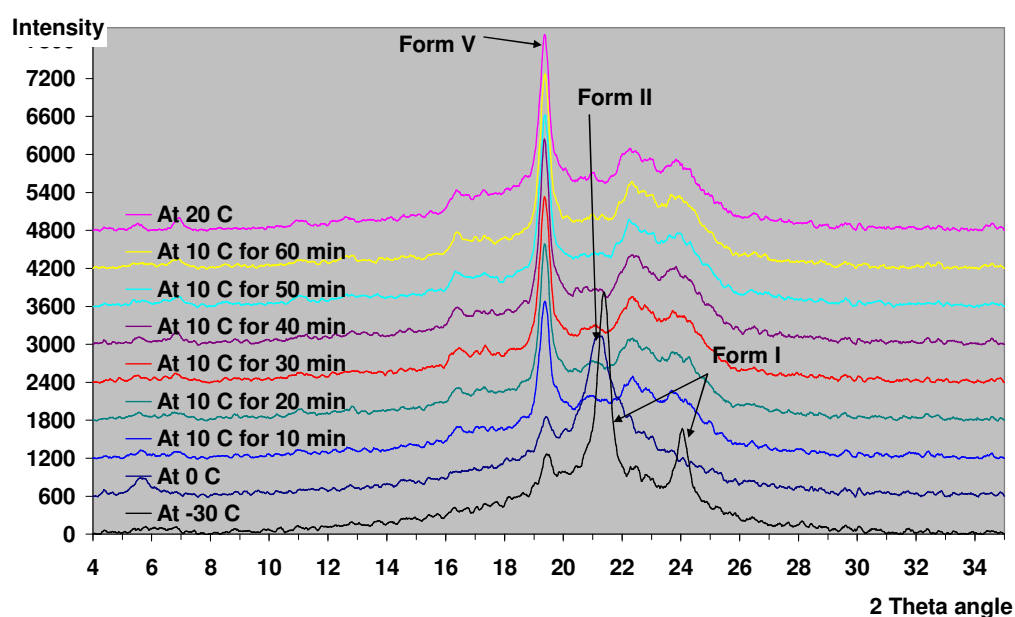


**Figure 6.22:** Tempered chocolate fats contact cooled at -30 °C then warmed at 1 °C.min<sup>-1</sup> to 20 °C. On contact at -30 C, Form I is formed. This transforms to Form II on warming.

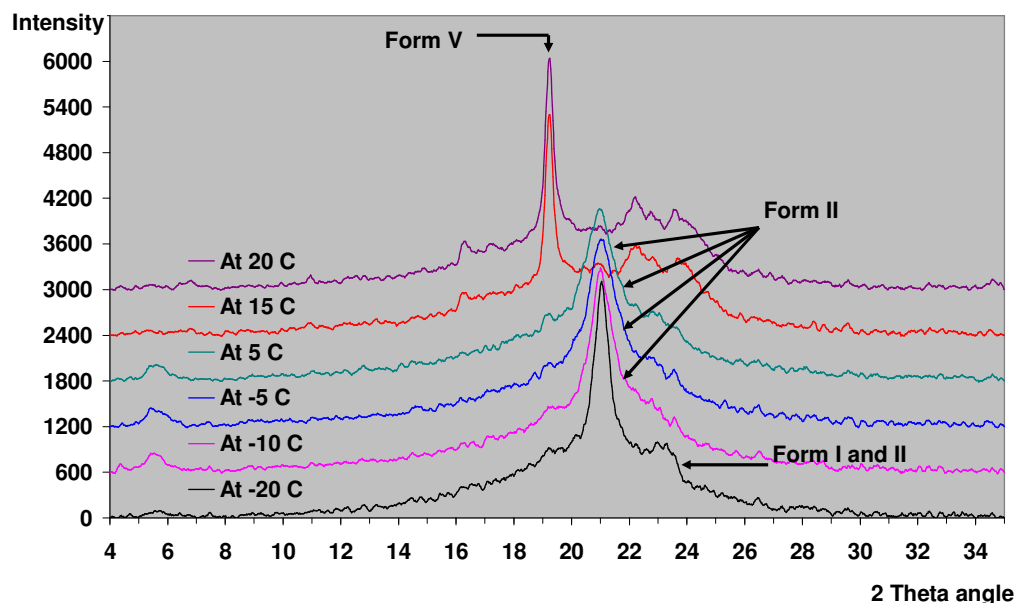


**Figure 6.23: Tempered chocolate fats contact cooled at -20 °C then warmed at 1 °C.min<sup>-1</sup> to 20 °C**

At -20 °C (Figure 6.23), however, Form II is formed and stickiness is observed. At temperatures of -15, -10 and -5 °C (results not shown), the proportion of Form II in the sample is seen to increase and no Form I is seen to be formed.. The adhesion of the sample to the holder also increases with increase in contact temperature and at a temperature of 0 °C (Figure 6.24), the chocolate fats stick completely to the surface of the sample holder, resulting in very poor release. At 5 °C (Figure 6.25), the sample sticks completely to the holder. As the result shows, the sample has very little crystalline material and the crystals present are mostly of polymorphic Form II. These results on the whole reinforce the idea that the properties of Form II are responsible for the poor release of the mould.

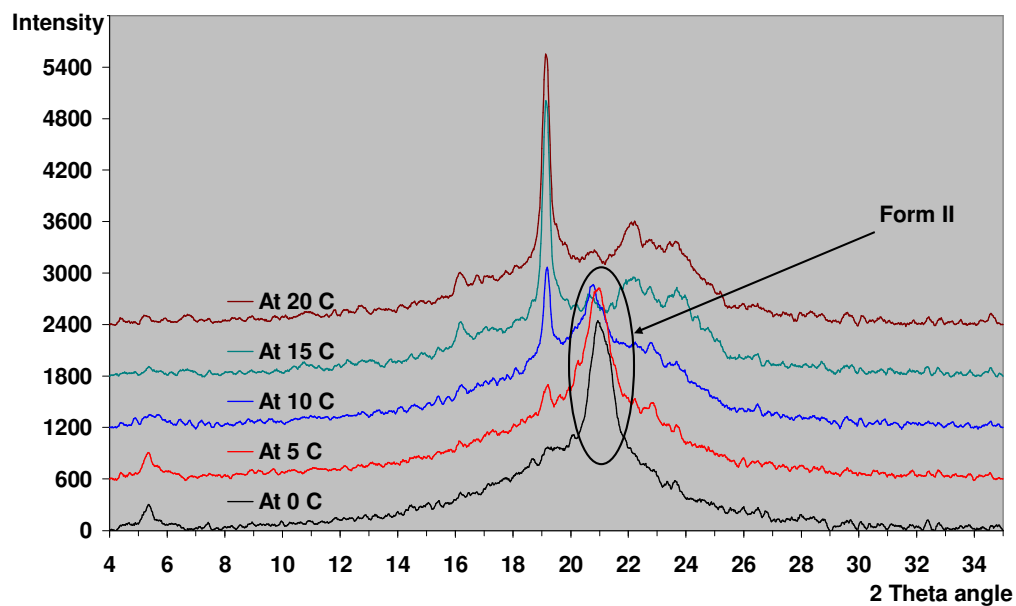


**Figure 6.24:** Tempered chocolate fats cooled at 0 °C then warmed at 1 °C.min<sup>-1</sup> to 20 °C. Form II is generated at this temperature.

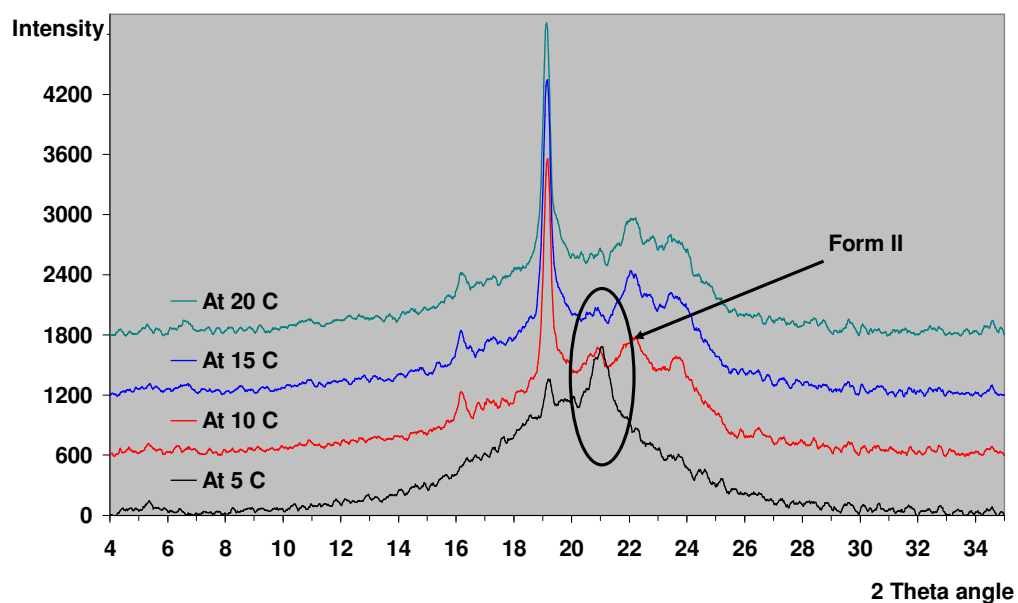


**Figure 6.25:** Tempered chocolate fats contact cooled at 5 °C then warmed at 1 °C.min<sup>-1</sup> to 20 °C. Form II is generated at this temperature

#### 6.4.3.1 Contact cooling of untempered chocolate fats

The results of contact cooling on untempered chocolate were similar to that for

untempered cocoa butter. At contact temperatures of -30, -20 and -15 °C, good release of the sample from the mould was observed, with Form I being present in the sample. When the temperature was increased from -15 °C, Form II was also present in the sample and its proportion increased as the contact temperature was increased. Stickiness of the sample was also seen to increase with temperature.

## **6.5 Conclusions**

This chapter looked at the effect of cooling rate X-ray diffraction. From DSC results (previous chapter), a hypothesis was formed whereby upon rapid cooling the formation of unstable polymorphs is favoured. Upon warming however, these melt and the thermodynamics shift back in favour of the higher polymorph (Form V). The X-ray results obtained seem to confirm this view and identification of the different forms was made. Rapid cooling generated the formation of Form I as identified by X-ray, which subsequently transforms to Form II, which in turns melts and recrystallises in polymorphic Form V. This recrystallisation is not solely responsible for the Form V being present in the final chocolate matrix. During the warming process, simultaneously while Form II is undergoing transformation, Form V nuclei initially generated during tempering also start to grow and stabilise. Direct contact cooling in the X-ray also allowed clarification as to which polymorph seems to be responsible for poor release/demoulding. Form I provided good release at temperature up to -15 °C for cocoa butter and up to -20 °C for chocolate fats. Poor release is observed as Form II is formed and the higher the proportions of Form II

present, the worse the release mechanism. These results indicate that both the nature of the polymorph and its properties are crucial for good release. The results also clearly showed that in order for a rapid cooled material to end up in solely Form V configuration, it is important to start with tempered material containing the Form V nuclei

## **Chapter 7: Use of Stepscan DSC to study the effect of cooling rate on chocolate**

*This chapter presents the results obtained by Stepscan DSC to study the effect of rapid cooling on chocolate. The limitations of the method are also described.*

## **7 Use of Stepscan DSC to study the effect of cooling rate on chocolate**

### **7.1 Introduction**

As discussed in the previous chapter, DSC has been an important technique in the investigation of the effect of cooling and heating rate on chocolate. Of particular interest were the results upon heating of the effect of rapid cooling ( $10\text{ }^{\circ}\text{C}\cdot\text{min}^{-1}$ ) on chocolate. These results showed melting of lower melting point polymorphs followed by a recrystallisation event and melting of the higher melting point polymorph.. This behaviour was not observed for all samples and was more common at the low cooling rates within the range of fast cooling rates studied. It was hoped that Stepscan DSC would provide some insight into this lack of reproducibility. As mentioned in the literature review, DSC results are often complex due to various transformations such as melting and recrystallisation occurring concurrently during heating. As previously discussed in the literature review, modulated DSC applies a sine wave function and Fourier transform to deconvolute data into reversing and non-reversing components and also obtain heat capacity data. Modulated DSC therefore allows the DSC thermogram upon heating to be deconvoluted into separate melting and crystallisation traces. For this work, Stepscan DSC, which is a variant of modulated DSC, was used. It utilises a series of short heating rates and isothermal segments to obtain thermodynamic (reversing) and Iso-kinetic (non-reversing) data. In order to optimise the results obtained from Stepscan DSC, it was first necessary to optimise the experimental conditions to be used.

Therefore, parameter determination was first carried out using tempered chocolate. For comparison of the difference between fat systems, Stepscan parameters were also determined for tripalmitin (PPP), a simple triacylglycerol system as opposed to the complex chocolate system.

## 7.2 Optimisation of Stepscan parameters

When using temperature-modulated methods it is important to decide on the step size, and isothermal equilibration time appropriate to the system to be studied. Schawe and Hohne, (1996) gave clear guidelines as to when the reversing and non-reversing signals may be accurately separated for temperature profiles having a sine wave oscillation of temperature superimposed on a linear temperature ramp. Briefly these authors state that for kinetically restricted transformation/reactions such as cold crystallization processes in polymers, Equation 1 (below) must apply in order to measure the reversing signal accurately from the oscillatory heat flow response and to allow the calculation of the non-reversing signal by subtracting the reversing component from the total heat flow (Schawe and Hohne, 1996) .

$$dH/dt = [C_p \beta_0 + H_r \alpha \beta_0] + C_p \omega_0 T_a \cos \omega_0 t \quad \text{Equation 7}$$

Where  $\beta_0$  is the underlying heating rate,  $H_r$  is the partial enthalpy of reaction,  $\alpha$  is the degree of the reaction,  $\omega_0$  is the frequency of modulation and  $T_a$  is the temperature amplitude of modulation.



This equation is an approximation in the sense that the reaction must be fast enough to be in equilibrium with the temperature change and that the amplitude of temperature modulation must be sufficiently small that high terms in the temperature dependent expansion of the reaction rate, can be neglected.

However the method of calculating signals is completely different in Stepscan compared with sine wave-modulated DSC and Equation 7 does not apply directly. As Figure 7.1 shows, the non reversing signal can more correctly be labelled the slow component, and is the power offset at the end of the isotherm, whilst the reversing trace is calculated from the amount of heat required to raise the sample temperature by a given amount-a conventional heat capacity measurement.

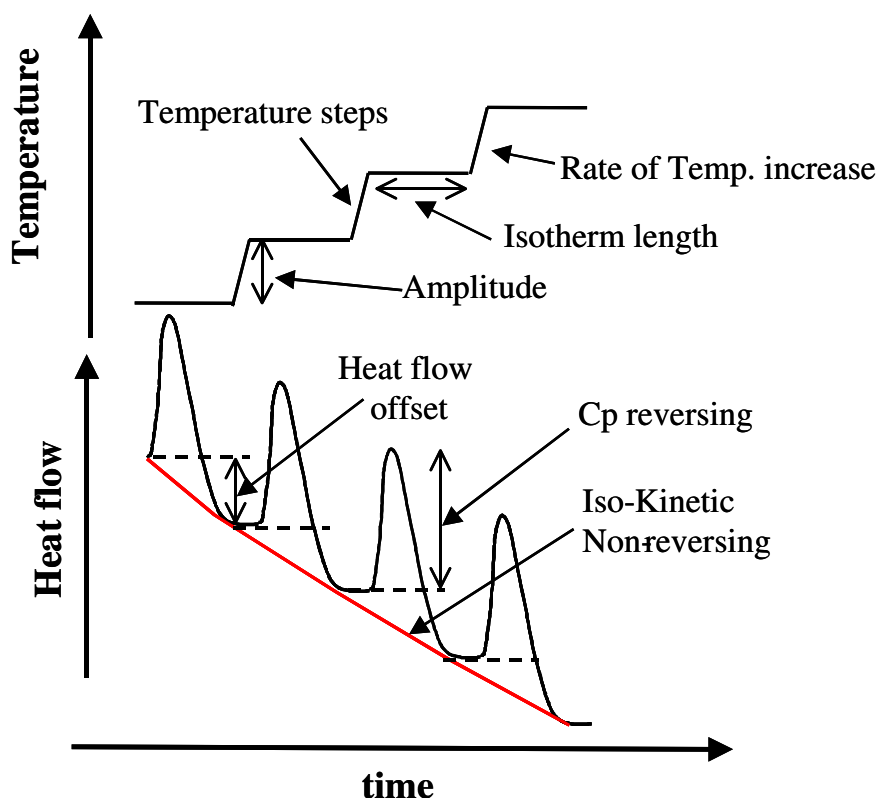


**Figure 7.1: Stepscan trace and the principle of separation into 1) heat capacity, rapid or reversing and 2) iso-kinetic, slow or non-reversing traces.**

Whilst the exact details of the algorithm, which is proprietary, are not available, the limitations of the method can be mapped experimentally. This was performed on tripalmitin and chocolate and the conclusions are described below.

## **7.3 Results and Discussion**

### **7.3.1 Results of parameter variation on tripalmitin**

The behaviour of the reversing and non-reversing heat flows was studied during the melting and recrystallisation of tripalmitin (PPP), which is a polymorphic system showing metastable phases and multiple transitions

including recrystallisation. The matrix of parameters used is illustrated in Table 7.1. These conditions gave underlying heating rates,  $\beta$ , between 0.1 and 2.5  $^{\circ}\text{C}.\text{min}^{-1}$ .

**Table 7.1: Matrix of Stepscan parameters for PPP**

<b>Parameter</b>	<b>Minimum</b>	<b>Maximum</b>
<b>Step size</b>	0.5 $^{\circ}\text{C}$	2 $^{\circ}\text{C}$
<b>Isothermal time</b>	1 min	3 min
<b>Step heating rate</b>	10 $^{\circ}\text{C min}^{-1}$	150 $^{\circ}\text{C min}^{-1}$

The melting DSC profiles of 2 samples of PPP are shown in Figure 7.2. These profile show the samples undergoing linear heating at a rate of 1 (A) and 2.5  $^{\circ}\text{C}.\text{min}^{-1}$  (B).

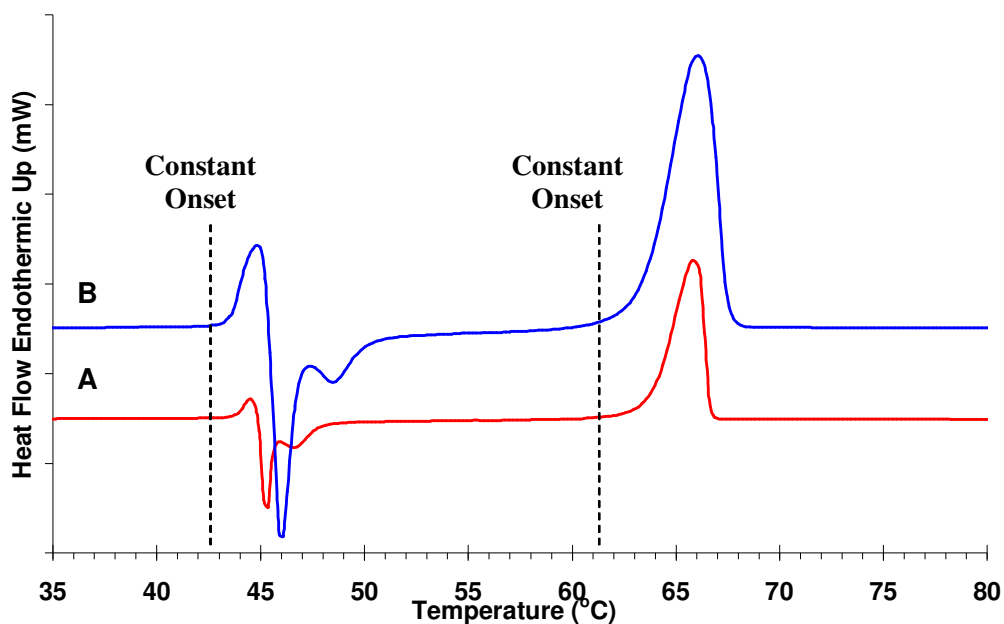


**Figure 7.2: Melting thermograms of PPP (A) at a rate of  $1\text{ }^{\circ}\text{C}.\text{min}^{-1}$  and (B) at  $2.5\text{ }^{\circ}\text{C}.\text{min}^{-1}$ . Samples were first cooled at  $40\text{ }^{\circ}\text{C}.\text{min}^{-1}$  from  $80\text{ }^{\circ}\text{C}$  to  $30\text{ }^{\circ}\text{C}$**

It can be seen in Figure 7.2, at  $1\text{ }^{\circ}\text{C}.\text{min}^{-1}$  (A), the first melting endotherm occurs at  $\sim 44.5\text{ }^{\circ}\text{C}$  and is due to the melting of the  $\alpha$ -form of PPP (MacNaughtan et al., 2006). This is followed by immediate recrystallisation at  $45\text{ }^{\circ}\text{C}$  and eventual melting at  $66\text{ }^{\circ}\text{C}$  which is attributed to the  $\beta$  form (MacNaughtan et al., 2006). Heating PPP at  $2.5\text{ }^{\circ}\text{C}.\text{min}^{-1}$  (B) shows similar melting behaviour but with the broadening and displacement of the endo- and exotherms due to the effect of higher heating rate (Cebula and Smith, 1991). The effect of Stepscan parameter variation on the reversing traces of the melting of PPP is shown in Figure 7.3 with the corresponding non-reversing traces shown in Figure 7.4

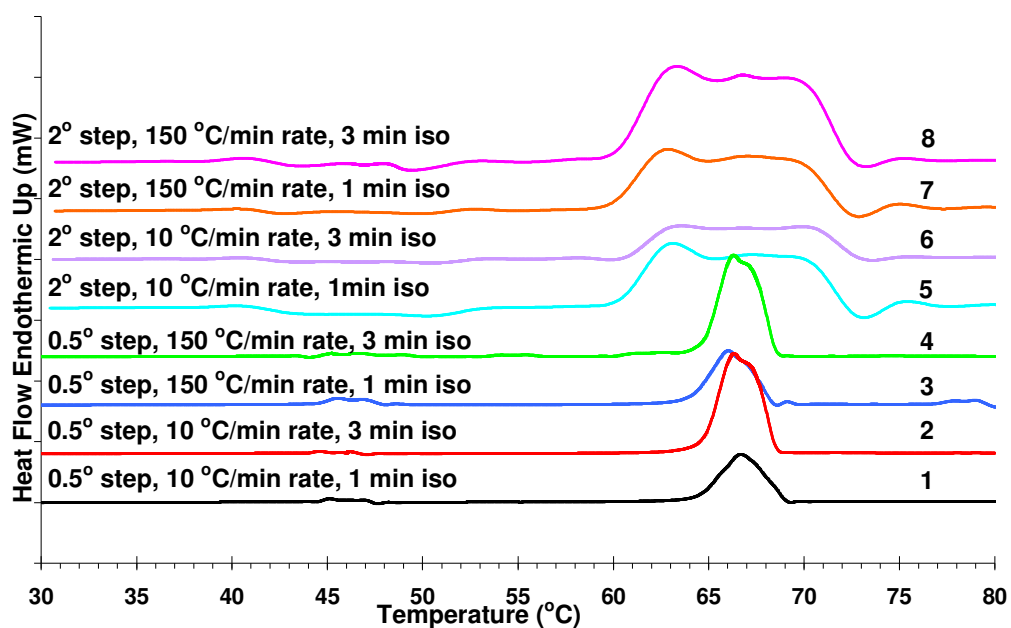


**Figure 7.3: Reversing traces of PPP results.** The Stepscan conditions are shown above each trace. The PPP samples were cooled to 30 °C prior to heating in Stepscan mode to 80 °C

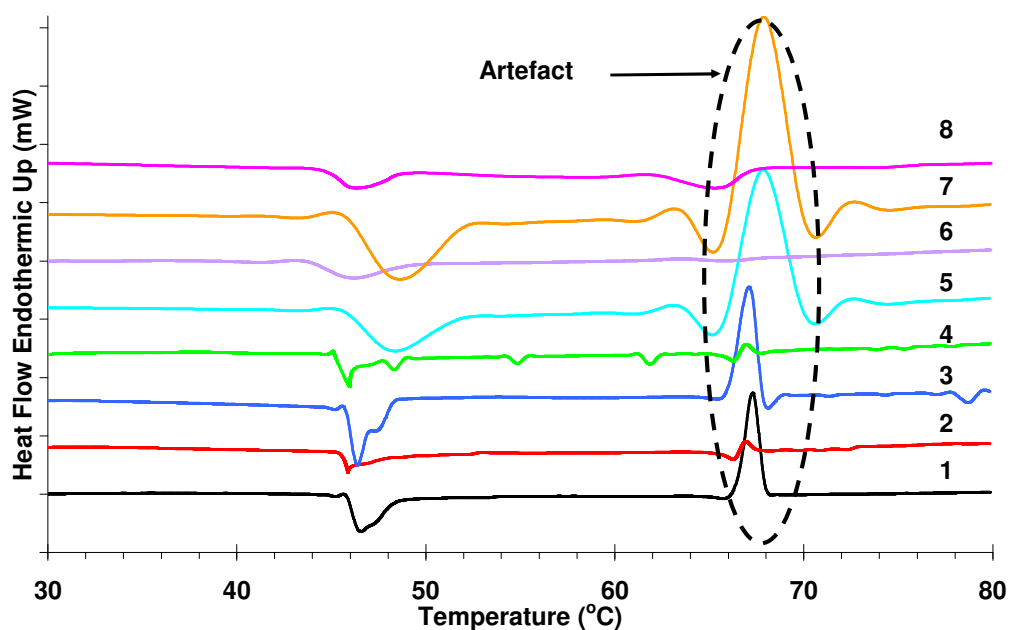


**Figure 7.4: Non-reversing traces for PPP.** Numbers 1-8 refer to the corresponding reversing traces on Figure 7.3

From the results shown in Figures 6.3 and 6.4, the following observations can be made:

1. A wide reversing melting trace is observed with a large step amplitude

2. A wide non-reversing recrystallisation trace is obtained with a large step amplitude
3. Short isothermal times produce smaller reversing melting trace
4. Large non-reversing melting trace results from short isothermal times, and
5. The initial step heating rate seems to have very little effect on the overall results.

Artefacts are also produced depending on the parameter chosen. In order to avoid artefacts and achieve at least an approximate separation into reversing (or rapid) and non-reversing (or slow signals), it is important to choose appropriate values for the 1) amplitude; 2) isotherm length and 3) step rate (Figure 7.1)

#### *7.3.1.1 Influence of step size (amplitude)*

The grossly widened traces recorded for large step sizes/amplitudes, both in the reversing and non-reversing traces are believed to be due to the averaging algorithm employed by the Stepscan software. In Stepscan, readings would be expected for the heat capacity and non-reversing heat flow every 2 K for a 2 K step size. There is more resolution on the curves than this, which must be produced by some form of interpolation. This is inferred as the exact algorithm is not available from the manufacturer. A method similar to a moving average would have the effect of smearing detail in the curves, i.e. at any one point there will be contributions from the nearest neighbour points. For large steps this will mean that points in a temperature range spanning the melting peak but outside of the peak itself will have contributions from the melting point and so

artificially broaden the peak. To preserve the resolution, small steps, should be chosen. This is particularly important for example when studying pure triacylglycerols such as PPP, where transitions occur over a narrower temperature range than in the case of a mixed system like chocolate. Short step size, in the case of PPP, enables the separation of transformation events from  $\alpha$  to  $\beta'$  and  $\beta'$  to  $\beta$  as shown on trace 3 in Figure 7.4. However the overall sensitivity is impaired by small values, with 1 to 2°C producing less noise compared to 0.5 °C.

#### *7.3.1.2 Isothermal length*

The length of the isotherm is a crucial parameter. As well as determining the underlying heating rate,  $\beta$ , which if small reduces the overall sensitivity of the measurement, it determines the value of the non-reversing component. Ideally this should settle down to a steady value. One type of artefact that can arise by choice of too short an isotherm can be seen on Figure 7.5.

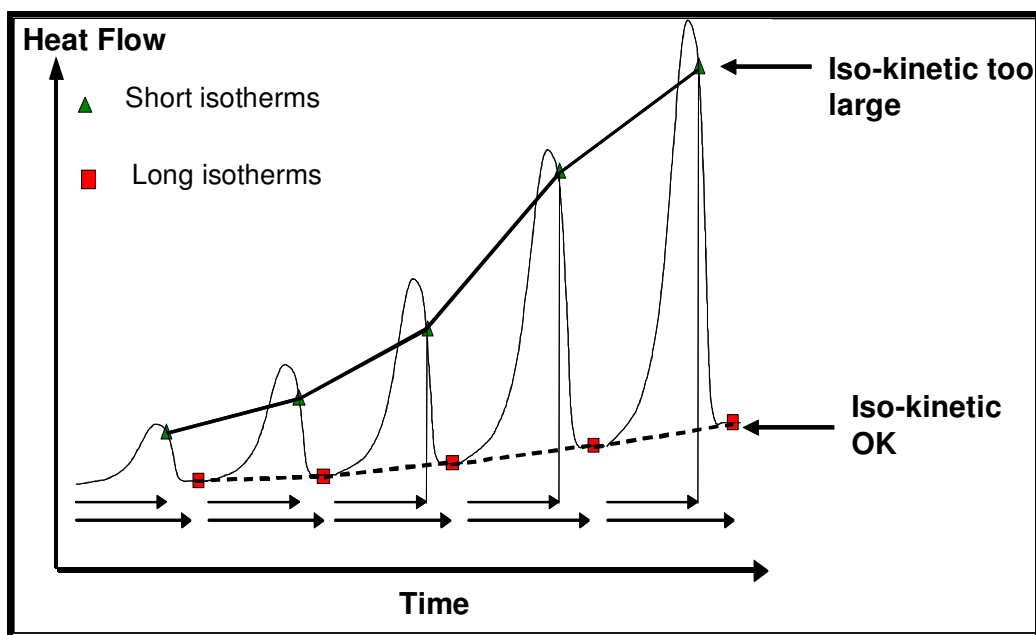


**Figure 7.5: The effect of isothermal time on the heat flow signal. Too short a time leads to the  $C_p$  or reversing signal appearing in the iso-kinetic or non-reversing trace.**

This produces an artificially high non-reversing trace. In addition if there is a limit to the amount of heat that can be supplied to the furnace, determined by the thermal resistance, the choice of too short an isotherm means that the heat flow value can become steadily greater as more time is taken for the instrument to react and can lead to reversing signal appearing in the non-reversing trace and inaccuracies appearing in the calculation of  $C_p$ . However, as shown on Figure 7.6, for tripalmitin, which exhibits rapid recrystallisation, if the choice of isotherm is long compared with the rate of recrystallisation, then the iso-kinetic baseline gives misleading estimates of the process.



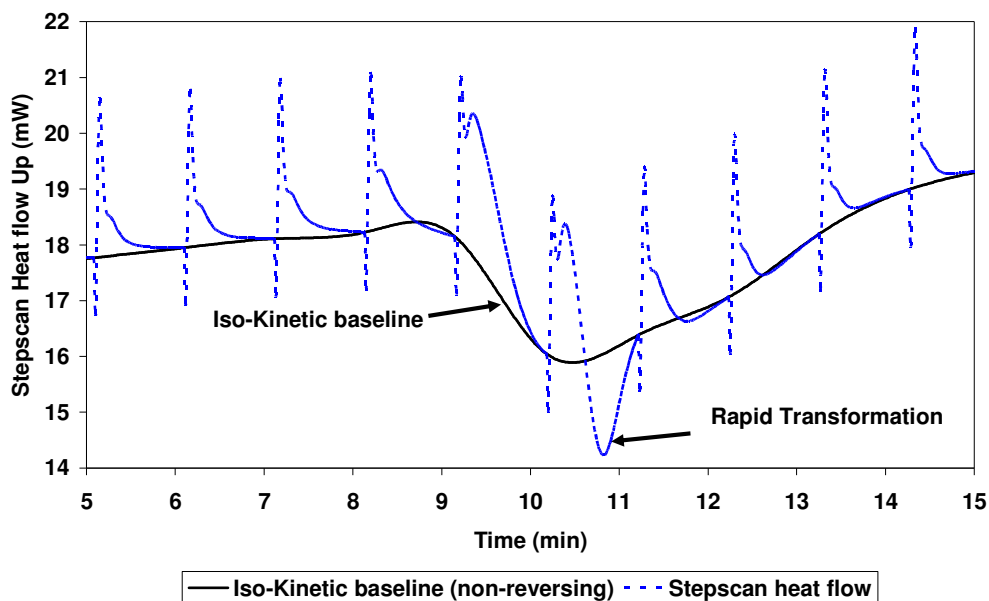


**Figure 7.6: Potential distortions in the non-reversing trace when the transformation is rapid. This trace is for the PPP (temperature step =  $0.5^{\circ}\text{C}$ , isotherm length = 1 minute and heating rate for the step =  $150^{\circ}\text{C}\cdot\text{min}^{-1}$ ), which rapidly transforms from the  $\alpha$  to the  $\beta$  polymorph. Too long an isothermal time results in the heat flow of the reaction being “missed”.**

For PPP, short isothermal times lead to an artificially high signal in the non-reversing trace as shown in Figure 7.4. However they also produced sharper recrystallisation peaks as shown in Figure 7.7. Long isothermal times also lead to artefacts in the recrystallisation event occurring at  $46^{\circ}\text{C}$  Figure 7.7. This is believed to occur due to the averaging algorithm used in data deconvolution. Long isothermal times also widened peaks and reduced the intensity of recrystallisation in PPP. A choice of smaller amplitude steps can help in such situations. In fact, in chocolate, the recrystallisation events are sufficiently fast that the Stepscan method, within the limits of the instrumentation, can only provide an approximation to the transformation.

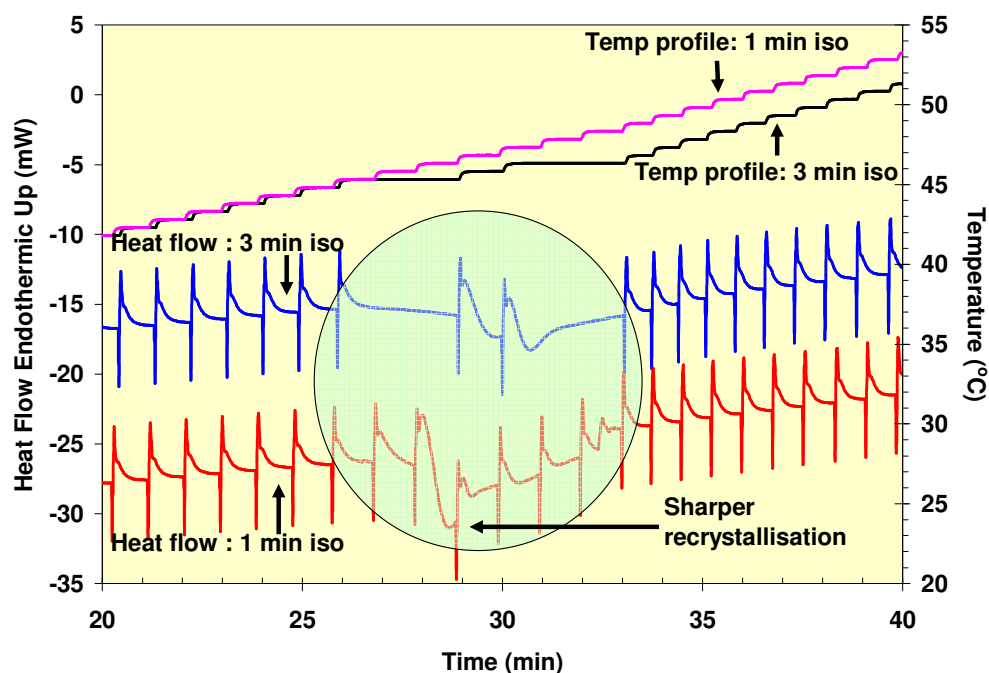


**Figure 7.7: Influence of isothermal length on artefacts produced in the recrystallisation area of PPP**

### 7.3.1.3 Influence of the step heating rate

The rate of temperature increase of the step was found to have little effect. This was expected as the calculation of  $C_p$  was simply made from the heat flow produced in response to the overall increase in temperature.

### 7.3.2 Parameter optimisation for chocolate

As has been discussed above, the choice of parameter value to optimize one feature, for instance the separation of reversing and non reversing signals (long isothermal time) could be in conflict with the value required to optimize another feature, for example the accurate recording of the non reversing signal (short isothermal time). In the light of the above results, it would appear that

the Stepscan method would cope better with broader melting and slower recrystallisation events as found in complex fat systems such as chocolate. These results with PPP suggested that an optimum step size and isotherm time would be in the region of 0.5 °C step size, step heating rate of 10 °C.min<sup>-1</sup> and isothermal time of 1 min. Initially conditions within this range were applied to tempered chocolate. As the results in Figure 7.8 show, these conditions resulted in large distortions in the non-reversing trace despite the DSC machine being correctly calibrated and sensitivity adjusted. Due to these distortions, the reversing trace appeared to have a much lower magnitude that that of the non-reversing trace, making interpretation of data difficult.

For this reason, further optimisation work was carried out on chocolate and the results are shown in Figure 7.9 and Figure 7.10.

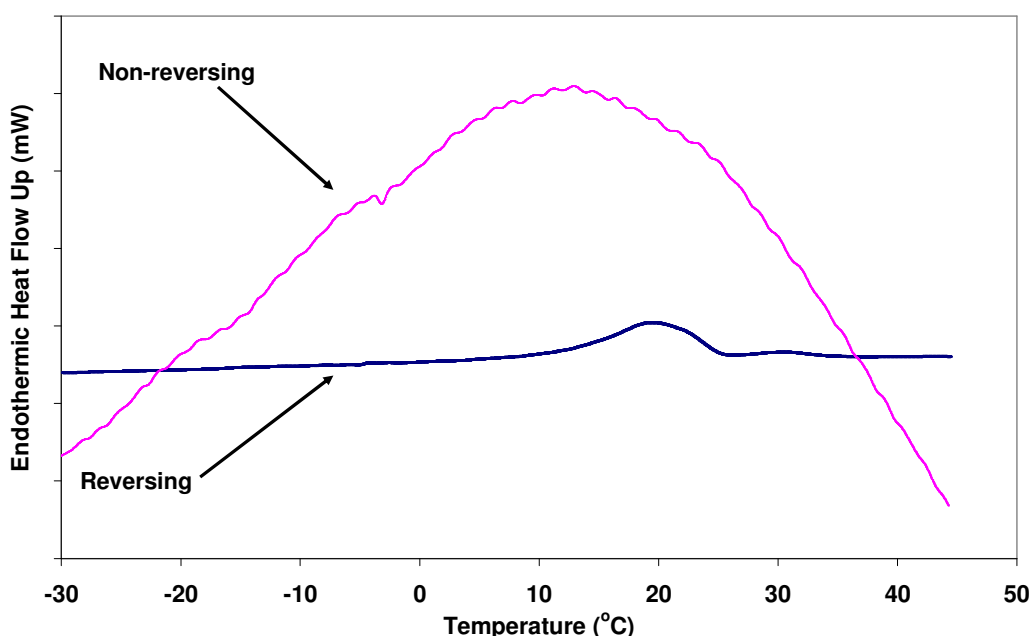


**Figure 7.8: Stepscan results for tempered chocolate (0.5 °C step size, 10 °C.min<sup>-1</sup> heating rate and 1 min isothermal time). The tempered chocolate was initially cooled at 1 °C.min<sup>-1</sup> prior to heating in Stepscan mode.**

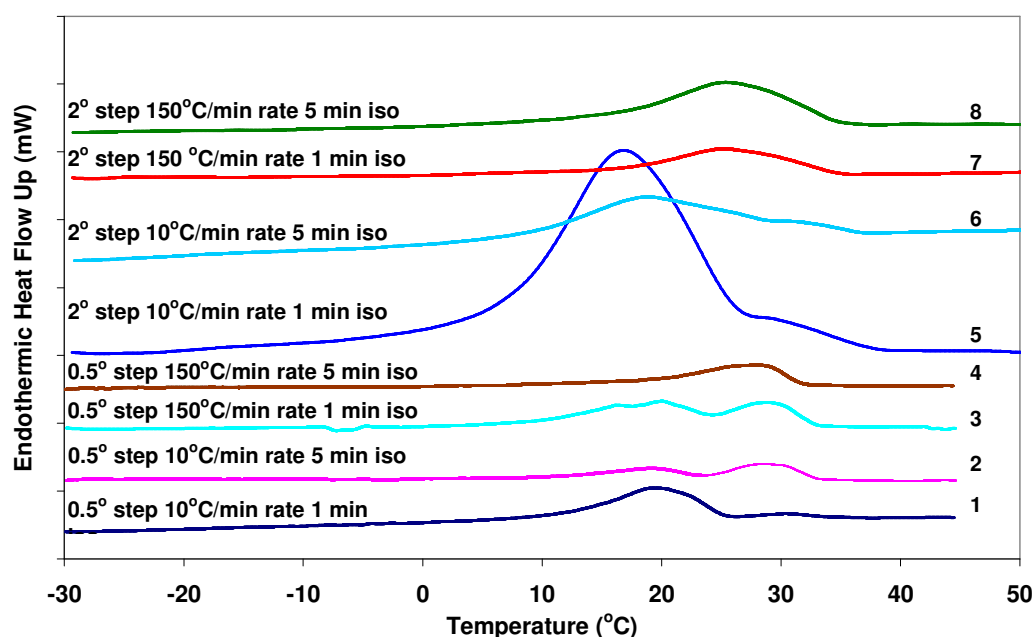


**Figure 7.9: Reversing traces of chocolate Stepscan optimisation results.** The Stepscan conditions are shown above each trace. The tempered chocolate samples were cooled to  $-30\text{ }^{\circ}\text{C}$  at  $1\text{ }^{\circ}\text{C}.\text{min}^{-1}$  prior to heating in Stepscan mode to  $50\text{ }^{\circ}\text{C}$ . Note: the initial cooling curves are not shown.

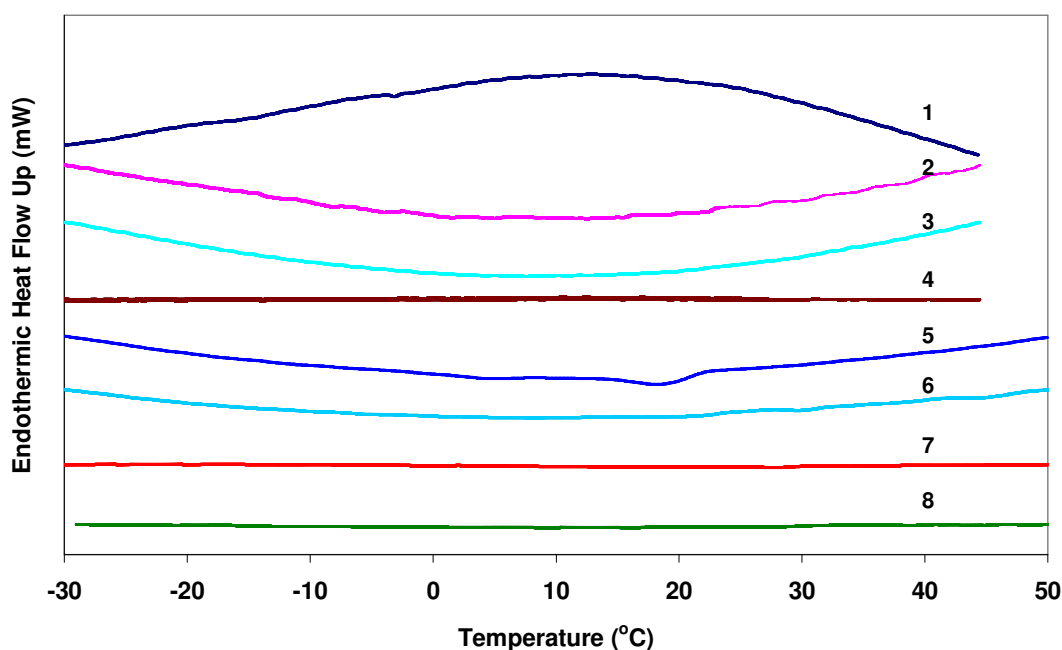


**Figure 7.10: Non-reversing traces of chocolate Stepscan optimisation results.** Numbers 1-8 refer to the corresponding reversing traces shown in Figure 7.9. The tempered chocolate samples were cooled to  $-30\text{ }^{\circ}\text{C}$  at  $1\text{ }^{\circ}\text{C}.\text{min}^{-1}$  prior to heating in Stepscan mode to  $50\text{ }^{\circ}\text{C}$ . The initial cooling curves are not shown.

As can be seen from Figure 7.9 and Figure 7.10, for chocolate, small step size

(0.5 °C) slow step heating rate (10 °C.min<sup>-1</sup>) and short isothermal time seem to lead to distortions in the non-reversing traces while increasing the step size, faster step heating rate and longer isothermal time lead to less distortion and minimise any potential artefact formation. Although resolution is better with smaller step size, sensitivity increases with a larger one. Hence, after this series of optimisation with both PPP and chocolate, a compromise set of parameters were chosen for chocolate: a step size of 2 °C, a step heating rate of 150 °C.min<sup>-1</sup> and an isothermal time of 5 minutes. These parameters will only be applicable for these samples and must be optimized for other systems.

### **7.3.3 Slow cooling experiments on tempered chocolate using conventional DSC and Stepscan DSC:**

The thermograms acquired using conventional DSC by heating at 2 °C.min<sup>-1</sup> on tempered chocolate, which had been cooled to -30 °C at 1°C.min<sup>-1</sup>, showed a series of endotherms with the main one having a peak temperature of ~28 °C. A typical conventional DSC result is shown in Figure 7.11. A heating rate of 2 °C.min<sup>-1</sup> was chosen in order to match the overall heating rate when the sample is heated in Stepscan mode. When heated in Stepscan mode, the overall heating rate ( $\beta$ ) is ~ 1.96 °C.min<sup>-1</sup>.

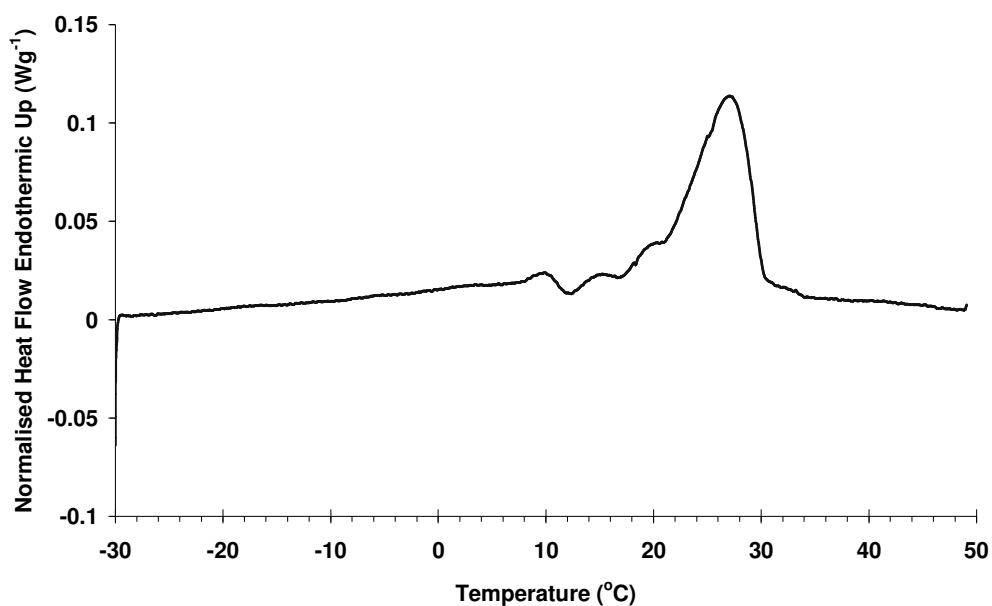


**Figure 7.11 : A conventional heating DSC thermogram for a tempered chocolate initially cooled at  $1^{\circ}\text{C}\cdot\text{min}^{-1}$  to  $-30^{\circ}\text{C}$ , followed by heating at  $2^{\circ}\text{C}\cdot\text{min}^{-1}$  to  $50^{\circ}\text{C}$ .**

As mentioned in previous chapters, the major melting event occurring at  $28^{\circ}\text{C}$  is that of the Form V polymorph, the value being depressed from  $33.8^{\circ}\text{C}$  (Wille and Lutton, 1966) due to the presence of milk and other vegetable fats (Reddy et al., 1996). Other minor melting events are observed at temperatures (peak) of  $\sim 9$ ,  $14$  and  $19^{\circ}\text{C}$ . These are attributed to low melting point triacylglycerols present in the fat fraction of chocolate solidifying due to the sample of chocolate being cooled to  $-30^{\circ}\text{C}$ . These triacylglycerols would normally be in the liquid phase at room temperature. Stepscan experiments were then performed and were used in order to facilitate the assignment of thermal events on the thermograms.

Figure 7.12 shows the processed Stepscan thermogram deconvoluted into the reversing and non-reversing heat flow components.

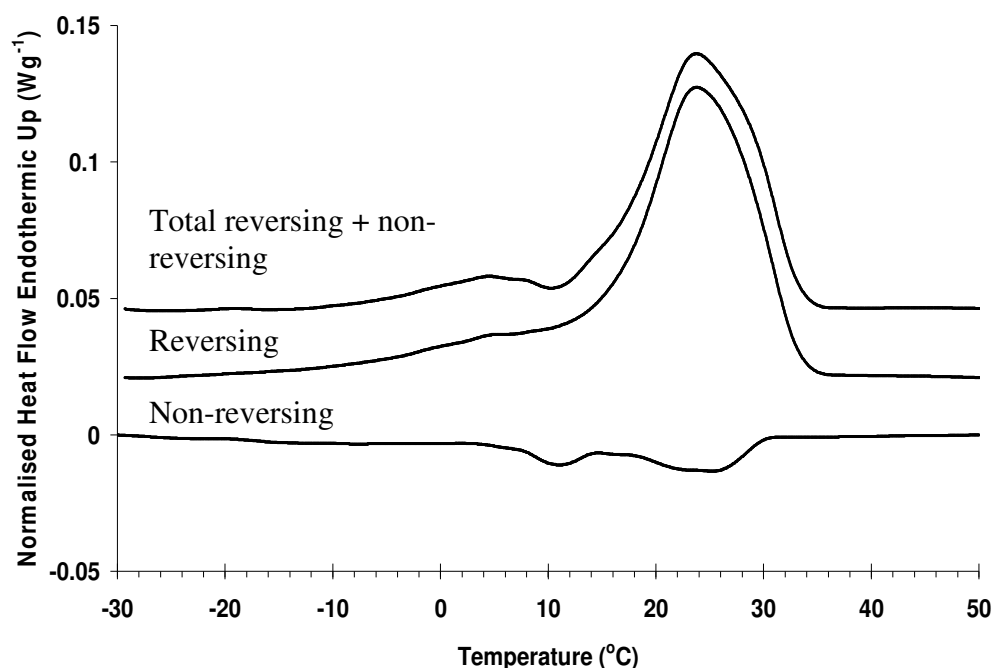


**Figure 7.12: Deconvolution of Stepscan data for a tempered chocolate initially cooled at  $1^{\circ}\text{C}.\text{min}^{-1}$  to  $-30^{\circ}\text{C}$  into reversing and non-reversing components.**

The total heat flow trace was only broadly similar to that obtained by conventional DSC (Figure 7.11). The reversing component showed similar melting endotherms to those in Figure 7.11, namely at peak temperatures of 5-9, 24 and  $29^{\circ}\text{C}$ . The non-reversing trace showed evidence of exothermic heat flow at  $\sim 11$ , 22 and  $26^{\circ}\text{C}$  suggesting that crystallization events occur during heating, i.e., overlapped with some of the melting events. This observation, which cannot be unequivocally implied using conventional DSC, is of significance, as it could lead to a range of artefacts in conventional DSC analysis of chocolate. Distortion of melting endotherms could lead to the underestimation of latent heat of melting, as the measured values reflect the overall sum of endothermic and exothermic heat components, together with errors in estimating peak temperatures.

However there are still significant artefacts present on the Stepscan thermograms. The resolution is poorer due to the large step amplitude (2 °C) (Figure 7.12), however, both of the major melting peaks on Figure 7.11 and Figure 7.12 are probably composite peaks composed of at least 2 underlying melting peaks. It is also worth noting that the peak temperature of the melting endotherm in both the reversing and the total heat flow of the Stepscan data is shifted to slightly lower values compared with the conventional DSC. This is thought to be due to the fact that the calibration is applied to the thermal data when the heating has stopped during the isothermal hold. For Stepscan, a small increment should be added to temperature onset values in this case typically of the order of 0.5 °C for a 10 °C.min<sup>-1</sup> calibration. The issue of calibration is complex and there has been no accepted protocol on what calibration should be applied when using Stepscan DSC. The difficulty is in the choice of time-temperature profile for the calibration and a suitable standard. In this study, a calibration performed at a constant heating rate of 2°C.min<sup>-1</sup> was used. This rate matches the underlying heating rate of the Stepscan time-temperature profile.

#### **7.3.4 Rapid cooling experiments on tempered chocolate using conventional DSC and Stepscan DSC:**

In order to assess the impact of rapid cooling on the DSC melting thermogram, tempered chocolate was cooled in the calorimeter at a rate of 10 °C.min<sup>-1</sup> followed by heating at a rate of 2 °C.min<sup>-1</sup> (Figure 7.13). As shown previously in Chapter 5, cooling at this rate leads to the formation of lower melting



polymorphs. The lower heating rate of  $2^{\circ}\text{C}\cdot\text{min}^{-1}$  was chosen to match the overall Stepscan heating rate. The melting of lower forms at  $\sim 6^{\circ}\text{C}$  and recrystallisation at  $\sim 13^{\circ}\text{C}$ , although present, appear to be less marked at a heating rate of  $2^{\circ}\text{C}\cdot\text{min}^{-1}$  compared with heating samples at  $10^{\circ}\text{C}\cdot\text{min}^{-1}$ . This may be due to lower sensitivity obtained at lower heating rates. As previously discussed, the results of heating at  $10^{\circ}\text{C}\cdot\text{min}^{-1}$  following rapid cooling at rates greater than  $10^{\circ}\text{C}\cdot\text{min}^{-1}$ , lacked consistency (Table 7.2). At a lower heating rate of  $2^{\circ}\text{C}\cdot\text{min}^{-1}$  the results appeared to be more reproducible and a typical response is shown in Figure 7.13. A likely explanation for this variability is that the inverse relationship between heating rate and time being allowed for recrystallisation events to proceed. A lower heating rate would allow more time for the system to convert to higher forms over a wider temperature range. Stepscan experiments, which incorporate an isothermal hold time, carried out on rapidly cooled chocolate samples (discussed below) showed the recrystallisation event in every run.

**Table 7.2: Number of experiments carried out at different cooling rates showing the recrystallisation exotherm upon melting.**

<b>Cooling rate</b>	<b>Number of experiments done</b>	<b>Number of experiments showing exotherms</b>	<b>% of experiments showing recrystallisation exotherm on heating</b>
<b><math>10^{\circ}\text{C}\cdot\text{min}^{-1}</math></b>	25	14	56 %
<b><math>20^{\circ}\text{C}\cdot\text{min}^{-1}</math></b>	20	7	35 %
<b><math>30^{\circ}\text{C}\cdot\text{min}^{-1}</math></b>	20	5	25 %
<b>Quenching in liquid nitrogen</b>	20	4	20 %

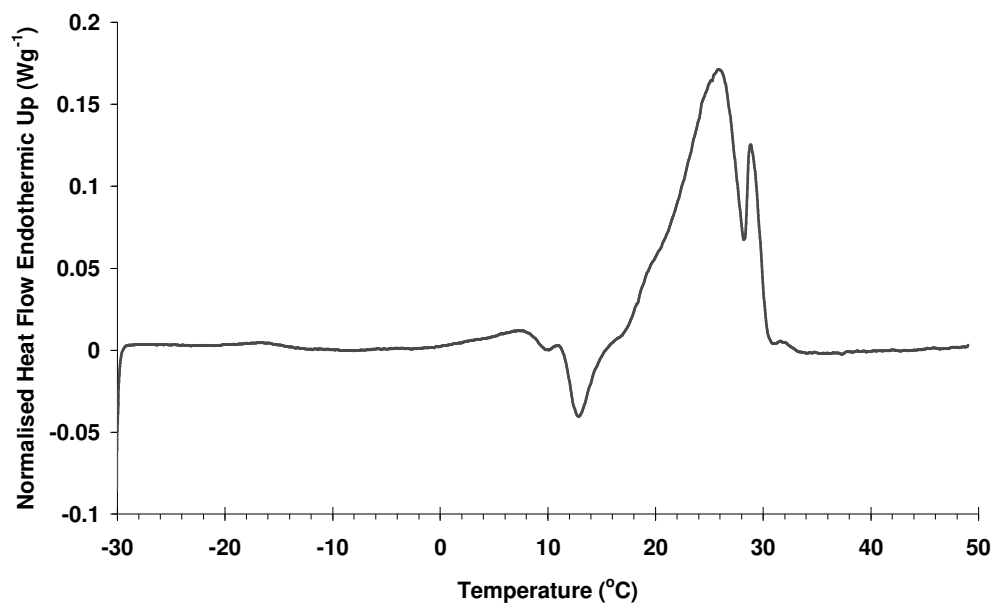


**Figure 7.13: A conventional heating DSC thermogram for a tempered chocolate initially cooled at  $10^{\circ}\text{C}.\text{min}^{-1}$  to  $-30^{\circ}\text{C}$  followed by heating at  $2^{\circ}\text{C}.\text{min}^{-1}$  to  $50^{\circ}\text{C}$ .**

Stepscan thermograms for a tempered chocolate sample that was cooled at  $10^{\circ}\text{C}.\text{min}^{-1}$  are shown in Figure 7.14.

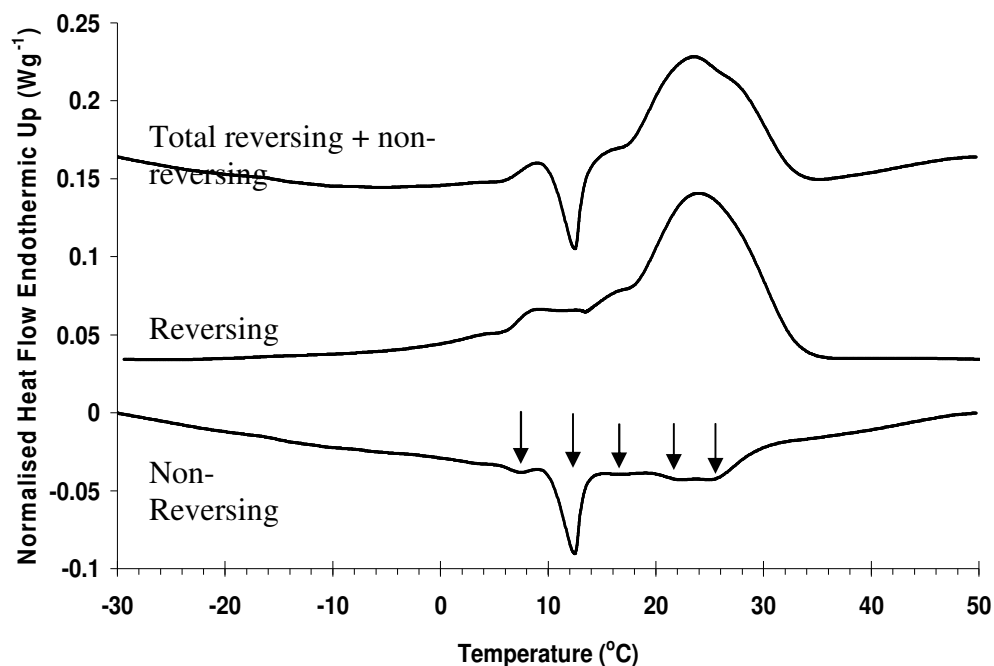


**Figure 7.14: Stepscan DSC results for tempered chocolate initially cooled at  $10^{\circ}\text{C}.\text{min}^{-1}$ . The recrystallisation events are shown by an arrow on the non-reversing trace.**

The results clearly show the large non-reversing heat flow component centred at  $\sim 12^{\circ}\text{C}$  relating to a recrystallisation exotherm. The non-reversing curve shows multiple crystallization events occurring at temperatures of  $\sim 7, 12, 17, 22$  and  $26^{\circ}\text{C}$  which cannot all be detected in the conventional DSC trace. The main difference between the conventional and Stepscan DSC result for rapid cooling is the absence in the Stepscan trace (Figure 7.14) of the very sharp recrystallisation event at  $28^{\circ}\text{C}$  seen on the conventional DSC trace (Figure 7.13). This is likely to be due to the fact that this event is so rapid that it is not picked up by the slower heating rate employed in Stepscan DSC. The observation of multiple crystallization events indicates that transformation processes are complex. The melting events are also clearly separated out and

hence it is possible to calculate the crystallization and melting enthalpies involved from the non-reversing and reversing traces respectively. Such a calculation, although possible, is of little quantitative value due to inaccuracies in the non-reversing trace and the fact that the melting enthalpy of cocoa butter is strongly dependent on its polymorphic form (Rudnicki and Niezgódka, 2002) which is not known accurately without recourse to simultaneous X-ray diffraction (XRD).

It is however interesting to compare the melting enthalpies obtained from the conventional and Stepscan DSC analysis. The overall endothermic melting enthalpy obtained by integrating the conventional DSC thermogram for the tempered chocolate cooled at  $1\text{ }^{\circ}\text{C}\cdot\text{min}^{-1}$  over the temperature range  $-10\text{ }^{\circ}\text{C}$  and  $40^{\circ}\text{C}$  was  $31\text{ J}\cdot\text{g}^{-1}$ . This value is comparable to that obtained from the equivalent total (reversing + non-reversing) Stepscan thermogram ( $34\text{ J}\cdot\text{g}^{-1}$ ) but smaller than that obtained from the reversing component of the thermogram ( $40\text{ J}\cdot\text{g}^{-1}$ ). The difference between the reversing Stepscan and the conventional DSC values reflects the inability of the latter to separate exothermic contributions from the crystallization events discussed above. Additionally, there is the contribution of milk fat to the enthalpy in this temperature range, and the presence of other materials such as sugar, which do not contribute. The net result is to render the absolute enthalpy calculation complex and cause the recorded values of between  $30$  and  $40\text{ J}\cdot\text{g}^{-1}$  to be much less than the values for pure cocoa butter. For example the  $\Delta H_m$  of Form II of cocoa butter ( $T_m = 23.3$ ) is  $\sim 86\text{ J}\cdot\text{g}^{-1}$  while that of Form V ( $T_m = 33.9^{\circ}\text{C}$ ) is  $\sim 137\text{ J}\cdot\text{g}^{-1}$  (Rudnicki and Niezgódka, 2002)

### 7.3.5 The effect of tempering on recrystallisation

While the transformation on heating of lower to higher melting point polymorphs is significant, even in chocolate cooled slowly ( $1^{\circ}\text{C}.\text{min}^{-1}$ ), it is not clear whether the existence of higher form nuclei (as a result of tempering) plays any role in this transformation. To answer this question, conventional and Stepscan DSC experiments were performed on untempered chocolate samples in rapid cooling conditions ( $10^{\circ}\text{C}.\text{min}^{-1}$ ). When comparing the result of conventional DSC melting of the untempered to tempered chocolate (Figure 7.15), it was clear that the untempered chocolate crystallised largely into an intermediate melting point polymorph believed to be Form II (confirmed by XRD, results not shown) which had a peak temperature of  $\sim 17^{\circ}\text{C}$ . Minor melting endotherms were observed at  $-11$  and  $25^{\circ}\text{C}$ . There was no evidence of any higher forms (Forms V and VI). The absence of a crystallization exotherm in the conventional DSC thermogram of the untempered sample was the most striking difference when compared with the behaviour of the tempered sample, suggesting that the existence of nuclei is necessary for the recrystallisation process. The free energy of formation of nuclei of the higher forms, despite being the most stable polymorphs, is high. Furthermore, there is insufficient time during a scan (Stepscan or conventional) for nucleation to occur.

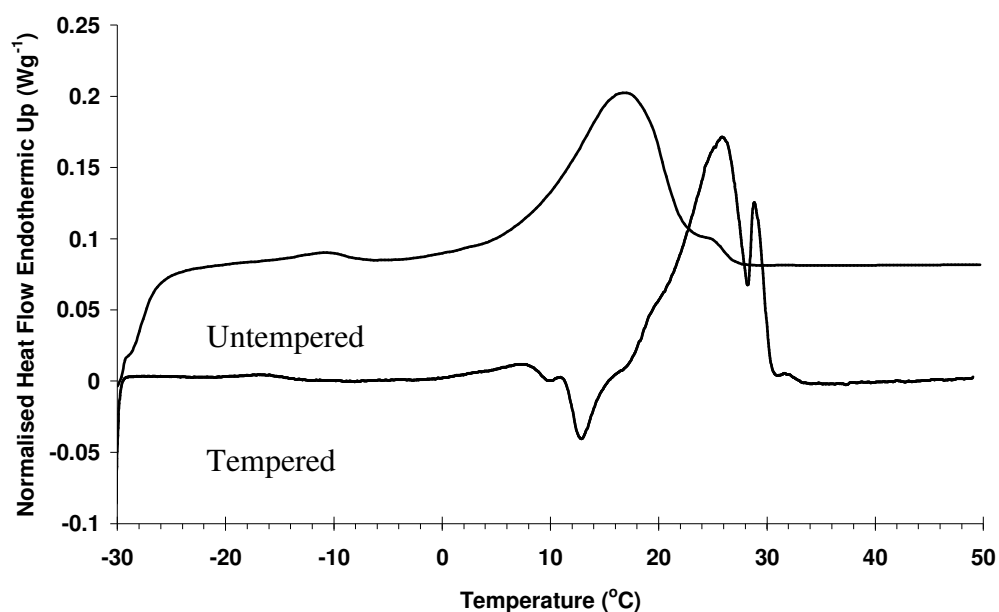


**Figure 7.15: Conventional heating DSC thermograms for tempered and untempered chocolate initially cooled at  $10\text{ }^{\circ}\text{C.min}^{-1}$  and heated at  $2\text{ }^{\circ}\text{C.min}^{-1}$ . Note that peak melting temperature is lower for the untempered sample, and no recrystallisation events are seen.**

Stepscan was performed on a sample of untempered chocolate cooled at  $10^{\circ}\text{C.min}^{-1}$  in order to test the above proposal, i.e. the absence of recrystallisation in non-nucleated systems. The results were compared with those obtained on the nucleated/tempered system (Figure 7.16). Although some evidence of multiple recrystallisation events can be seen on the non-reversing trace, they were of a much smaller magnitude compared to the results obtained with tempered chocolate under the same experimental conditions. This confirms the suggestion made above that nuclei of a higher form (Form V in this instance) are required in order for well-defined recrystallisation to take place.

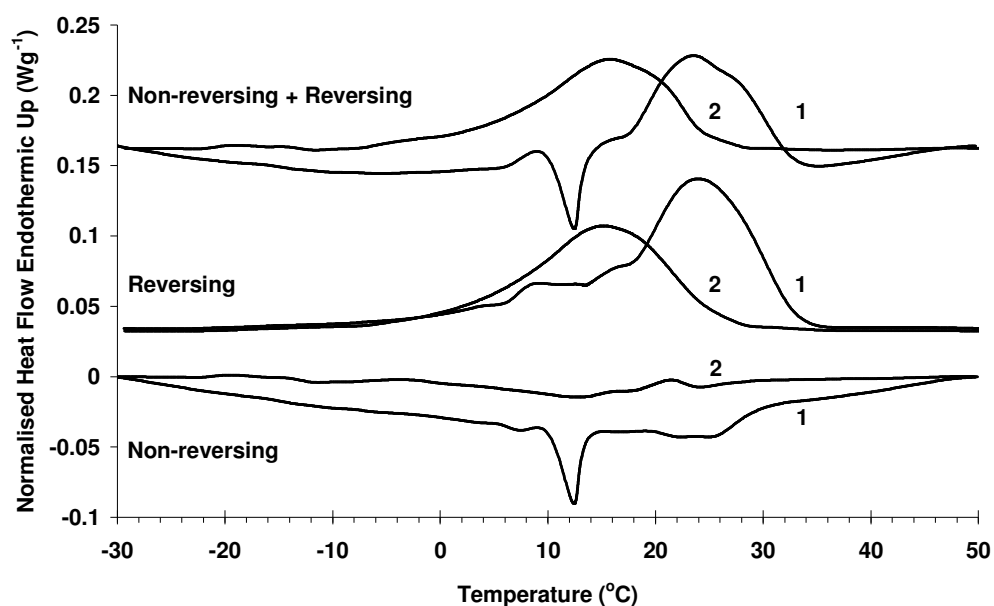


**Figure 7.16: Stepscan thermograms for tempered (1) and untempered (2) chocolate initially cooled at  $10^{\circ}\text{C}.\text{min}^{-1}$  then heated in the Stepscan mode.**

## 7.4 Conclusion

Stepscan is a useful addition to conventional DSC modes and offers additional information in the thermal analysis of tempered and untempered chocolate. The technique demonstrated that even in slowly cooled tempered chocolate, there is the formation of low melting point polymorphs. This is more pronounced for rapidly cooled chocolate. These low melting polymorphs melt on heating and the liquid formed is consumed in the growth of existing high melting point nuclei. This finding questions the validity of DSC determined melting enthalpies and temperatures of polymorphs of mixed systems.

However, the iso-kinetic (non-reversing) recording of kinetic processes is poor if the process is fast or if incorrect parameters are chosen, nevertheless the information even if approximate is useful. There are further limitations to the

technique. A Stepscan measurement generally requires more time than conventional DSC, since a lower underlying heating rate is normally used. Moreover, care and time must be taken in determining the Stepscan parameters (step size, isothermal time and step heating rate) and interpreting their effect on the results.

The Stepscan DSC results support and indeed strengthen the overall hypothesis that rapid cooling results in the production of lower melting polymorphs of cocoa butter that subsequently melt and recrystallise into higher forms. It is encouraging to note that the results obtained with Stepscan DSC are more consistent and reproducible compared to those obtained with conventional DSC. We interpret this in terms of both a lower overall heating rate in the case of Stepscan DSC and also the importance of the isothermal segments which allows the sample sufficient time to melt and recrystallise. Hence, these events are consistently obtained during Stepscan heating. It has also been seen that Stepscan results can provide additional information such as small underlying crystallisation events occurring simultaneously during melting which are difficult to deconvolute from a conventional DSC scan. This could be of significance as it can lead to underestimation of enthalpy calculations and possibly solid-liquid ratio estimation if based solely on partial areas and enthalpy calculations.



## **Chapter 8: General Discussion and Future work**

*In this chapter, the results are discussed as a whole and suggestions are made for future work.*

## 8 General conclusions

The aim of this work was to try to understand how the Frozen cone® process works and the two main questions that one aimed to explain concerning this process were:

1. The ability to rapidly cool chocolate and end up with the correct polymorphic Form V in the final product
2. Understanding how good demoulding is achieved following rapid cooling.

This section will discuss these two areas separately with reference to the experimental results.

### 8.1 Rapid cooling to produce Form V

The hypothesis derived from preliminary DSC results stated that actually, rapid cooling of tempered chocolate leads to the formation of lower melting point polymorphs at the expense of the further growth and stabilisation of Form V ( $\beta_2$ ) nuclei formed during tempering. It is only upon subsequent warming of the chocolate that the kinetics shift in favour of Form V growth. Simultaneously, the lower melting polymorphs melt and recrystallise in the more stable Form V. From X-ray diffraction data, these lower forms were identified as Forms I ( $\gamma$ - or sub- $\alpha$  polymorph) and II ( $\alpha$ -polymorph). Form I is first created upon rapid cooling and upon warming it transforms to Form II, which eventually transforms to Form V. This further enhances the growth of Form V and hence, in the final product, only Form V is present in the chocolate matrix. From the

experimental results obtained, it is the Form I or sub- $\alpha$  phase that forms first because although Form V ( $\beta_2$ ) nuclei are present, their kinetics of formation is greater than that of Form I.

Another observation made from the DSC results is that recrystallisation following melting of lower melting polymorph is strongly dependent on the heating rate. Slow heating combined with isothermal periods, like the conditions in Stepscan heating, favours this event and recrystallisation is consistently occurs. This can also be explained in terms of kinetics. During Stepscan heating, the heating rate is sufficiently slow to favour the formation of the more stable phase which grows at a very slow rate. The isothermal period allow the system more time to complete any transformations occurring.

The recrystallisation of lower melting polymorph to Form V also raises the question of whether this transition is a solid-solid one or is it a solid-liquid-solid transition. According to Sato, (1989) a melt-mediated transformation is said to occur after the rapid melting of less stable forms. From the DSC data obtained, one may assume that the transformation of unstable  $\beta'$  to more stable  $\beta$  (Form V) form was indeed a melt-mediated one or a solid-liquid-solid transformation. However, once has to bear in mind that the sample was being heated during the DSC experiment, so the melting of the lower forms could have been a consequence of this application of heat. The X-ray diffraction pattern for a rapidly cooled tempered cocoa butter sample is reproduced in Figure 8.1. From the different X-ray patterns acquired as the sample was being warmed, it is not clear whether the transformation is actually melt mediated. It appears to be more via a solid to solid transformation due to the absence of a

significant amorphous phase. A possible way to determine whether the Form II underwent melt-mediated or solid-solid transformation to Form V would be to calculate the % crystallinity and amorphous ratio of the sample with increasing temperature. To do this however, one would need to know beforehand the crystallinity values of each polymorph of cocoa butter at different temperatures. Another way to determine the type of transformation taking place would be to carry out pulse NMR (pNMR) experiments to determine solid/liquid ratios. In this case as well, one would need to previously determine the solid/liquid ratios for each polymorph at different temperature and derive the proportion of the polymorphs present in a sample at a particular temperature. Kevin Smith's team at Unilever Research, UK has used a combination of pNMR results and X-ray diffraction data (personal communication) in order to quantify the amount of polymorphs present in a mixture. It would necessary to adapt the method he developed in order to apply it to the results obtained in this work.

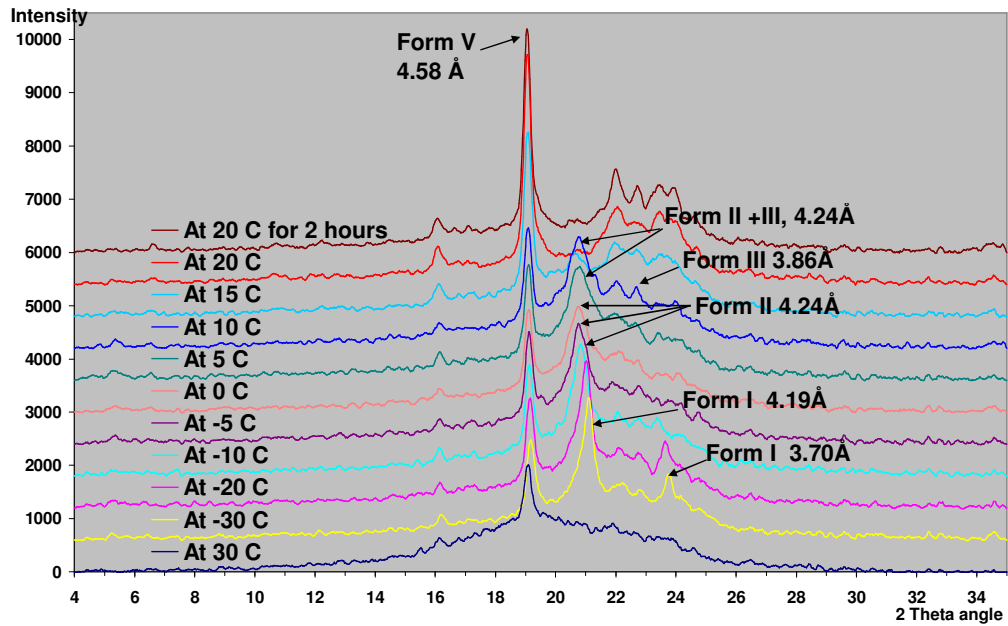


**Figure 8.1: Tempered cocoa butter (CB) cooled at 20 °C.min<sup>-1</sup> to -30 °C then warmed at 1 °C.min<sup>-1</sup> with scans acquired at every 5-10 °C interval up to 20 °C**

Tempering has also been shown to be crucial in order that a rapidly cooled material ends up in the stable Form V. Within the time frame of the industrial Frozen cone process and indeed the lab experiment (~1 hour), it is necessary to have the presence of Form V nuclei in the material to be rapidly cooled. If untempered material were indeed to be used, the process would not be economically viable as it would require a long holding process at 20 °C for hours if not days in order to allow the unstable phases to eventually transform to the stable Form V phase. This would also result in bloom defects, making the product of unacceptable quality.

## **8.2 Good demoulding properties following rapid cooling**

Good release from the stamp and good demoulding properties is of crucial importance to the Frozen cone process. When these are achieved, the process is considered to be successful. There are two possibilities to explain the release mechanism of the cold stamp from the chocolate.

1. The adhesive property of the material at a given temperature
2. The nature of the polymorph formed

### **8.2.1 The adhesive property of the material formed at low temperature**

As mentioned in Chapter 6, it is possible that the adhesive property of the specific polymorph formed may be responsible for the release of the material from the X-ray holder or in the case of the industrial Frozen Cone process, release of the chocolate from the cold stamp.

Adhesion can be described as the interactions that form between two objects that are in contact. It can be measured by the force required to separate the two and overcome these interactions. The theory of adhesion can be found in works by Allen, (1993), Houwink and Salomon, (1995), and Gierenz and Karmann, (2001).

The mechanism by which an adhesive bond fractures is very important in determining the overall amount of adhesion. One type of adhesive that exist is the pressure sensitive adhesive (PSA). Traditional PSAs are made of soft

viscoelastic materials. PSAs display tack, the property of instantaneously “wetting” an opposing substrate under little or no applied pressure (Pocius, 2002). This means that they can be applied to a surface and adhere instantly under only light pressure. To do so, PSAs are found to satisfy the “Dahlquist criterion for tack,” which states that the modulus should be less than 300kPa when measured at 1Hz (Dahlquist, 1989). Adhesion will not occur when the adhesive storage modulus ( $G'$ ) is greater than  $10^6$ Pa and at this point the adhesive is unable to wet the surface it is applied to, to produce the contact required for good adhesion. Assuming that the polymorphic forms of cocoa butter behave like PSAs, this would explain their adhesion or lack of adhesion to the cold surfaces. It is possible that Form I, at temperatures where cocoa butter and chocolate fats do not adhere to the cold surface, possesses a storage modulus greater than  $10^6$ Pa. As temperature increases and Form I transforms to Form II, the storage modulus may decrease, hence increasing the ‘wetting ability’ of the material, resulting in adhesion to the mould/stamp surface. It is possible that the storage modulus will depend on both temperature and polymorphic form present in the material. To measure this stickiness factor in chocolate, it would be interesting to measure its storage modulus and that of its fats using dilatometry and dynamic mechanical thermal analysis (DMTA).

#### *8.2.1.1 Presence of a liquid phase at the surface*

Another possibility to explain the adhesion of the chocolate to the Frozen Cone stamp could be the presence of a liquid phase at the surface. As the temperature of the stamp is increased, instead of a solid layer of material being produced

upon contact, the material may be in a semi solid or liquid state. This ‘slippery’ surface will cause the bulk of the material to adhere to the surface of the stamp, resulting in poor release. The presence of any liquid phase could be detected by carrying pNMR studies on both tempered and untempered material and calculating the solid: liquid ratios at different temperatures. Although this type of experiment was not investigated in this study, some preliminary NMR work (not shown in this study) was carried out to determine solid: liquid ratios in tempered chocolate fats at temperatures between -30 and 20 °C. These preliminary results showed however that from -30 to 0 °C, the samples were solid and no liquid signal was detected. However, it must be pointed out that the temperature on the NMR could not be controlled accurately and the design of the experiment would need to be proper set up and modification in order to mimic the Frozen Cone® process accurately.

### **8.2.2 The nature of the polymorph**

The X-ray results of the direct contact cooling experiments showed that good release was obtained when Form I was present in the matrix. This could lead to the speculation that the actual molecular arrangement present in Form I may be responsible for this. Form I or sub- $\alpha$  was found to be generated upon fast cooling by Loisel et al., (1998) and Marangoni and McGauley, (2003). Loisel et al., (1998) describe this phase as being less organised than the  $\alpha$ -form (Form II) and that it transforms irreversibly upon heating into the  $\alpha$ -form. This was confirmed by the results obtained in this work. Loisel et al., (1998) also deduced from their long and short spacing data that the sub-  $\alpha$  (Form I) has a



packing that is more compact than the hexagonal arrangement of the  $\alpha$ -form (double chain structure) and it resembles more that of the  $\beta'$  type (triple chain structure). From their data, the same authors also state that while the whole organisation of the sub-  $\alpha$  is less stable than of the  $\alpha$ , part of it corresponds to a phase much more ordered than  $\alpha$  and this indicates that only part of the structure is ordered while the rest is not. They thus put forward the theory that there might be two levels of organisation in the sub-  $\alpha$  phase: one crystalline and the other a liquid –like moiety. The presence of a liquid crystalline moiety in the structure would also explain why it progressively transforms to  $\alpha$  because according to Timms, (1984), the presence of a liquid favours the evolution of unstable species towards more stable forms.

It is possible that the molecular structure of this sub-  $\alpha$  phase is responsible for its adhesive properties (in our case, non-adhesive property). Its subsequent transformation to the  $\alpha$ -phase, i.e., the change from a triple chain structure to a double chain one could be responsible for the interactions at the surface of the molecule. Roughness is one of the factors that affect adhesion. The roughened surface provides a larger interface for interaction between the adhesive and the surface. In the case of a liquid adhering to a solid surface, increased roughness will improve adhesion as the liquid will wet the entire surface (Mittal, 1977) . For solid and semi-solids however, the roughness of the surfaces is likely to reduce the area of contact between them and cause a reduction in adhesion. It would therefore be of interest to measure and compare the surface roughness of the sub-  $\alpha$  and  $\alpha$ -phases and relate this property to surface adhesion.

### 8.3 Future Implications

Having seen that rapid cooling can result in the eventual formation of Form V in chocolate, what implications can this have on chocolate manufacture? Is it possible that rapid cooling can be applied not only to chocolate shells, but also chocolate bars? Chocolate bars are the most popular form in which chocolate is consumed. It might be possible to use rapid cooling in order to quicken the solidification process and the growth of stable Form V nuclei. Tempered chocolate could be deposited on cold polycarbonate moulds  $\sim -30\text{ }^{\circ}\text{C}$  which would result in the formation of Form I crystals on the surface in contact with the mould. Form I crystals could then act as seed crystals which would quicken the growth of Form V crystals upon warming. The warming period from a temperature of  $-30\text{ }^{\circ}\text{C}$  to  $10\text{ }^{\circ}\text{C}$  would be taking place when the moulded bars are kept at a temperature of  $10\text{ }^{\circ}\text{C}$ , enabling transformation of Form I to Form II and eventually Form V to occur while at the same time, Form V nuclei generated during tempering would also be growing. The rate at which warming takes place would need to be carefully controlled and therefore more work would need to be done to investigate the proper heating rate required, depending on the composition and thickness of chocolate being moulded.

## 9 References

- AASTED L., (1993); Aasted- Mikroverk APS, assignee. A method and device for moulding of chocolate articles. DENMARK patent 0 589 820 A1.
- ABERS D. (1928) De eigenschappen van cacaoboter in verband met het aantoonen van vreemde vetten in chocolade. *Cherni. Week*; 25:235-240
- ADENIER H., CHAVERON H. and OLLIVON M. (1984) Chocolate tempering control by simple differential thermal analysis. *Sciences des Aliments*; 4 (2):213-231
- ADENIER H., OLLIVON M., PERRON R. and CHAVERON H. (1975) Le blanchiment gras: Observations et commentaires. *Chocolaterie, Confiserie de France*; 315 (8):7-14
- ALEXANDER L. E. (1969) *X-ray diffraction methods in polymer science*. Wiley & Sons; New York.
- ALI A. R. M. and DIMICK P. S. (1994a) Melting and solidification characteristics of confectionery fats - anhydrous milk-fat, cocoa butter and palm kernel stearin blends. *Journal of the American Oil Chemists Society*; 71 (8):803-806
- ALI A. R. M. and DIMICK P. S. (1994b) Thermal-analysis of palm mid fraction, cocoa butter and milk- fat blends by differential scanning calorimetry. *Journal of the American Oil Chemists Society*; 71 (3):299-302
- ALLEN K. W. (1993) Current theories of adhesion and their relevance to adhesive technology. *Journal De Physique Iv*; 3 (C7):1511-1516
- BECKETT S. T. (1999) Non-conventional machines and processes. In: *Industrial chocolate manufacture and use*, Ed. by Beckett S. T., 3rd ed, Blackwell science, Oxford. p. 423-427.
- BECKETT S. T. (2000) *The science of chocolate*. Royal Society of Chemistry; Cambridge.
- BERBERT P. R. F. (1976) Influência das condições climáticas na composição química e características físicas da manteiga de cacau. *Revista Theobroma*; 6 (3):67-76
- BERBERT P. R. F. and ALVIM P. T. (1972) Fatores que afetam o índice de iodo da manteiga de cacau do brasil. *Revista Theobroma*; 2 (1):3-16
- CARTER M. G. R. and MALKIN T. (1939) An X-ray and thermal examination of the glycerides part v unsymmetrical mixed triglycerides,  $\text{ch}_2(\text{o cor}) \text{ch}(\text{o cor}) \text{ch}_2(\text{o cor})$ . *Journal of the Chemical Society*: 577-

- CEBULA D., DILLEY K. M. and SMITH K. (1991) Continuous tempering studies on model confectionery systems. *Manufacturing Confectioner*; (May):131-136
- CEBULA D. J. and SMITH K. W. (1991) Differential scanning calorimetry of confectionery fats - pure triglycerides - effects of cooling and heating rate variation. *Journal of the American Oil Chemists Society*; 68 (8):591-595
- CEBULA D. J. and SMITH K. W. (1992) Differential scanning calorimetry of confectionery fats .2. Effects of blends and minor components. *Journal of the American Oil Chemists Society*; 69 (10):992-998
- CEBULA D. J. and SMITH P. R. (1990) Dynamic polymorphic phase-transitions in a model binary triglyceride system measured by position-sensitive x-ray-diffraction methods. *Journal of the American Oil Chemists Society*; 67 (11):811-814
- CHASERI S. and DIMICK P. S. (1989) Lipid and hardness characteristics of cocoa butters from different geographic regions. *Journal of the American Oil Chemists Society*; 66 (12):1771-1776
- CHAPMAN D. (1956) Infrared spectra and the polymorphism of glycerides .1. *Journal of the Chemical Society*; (JAN):55-60
- CHAPMAN D. (1962) Polymorphism of glycerides. *Chemical Reviews*; 62 (5):433-&
- CHAPMAN G., AKEHURST E. and WRIGHT W. (1971) Cocoa butter and confectionery fats. Studies using programmed temperature X-ray diffraction and differential scanning calorimetry. *Journal of the American Oil Chemists' Society*; 48 (12):824-830
- DAHLQUIST C. A. (1989) In: *Handbook of pressure sensitive adhesives*, Ed. by Satas D., 3rd ed ed, Van Nostrand Reinhold, New York. p. 97.
- DE GRAEF V., FOUBERT I., AGACHE E., BERNAERT H., LANDUYT A., VANROLLEGHEM P. A. and DEWETTINCK K. (2005) Prediction of migration fat bloom on chocolate. *European Journal of Lipid Science and Technology*; 107 (5):297-306
- DE MEUTER P., RAHIER H. and VAN MELE B. (1999) The use of modulated temperature differential scanning calorimetry for the characterisation of food systems. *International Journal of Pharmaceutics*; 192 (1):77-84
- DEMMER T., WUTZ H., BAXTER J. F., KIRTLEY N. and EBBINGHAUS L., (2002); Kraft Foods R&D Ltd, assignee. Chocolate production by supercooling and press-forming. USA patent US 2002/00015775 A1.

- DIMICK P. S., ZIEGLER G. R., FULL N. A. and REDDY S. Y. (1996) Formulation of milk chocolate using milkfat fractions. *Australian Journal of Dairy Technology*; 51 (2):123-126
- DUCK W. (1958) A study of viscosity increase due to solid fat formation in tempering chocolate coatings. *Manufacturing Confectioner*; 38:9-12
- DUCK W. N. (1964) Determination of solid fat in melted fat, their role in the formation and polymorphic form by viscometry, Master Thesis. Lancaster.
- DUFFY P. (1853) On certain isomeric transformations of fats. *Journal of Chemical Society*; 5:197-210
- FESSAS D., SIGNORELLI M. and SCHIRALDI A. (2005) Polymorphous transitions in cocoa butter. *Journal of Thermal Analysis and Calorimetry*; 82 (3):691-702
- GARTI N. and SATO K. (1988) *Crystallization and polymorphism of fats and fatty acids*. Marcel Dekker; New York.
- GIBON V., DURANT F. and DEROANNE C. (1986) Polymorphism and intersolubility of some palmitic, stearic and oleic triglycerides - ppp, psp and POP. *Journal of the American Oil Chemists Society*; 63 (8):1047-1055
- GIERENZ G. and KARMANN W. (2001) *Adhesives and adhesive tapes*. Wiley-VCH; New York.
- GILL P. S., SAUERBRUNN S. R. and READING M. (1993) Modulated differential scanning calorimetry. *Journal of Thermal Analysis*; 40 (3):931-939
- GRAY M., LOVEGREN N. and MITCHAM D. (1976) Cold stage for X-ray diffractometer studies of lower-melting polymorphs of triglycerides. *Journal of the American Oil Chemists' Society*; 53 (5):196-197
- GUNARATNE L. M. W. K., SHANKS R. A. and AMARASINGHE G. (2004) Thermal history effects on crystallisation and melting of poly(3-hydroxybutyrate). *Thermochimica Acta*; 423 (1-2):127-135
- HACHIYA I., KOYANO T. and SATO K. (1989) Seeding effects on solidification behavior of cocoa butter and dark chocolate .1. Kinetics of solidification. *Journal of the American Oil Chemists Society*; 66 (12):1757-1762
- HAGEMANN J. W. (1988) Thermal behaviour and polymorphism of acylglycerides. In: *Crystallisation and polymorphism of fats and fatty acids*, Ed. by Garti N. and Sato K.. p. 10-87.
- HERNQVIST L. (1984) Polymorphism of fats, PhD Thesis. Lund: Lund University.

- HERNQVIST L. (1988) Crystal structures of fats and fatty acids. In: *Crystallisation and polymorphism of fats and fatty acids*, Ed. by Garti N. and Sato K., Marcel Dekker Inc., New York. p. 97-137.
- HIGAMI M., UENO S., SEGAWA T., IWANAMI K. and SATO K. (2003) Simultaneous synchrotron radiation X-ray diffraction - DSC analysis of melting and crystallization behavior of trioleoylglycerol in nanoparticles of oil-in-water emulsion. *Journal of the American Oil Chemists Society*; 80 (8):731-739
- HOUWINK R. and SALOMON G. (1995) *Adhesion and adhesives*. Elsevier; Amsterdam.
- HUYGHEBAERT A. and HENDRICKX H. (1971) Polymorphism of cocoa butter, shown by differential scanning calorimetry. *Lebensmittel-Wissenschaft Und-Technologie-Food Science and Technology*; 4 (2):59-63
- JOVANOVIC O., KARLOVIC D. J. and JAKOVLJEVIC J. (1995) Chocolate pre-crystallization: A review. *Acta Alimentaria*; 24 (3):225-239
- KALNIN D., LESIEUR P., ARTZNER F., KELLER G. and OLLIVON M. (2005) Systematic investigation of lard polymorphism using combined DSC and time-resolved synchrotron X-ray diffraction. *European Journal of Lipid Science and Technology*; 107 (9):594-606
- KELLENS M., MEEUSSEN W., HAMMERSLEY A. and REYNAERS H. (1991) Synchrotron radiation investigations of the polymorphic transitions in saturated monoacid triglycerides .2. Polymorphism study of a 50-50 mixture of tripalmitin and tristearin during crystallization and melting. *Chemistry and Physics of Lipids*; 58 (1-2):145-158
- KELLER G., LAVIGNE F., LOISEL C., OLLIVON M. and BOURGAUX C. (1996) Investigation of the complex thermal behavior of fats - combined DSC and X-ray diffraction techniques. *Journal of Thermal Analysis*; 47 (5):1545-1565
- KLUG H. P. and ALEXANDER L. E. (1974) *X-ray diffraction procedures: For polycrystalline and amorphous materials*. 2nd edition. Wiley-Interscience; UK.
- LARSSON K. (1994) *Lipids-molecular organization, physical functions and technical applications*. The Oily Press; Dundee.
- LAVIGNE F., BOURGAUX C. and OLLIVON M. (1993) Phase-transitions of saturated triglycerides. *Journal De Physique Iv*; 3 (C8):137-140
- LEHRIAN D. W., KEENEY P. G. and BUTLER D. R. (1980) Triglyceride characteristics of cocoa butter from cacao fruit matured in a microclimate of elevated-temperature. *Journal of the American Oil Chemists Society*; 57 (2):66-69

- LOISEL C., KELLER G., LECQ G., BOURGAUX C. and OLLIVON M. (1998) Phase transitions and polymorphism of cocoa butter. *Journal of the American Oil Chemists Society*; 75 (4):425-439
- LOISEL C., KELLER G., LECQ G., LAUNAY B. and OLLIVON M. (1997) Tempering of chocolate in a scraped surface heat exchanger. *Journal of Food Science*; 62 (4):773-780
- LOVEGREN N. V., GRAY M. S. and FEUGE R. O. (1976a) Effect of the liquid fat on melting point and polymorphic behaviour of cocoa butter and a cocoa butter fraction. *Journal of The American Oil Chemists' Society*; 53:108-112
- LOVEGREN N. V., GRAY M. S. and FEUGE R. O. (1976b) Polymorphic changes in mixtures of confectionery fats. *Journal of the American Oil Chemists Society*; 53 (2):83-88
- MACMILLAN S. D., ROBERTS K. J., ROSSI A., WELLS M. A., POLGREEN M. C. and SMITH I. H. (2002) In situ small angle X-ray scattering (saxs) studies of polymorphism with the associated crystallization of cocoa butter fat using shearing conditions. *CRYSTAL GROWTH & DESIGN*; 2 (3):221-226
- MACNAUGHTAN W., FARHAT I. A., HIMAWAN C., STAROV V. M. and STAPLEY A. G. F. (2006) A differential scanning calorimetry study of the crystallization kinetics of tristearin-tripalmitin mixtures. *Journal of the American Oil Chemists Society*; 83 (1):1-9
- MALKIN T. and MEARA M. L. (1939) An X-ray and thermal examination of the glycerides - part iv symmetrical mixed triglycerides,  $\text{ch(o cor')(ch}_2\text{ o cor)(2)}$ . *Journal of the Chemical Society*:103-108
- MARANGONI A. G. and MCGAULEY S. E. (2003) Relationship between crystallization behavior and structure in cocoa butter. *CRYSTAL GROWTH & DESIGN*; VOL.3, (NO.1):95-108
- MAZZANTI G., GUTHRIE S. E., SIROTA E. B., MARANGONI A. G. and IDZIAK S. H. J. (2003) Orientation and phase transitions of fat crystals under shear. *CRYSTAL GROWTH & DESIGN*; 3 (5):721-725
- MERKEN G. V. and VAECK S. V. (1980) Etude du polymorphisme du beurre de cacao par calorimétrie DSC. *Lebensmittel-Wissenschaft Und-Technologie-Food Science and Technology*; 13:314-317
- METIN S. and HARTEL R. W. (1996) Crystallization behaviour of blends of cocoa butter and milk fat or milk fat fractions. *Journal of Thermal Analysis*; 47:1527-1544
- MINIFIE B. W. (1989) *Chocolate, cocoa, and confectionery: Science and technology*. 3rd. Van Nostrand Reinhold Ltd; New York.
- MITTAL K. L. (1977) Role of interface in adhesion phenomena. *Polymer*

- MYKHAYLYK O. O., CASTELLETTO V., HAMLEY I. W. and POVEY M. J. W. (2004) Structure and transformation of low-temperature phases of 1,3-distearoyl-2-oleoyl glycerol. *European Journal of Lipid Science and Technology*; 106 (5):319-324
- NELSON R. B. (1999a) Enrobers, moulding equipment and coolers. In: *Industrial chocolate manufacture and use*, Ed. by Beckett S. T., 3rd ed, Blackwell science, Oxford. p. 259-286.
- NELSON R. B. (1999b) Tempering. In: *Industrial chocolate manufacture and use*, Ed. by Beckett S. T., 3rd ed, Blackwell science, Oxford. p. 231-258.
- NICE G. (2005) Chocolate moulding- soup to nuts. *Manufacturing Confectioner*; 85 (6):71-77
- OLLIVON M. (2004) Chocolate, a mysteriously appealing food. *European Journal of Lipid Science and Technology*; 106 (4):205-206
- OLLIVON M., LOISEL C., LOPEZ C., LESIEUR P., ARTZNER F. and KELLER G. (2001) Simultaneous examination of structural and thermal behaviors of fats by coupled X-ray diffraction and differential scanning calorimetry: Application to cocoa butter polymorphism. In: *Crystallization and solidification properties of lipids*, Ed. by Widlak N., Hartel R. W. and Narine S. S., AOCS, Chicago. p. 34-41.
- POCIUS A. V. (2002) *Adhesion and adhesives technology: An introduction*. 2nd Ed. Hanser Gardner; Cincinnati.
- READE M. G. (1985) Cooling processes: The natural rate of solidification of chocolate. *Manufacturing Confectioner*; 65 (1):59-65
- READING M., LUGET A. and WILSON R. (1994) Modulated differential scanning calorimetry. *Thermochimica Acta*; 238:295-307
- REDDY S. Y., FULL N., DIMICK P. S. and ZIEGLER G. R. (1996) Tempering method for chocolate containing milk-fat fractions. *Journal of the American Oil Chemists Society*; 73 (6):723-727
- RIINER U. (1970) Investigation of the polymorphism of fats and oils by temperature programmed X-ray diffraction. *Lebensmittel-Wissenschaft Und-Technologie-Food Science and Technology*; 3 (6):101-106
- ROBERTS K. J., WELLS M., POLGREEN M. and SMITH I. (1999) In situ x-ray diffraction studies on single and mixed confectionery fats using synchrotron radiation. *Abstracts of Papers of the American Chemical Society*; 218:U38-U38
- ROBINSON P. and SICHINA W. J. (2000) Characterization of chocolate using power compensated DSC. In: PerkinElmer Technical Note; PETech-43



1.

- ROUSSET P. (2002) Modelling crystallization kinetics of tags. In: *Physical properties of lipids*, Ed. by Marangoni A. and Narine S. S., Marcel Dekker, Inc., New York. p. 1-57.
- RUDNICKI W. R. and NIEZGÓDKA M. Modelling phase transitions in chocolate. 4th International Symposium on Confectionery Science.; Hershey, Penn., USA; 2002.
- SANDOR M., BAILEY N. A. and MATHIOWITZ E. (2002) Characterization of polyanhydride microsphere degradation by DSC. *Polymer*; 43 (2):279-288
- SATO K. (1989) Crystallization of fats and fatty acids. In: *Crystallisation and polymorphism of fats and fatty acids*, Ed. by Garti N. and Sato K.. p. 227-260.
- SATO K. (1999) Solidification and phase transformation behaviour of food fats - a review. *Fett-Lipid*; 101 (12):467-474
- SATO K. (2001) Crystallization behaviour of fats and lipids - a review. *Chemical Engineering Science*; 56 (7):2255-2265
- SATO K., ARISHIMA T., WANG Z. H., OJIMA K., SAGI N. and MORI H. (1989) Polymorphism of POP and SOS .1. Occurrence and polymorphic transformation. *Journal of the American Oil Chemists Society*; 66 (5):664-674
- SATO K. and KOYANO T. (2001) Crystallization properties of cocoa butter. In: *Crystallization processes in fats and lipid systems*, Ed. by Garti N. and Sato K., Marcel Dekker, New York. p. 429-457.
- SATO K., UENO S. and YANO J. (1999) Molecular interactions and kinetic properties of fats. *Progress in Lipid Research*; 38 (1):91-116
- SAUER B. B., KAMPERT W. G., NEAL BLANCHARD E., THREEFOOT S. A. and HSIAO B. S. (2000) Temperature modulated DSC studies of melting and recrystallization in polymers exhibiting multiple endotherms. *Polymer*; 41 (3):1099-1108
- SCHAWWE J. E. K. (1995) A comparison of different evaluation methods in modulated temperature DSC. *Thermochimica Acta*; 260 (1-2):1-16
- SCHAWWE J. E. K. and HOHNE G. W. H. (1996) The analysis of temperature modulated DSC measurements by means of the linear response theory. *Thermochimica Acta*; 287 (2):213-223
- SCHLICHTER-ARONHIME J. and GARTI N. (1988) Solidification and polymorphism in cocoa butter and the blooming problems. In: *Crystallisation and polymorphism of fats and fatty acids*, Ed. by Garti N. and Sato K., Marcel Dekker, Inc.. p. 363-391.

- SCHLICHTER-ARONHIME J., SARIG S. and GARTI N. (1988)  
Reconsideration of polymorphic transformations in cocoa butter using the DSC. *Journal of the American Oil Chemists' Society*; 65 (7):1140-1143
- SEGUINE E. S. Tempering- the inside story. 45th P.M.C.A Production Conference; Pennsylvania, USA; 1991. p. 21- 30.
- SINGH S. K., JALALI A. F. and ALDEN M. (1999) Modulated temperature differential scanning calorimetry for examination of tristearin polymorphism: I. Effect of operational parameters. *Journal of the American Oil Chemists' Society [print]* 76; 76 (4):499-505
- SPIGNO G., PAGELLA G. and DE FAVERI D. M. (2001) DSC characterisation of cocoa butter polymorphs. *Italian Journal of Food Sciences*; 13 (3):275-284
- STAPLEY A. G. F., TEWKESBURY H. and FRYER P. J. (1999) The effects of shear and temperature history on the crystallization of chocolate. *Journal of the American Oil Chemists Society*; 76 (6):677-685
- TAKEUCHI M., UENO S., FLOTER E. and SATO K. (2002) Binary phase behavior of 1,3-distearoyl-2-oleoyl-sn-glycerol (SOS) and 1,3-distearoyl-2-linoleoyl-sn-glycerol (sls). *Journal of the American Oil Chemists Society*; 79 (7):627-632
- TAKEUCHI M., UENO S. and SATO K. (2003) Synchrotron radiation saxs/waxs study of polymorph-dependent phase behavior of binary mixtures of saturated monoacid triacylglycerols. *CRYSTAL GROWTH & DESIGN*; 3 (3):369-374
- TALBOT G. (1999) Chocolate temper. In: *Industrial chocolate manufacture and use*, Ed. by Beckett S. T., 3rd edition ed, Blackwell Science. p. 218-230.
- TEWKESBURY H., STAPLEY A. G. F. and FRYER P. J. (2000) Modelling temperature distributions in cooling chocolate moulds. *Chemical Engineering Science*; 55 (16):3123-3132
- TIMMS R. E. (1980) The phase-behavior of mixtures of cocoa butter and milk-fat. *Lebensmittel-Wissenschaft & Technologie*; 13 (2):61-65
- TIMMS R. E. (1984) Phase behaviour of fats and their mixtures. *Progress in Lipid Research*; 23 (1):1-38
- TIMMS R. E. (2003) *Confectionery fats handbook: Properties, production and applications*. The Oily Press; Bridgewater,UK.
- TIMMS R. E. and PAREKH J. V. (1980) The possibilities for using hydrogenated, fractionated or interesterified milk-fat in chocolate. *Lebensmittel-Wissenschaft & Technologie*; 13 (4):177-181

- UENO S., MINATO A., SETO H., AMEMIYA Y. and SATO K. (1997) Synchrotron radiation X-ray diffraction study of liquid crystal formation and polymorphic crystallization of SOS (sn-1,3-distearoyl-2-oleoyl glycerol). *Journal of Physical Chemistry B*; 101 (35):6847-6854
- UENO S., RISTIC R. I., HIGAKI K. and SATO K. (2003) In situ studies of ultrasound-stimulated fat crystallization using synchrotron radiation. *Journal of Physical Chemistry B*; 107 (21):4927-4935
- VAECK S. V. (1951) The polymorphism of certain natural fats. *Rev. Int. Choc*; 6:100-113
- VAECK S. V. (1960) Cacao butter and fat bloom. *Manufacturing Confectioner*; 40:35-73
- VAN LANGEVELDE A., DRIESSEN R., MOLLEMAN W., PESCHAR R. and SCHENK H. (2001a) Cocoa-butter long spacings and the memory effect. *Journal of the American Oil Chemists Society*; 78 (9):911-918
- VAN LANGEVELDE A., VAN MALSSSEN K., PESCHAR R. and SCHENK H. (2001b) Effect of temperature on recrystallization behavior of cocoa butter. *Journal of the American Oil Chemists Society*; 78 (9):919-925
- VAN MALSSSEN K., PESCHAR R., BRITO C. and SCHENK H. (1996) Real-time X-ray powder diffraction investigations on cocoa butter .3. Direct beta-crystallization of cocoa butter: Occurrence of a memory effect. *Journal of the American Oil Chemists Society*; 73 (10):1225-1230
- VERDONCK E., SCHAAP K. and THOMAS L. C. (1999) A discussion of the principles and applications of modulated temperature DSC (mtdsc). *International Journal of Pharmaceutics*; 192 (1):3-20
- WHYMPER R. (1912) *Cocoa and chocolate. Their chemistry and manufacture*. Churchill; London.
- WILLCOCKS N. A., EARIS F. W., COLLINS T. M., LEE R. D., PALMER W. R. and HARDING W., (2002); Mars Incorporated, McLean, VA (US), assignee. Methods of setting chocolate and products produced by same. USA patent US 6, 419, 970 B1. July 16.
- WILLE R. L. and LUTTON E. S. (1966) Polymorphism of cocoa butter. *Journal of the American Oil Chemists Society*; 43 (8):491-496
- WUNDERLICH B., BOLLER A., OKAZAKI I. and ISHIKIRIYAMA K. (1997) Heat-capacity determination by temperature-modulated DSC and its separation from transition effects. *Thermochimica Acta*; 305:125-136